

REMARKS

I. PRELIMINARY REMARKS

No claims have been amended, added or canceled. Claims 1-4, 6-19, 21-23 and 43-45 remain in the application. Claims 3, 4, 17, 43 and 45 have been withdrawn from consideration. Reexamination and reconsideration of the application are respectfully requested.

Applicant respectfully submits that the present response, including Exhibits 1-9 that are attached hereto and discussed below, should be entered for purposes of appeal in accordance with 37 C.F.R. § 1.116(e) because there are “good and sufficient reasons why the affidavit or other evidence is necessary and was not earlier presented.” Specifically, the issues to which the Exhibits 1-9 pertain were raised by the Examiner for the first time in the outstanding Final Office Action despite three prior Office Actions on the merits. Should the Examiner determine that the response (and Exhibits) will not be entered, applicant hereby requests that the Examiner fully explain her position in order to clarify the issues to be decided by petition.

II. REJECTIONS UNDER 35 U.S.C. §§ 101 AND 112, FIRST PARAGRAPH

A. The Rejections

Claims 1, 2 and 6-13 have been rejected under 35 U.S.C. § 101 because the claimed invention is purportedly not supported by either a substantial asserted utility or a well-established utility. The Office Action stated:

The fuel cell assembly has operability for a wherein an empty space for a fuel path extends from an anode to another anode, but not for an anode to a cathode. It is noted that when a fuel gas and an oxidant gas mix, it is well-known that combustion occurs, and does not generate electricity to make the fuel cell operable.

[Office Action at page 3.]

Claims 1, 2 and 6-13 have also apparently been rejected under 35 U.S.C. § 112, first paragraph, for two different reasons. The Office Action stated:

Specifically, since the claimed invention is not supported by either a substantial asserted utility or a well established utility for the reasons set forth above, one skilled in the art clearly would not know how to use the claimed invention.

* * *

[T]he specification, while being enabling for an anode to anode space, does not reasonably provide enablement for a cathode to anode space. The specification does not enable any person skilled in the art to which it pertains, or with which it is most nearly connected, to use the invention commensurate in scope with these claims.

[Office Action at page 3.]

The rejections under 35 U.S.C. §§ 101 and 112, first paragraph, are respectfully traversed. Reconsideration thereof is respectfully requested.

B. Discussion

There are a plethora of legal and factual errors associated with the rejections under 35 U.S.C. §§ 101 and 112, first paragraph. Nevertheless, in the interest of brevity, the focus of this response is one fundamental error that is clearly dispositive. The fundamental error involves the Examiner's implicit assertion that her opinions concerning "single chamber" fuel cells are entitled to greater weight than the knowledge of the inventor named in the present application, who is also named in many issued U.S. patents in the fuel cell area, including a number of which are directed to various types of "single chamber" fuel cells.¹

The present application discloses a variety of fuel cell assemblies that fall within the scope of, *inter alia*, independent claim 1. The assembly illustrated in Figures 14 and 15 is "single chamber" assembly in which "the fuel cell 114 is arranged in such a manner that the anode 118 and cathode 120 face one another (or face a portion of the housing main wall) with a combined fuel/oxidant passage 135 defined therebetween."

¹ See, e.g., U.S. Patent Nos. 6,893,769; 7,014,929; 7,045,244; 7,067,215; 7,118,826; 7,147,948; and 7,153,601.

[Application at page 9, lines 21-25.] The crux of the Examiner's arguments appears to be that "single chamber" fuel cells, which are sometimes referred to as "mixed reactant" fuel cells, were not known to those of skill in the art as of the filing date of the present application and, to the contrary, "when a fuel gas and an oxidant gas mix, ***it is well-known that combustion occurs, and does not generate electricity to make the fuel cell operable.***" [Office Action at page 3, emphasis added.]

The statement quoted in the previous paragraph begs the relatively straightforward question, "to whom was it well-known that combustion occurs and electricity is not generated?" The unmistakable answer is "certainly not to those of skill in the art." To that end, attached hereto are nine (9) Exhibits which show that single chamber fuel cells were, in fact, "well-known" to those of ordinary skill in the art prior to the July 15, 2003 filing date of the present application. Exhibits 1 and 2 are U.S. patents that issued one decade or two decades before the present application was filed, Exhibits 3-7 are scholarly articles that were published prior to 2003, and Exhibit 9 is a news article from 2000. Each Exhibit is discussed briefly below.

Exhibit 1 – Referring to Figures 1 and 2, U.S. Patent No. 4,248,941 discloses a "mixed reactant" fuel cell in which a fuel/oxygen mixture is supplied to the anode electrode 18 and cathode electrode 20. [Column 4, line 47 to column 5, line 46.]

Exhibit 2 - Referring to Figure 4, U.S. Patent No. 5,102,750 discloses a fuel cell that consumes a "fuel/oxidizer mixture." [Column 2, lines 30-35; and column 5, lines 46-64.]

Exhibit 3 – Takashi Hibino et al., *Single Chamber Solid Oxide Fuel Cell Constructed from an Yttria-Stabilized Zirconia Electrolyte*, The Electrochemical Society Electrochemical and Solid-State Letters, Volume 2, Issue 7, pp. 317-319 (1999). This article discusses materials-related improvements to single chamber fuel cells.

Exhibit 4 – Takashi Hibino et al., *A Low-Operating-Temperature Solid Oxide Fuel Cell in Hydrocarbon-Air Mixtures*, Science, Vol. 288, pp. 2031-2033 (2000). This article discusses materials-related improvements to single chamber fuel cells.

Exhibit 5 – Takashi Hibino et al., *Improvement of a Single-Chamber Solid-Oxide Fuel Cell and Evaluation of New Cell Designs*, Journal of the Electrochemical Society, Volume 147, Issue 4, pp. 1338-1343 (2000). This article discusses materials-related improvements to single chamber fuel cells.

Exhibit 6 – Takashi Hibino et al., *A Solid Oxide Fuel Cell Using an Exothermic Reaction as the Heat Source*, Journal of the Electrochemical Society, Volume 148, Issue 6, pp. A544-A549 (2001). This article discusses single chamber fuel cells that are capable of low temperature startup.

Exhibit 7 – Takashi Hibino et al., *High Performance Anodes for SOFCs Operating in Methane-Air Mixture at Reduced Temperatures*, Journal of the Electrochemical Society, Volume 149, Issue 2, pp. A133-A136 (2001). This article discusses materials-related improvements to single chamber fuel cells. [Note the Abstract.]

Exhibit 8 – Michael Priestnall et al., *Compact Mixed-Reactant Fuel Cells*, Journal of Power Sources, Volume 106 (1-2), pp. 21-30 (2002). This article discusses a mixed reactant PEM stack.

Exhibit 9 – “Hot” Fuel Cells Get Cooler and Cooler, CNN.com (2000). This article mentions single chamber fuel cells.

As illustrated above, single chamber fuel cells were “well-known” to those of ordinary skill in the art prior to the July 15, 2003 filing date of the present application. Applicant respectfully submits, therefore, that (1) the inventions defined by claims 1, 2 and 6-13 are supported by a well-established utility and (2) the specification, as originally filed, would have enabled a person of ordinary skill in the art to make and use the invention defined by claims 1, 2 and 6-13. As such, the rejections under 35 U.S.C. §§ 101 and 112, first paragraph, are improper and should be withdrawn.

III. REJECTIONS UNDER 35 U.S.C. § 112, SECOND PARAGRAPH

A. The Rejection

Claims 1, 2, 6-13 and 44 have been rejected under 35 U.S.C. § 112, second paragraph, as being indefinite for failing to particularly point out and distinctly claim the subject matter which applicant regards as the invention. The Office Action stated:

The limitation “an electrode surface to a radially spaced electrode surface” in claim 1 is unclear. Do these electrodes refer back to the aforementioned electrodes, anode electrode and a cathode electrode?

[Office Action at page 6.] The rejection under 35 U.S.C. § 112, second paragraph, is respectfully traversed. Reconsideration thereof is respectfully requested.

B. Discussion

At the outset, applicant notes for the record the rejections under 35 U.S.C. §§ 101 and 112, first paragraph, and the “election/restriction” discussion on page 2 of the Office Action show that the Examiner clearly understands what is set forth in independent claim 1. Should the rejection be maintained, applicant hereby requests that the Examiner explain why one of skill in the art who had reviewed the present application would not be able to understand at least as much as the Examiner.

That issue notwithstanding, 35 U.S.C. § 112, second paragraph, merely requires that the claims set forth and circumscribe a particular area with a reasonable degree of precision and particularity. The definiteness of the claim language employed must not be analyzed in a vacuum, ***but always in light of the teachings of the prior art and of the particular application disclosure*** as it would be interpreted by one having ordinary skill in the pertinent art. *Ex parte Moelands*, 3 USPQ2d 1474,1476 (PTO Bd. App. & Int’f 1987), quoting *In re Moore*, 169 USPQ 236, 238 (CCPA 1971).

With respect to the language employed in independent claim 1, claim 1 calls for “at least one spiral shaped fuel cell, including an anode electrode and a cathode electrode, that defines a fuel path.” Claim 1 also indicates that the fuel path is “in the form of an empty space that extends from an electrode surface to a radially spaced electrode surface.” Applicant respectfully submits that one of skill in the art who had reviewed the present application would understand that the claimed electrode surfaces are being recited in the generic sense, i.e. that the claim covers a ***fuel*** path that is in the form of (1) an empty space that extends from an ***anode electrode*** surface to a radially spaced ***anode electrode*** surface, or (2) an empty space that extends from an ***anode electrode*** surface to a radially spaced ***cathode electrode*** surface.

Applicant respectfully submits that one of ordinary skill in the art would understand what applicant regarded as the invention defined by independent claim 1 without any review of the remainder of the application. Nevertheless, even a cursory review of the remainder of the application would have left no doubt as to what is being

claimed. In particular, the specification indicates that a fuel cell that is bent during manufacture in the manner illustrated in Figures 13A and 13B will have an “anode electrode surface to anode electrode surface” empty space therebetween. One example of such an empty space is the fuel passage 134 illustrated in Figure 5, which is reproduced below. [Note anodes 118.] The specification also indicates that, alternatively, a fuel cell which is bent during manufacture in the manner illustrated in Figure 14 will have an “anode electrode surface to cathode electrode surface” empty space therebetween. Here, oxidant is combined with the fuel in the fuel/oxidant passage 135. One example of such an empty space is illustrated in Figure 15, which is reproduced below. [Note anode 118 and cathode 120.]

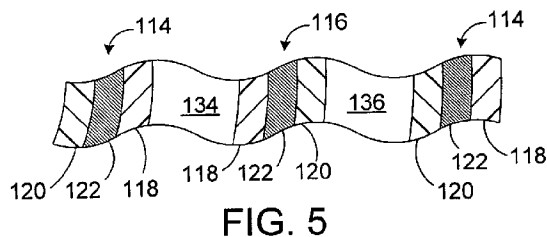


FIG. 5

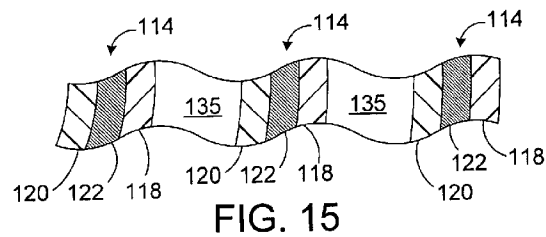


FIG. 15

Finally, with respect to the claims that depend from independent claim 1, applicant respectfully submits that one of ordinary skill in the art would understand that dependent claim 44 covers the embodiment illustrated in Figure 5,² and that dependent claim 45 covers the embodiment illustrated in Figure 15.³ As such, one of ordinary skill in the art would understand that both embodiments are covered by independent claim 1.

In view of the forgoing, applicant respectfully submits that one of skill in the art who had reviewed the present application would understand what applicant regards as the invention. The rejection under the second paragraph of 35 U.S.C. § 112 is, therefore, improper and should be withdrawn.

² Dependent claim 44 states that “the fuel path is in the form of an empty space that extends from an **anode** electrode surface to a radially spaced **anode** electrode surface.”

³ Dependent claim 45 states that “the fuel path is in the form of an empty space that extends from an **anode** electrode surface and a radially spaced **cathode** electrode surface.”

IV. PRIOR ART REJECTIONS

A. The Rejections

Claims 14-16 and 18 have been rejected under 35 U.S.C. § 102 as being anticipated by U.S. Patent No. 6,063,517 to Montemayor et al. ("the Montemayor '517 patent"). Claims 19, 22 and 23 have been rejected under 35 U.S.C. §§ 102 or 103 as being anticipated by, or unpatentable over, the Montemayor '517 patent. Claim 21 has been rejected under 35 U.S.C. § 103 as being unpatentable over the combined teachings of the Montemayor '517 patent and U.S. Patent Pub. No. 2003/0011721 to Wattelet et al. ("the Wattelet '721 publication").

The rejections under 35 U.S.C. §§ 102 and 103 are respectfully traversed. Reconsideration thereof is respectfully requested.

B. The Cited References

As illustrated in Figure 1, the Montemayor '517 patent discloses a fuel cell apparatus including a fuel cell with an anode 14 and hydrogen injection tubes 22 and 24 at the longitudinal edges of the anode. The fuel cell is rolled in the manner illustrated in Figure 2 and placed in the casing 30 illustrated in Figure 3. During operation, hydrogen is forced into both longitudinal ends of the anode 14 by way of the hydrogen injection tubes 22 and 24 under sufficient pressure to force the hydrogen through the anode. [Note arrows 34 in Figure 3.] Oxidant is supplied to the rolled fuel cell by way of the gaps adjacent to the cathode 26. Additionally, and although it is not entirely clear, it appears that hydrogen which was not forced into the anode 14 exits the apparatus by way of the injection tubes 22 and 24. [Note the arrows at the bottom of Figure 3.]

The Wattelet publication has been cited for its purported heat exchanger teachings.

C. Discussion Concerning Claims 14-16 and 18

Independent claim 14 is directed to a combination of elements comprising “a housing including an inlet and an exhaust port located radially inward of the inlet,” “an exhaust region connected to the housing exhaust port” and “at least one anode and cathode arrangement having a spiral shape that extends outwardly of and more than once around the perimeter of the exhaust region and defines a reactant path having an outlet end associated with the exhaust region and an inlet end connected to the housing inlet.” Claim 14 also indicates that “the housing and the anode and cathode arrangement are constructed and arranged relative to one another such that ***the only reactant flow direction is inward toward the housing exhaust port that is located radially inward of the housing inlet.***” The respective combinations defined by claims 15, 16 and 18 include, *inter alia*, the elements recited in claim 14.

The Montemayor '517 patent fails to teach or suggest the claimed combinations. For example, and referring to Figures 2 and 3, the Montemayor '517 patent discloses a fuel cell apparatus including a casing 30, a fuel cell within the casing, and hydrogen injection tubes 22 and 24 that force hydrogen into the inner and outer ends of the fuel cell anode 14. [Note arrows 34 in Figure 3.] In contrast to the claimed combination, there is clearly some flow that is not ***inward toward a housing exhaust port that is located radially inward of the housing inlet***, as is evidenced by the arrow labeled 24 in Figure 3.

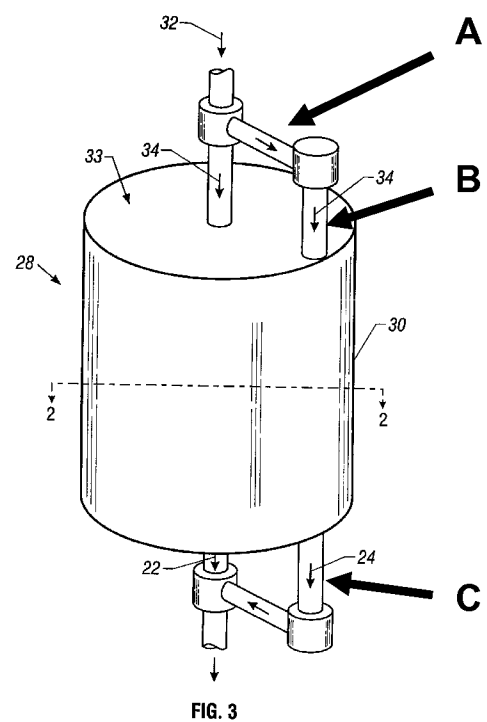
In response to the arguments in the preceding paragraph, the Examiner has taken the following position:

Applicant asserts that there is some flow in Montemayor that does not flow toward a housing exhaust port that is located radially inward of the housing inlet.

The Examiner disagrees. The Applicant has specified the location of the exhaust, but has not specified what is meant by "inward". Since Montemayor's housing exhaust port is located radially inward of the housing inlet, all the reactant flows ultimately lead toward the housing exhaust and thus, necessarily flow only inward toward the housing exhaust port.

[Office Action at page 13.] This statement shows that the Examiner's interpretation of claim 14 is utterly unreasonable. First, there is simply no reason for applicant's specification to include a "definition" of a common English word such as "inward." In order to clarify the issues for appeal, applicant hereby requests the Examiner clearly indicate how she is interpreting the word "inward" in the context of claim 14 and the disclosure of the present application. Second, the claim does not indicate "all the reactant flows *ultimately lead* toward the housing exhaust." Instead, claim 14 indicates *without equivocation* that "**the only reactant flow direction** is inward toward the housing exhaust port that is located radially inward of the housing inlet." To the extent that the Examiner is unaware of the meaning of the word "only," a typical definition is "without others or anything further; alone; solely; exclusively."⁴

In order to clarify the issues for appeal, Figure 3 of the Montemayor '517 patent is reproduced here with reference characters A, B and C added. Applicant hereby requests that the Examiner explain (1) how reactant flowing in the direction of arrow A falls within the scope of "**the only** reactant flow direction is inward" portion of independent claim 14, and (2) how reactant flowing in from arrow B to arrow C falls within the scope of "**the only** reactant flow direction is inward" portion of independent claim 14.



⁴ Dictionary.com Unabridged (v 1.1). Random House, Inc. <http://dictionary.reference.com/browse/only> (accessed: April 18, 2007).

As illustrated above, the Montemayor '517 patent fails to teach or suggest each and every element of the combination recited in independent claim 14. Applicant respectfully submits, therefore, that claims 14-16 and 18 are patentable thereover and that the rejection under 35 U.S.C. § 102 should be withdrawn.

E. Discussion Concerning Claims 19 and 21-23

1. The Claimed Combinations

Independent claim 19 is directed to a combination of elements comprising "**a housing having** an outer region, an inner region defining a perimeter and exhaust port connected to the inner region" and "**means for** converting reactants into electricity and byproducts and directing the reactants and byproducts from the outer region to the inner region, and at least once around the perimeter of the inner region, as the reactants are being converted into electricity and byproducts, **such that all of the byproducts and any unused reactants** that exit the fuel cell assembly exit by way of the inner region." The respective combinations defined by claims 21-23 include, *inter alia*, the elements recited in claim 19.

2. The Rejection Under 35 U.S.C. § 102

The Manual of Patent Examining Procedure ("MPEP") requires a two-part analysis of means-plus-function elements. **First**, "the application of a prior art reference to a means or step plus function limitation **requires** that the prior art element **perform the identical function** specified in the claim." [MPEP § 2182, emphasis added.] Second, "**if a prior art reference teaches identity of function** to that specified in a claim, **then** under Donaldson an examiner carries the initial burden of proof for showing that the prior art structure or step is the same as or equivalent to the structure, material, or acts described in the specification which has been identified as corresponding to the claimed means or step plus function." [Id., emphasis added.] Along these lines, the Federal

Circuit stated that "[t]he corresponding structure to a function set forth in a means-plus-function limitation **must actually perform the recited function, not merely enable the pertinent structure to operate as intended.**" *Asyst Technologies Inc. v. Empak Inc.*, 60 USPQ2d 1567, 1672-73 (Fed. Cir. 2001), emphasis added. With respect to the function itself, it is well settled that **all functional statements** which follow the "means for" language must be considered. See, e.g., *Sage Products Inc. v. Devon Industries Inc.*, 44 USPQ2d 1103, 1110 (Fed. Cir. 1997).

The Montemayor '517 patent fails to teach or suggest the claimed combinations. For example, the function recited in the means-plus-function element is not being performed because what appears to be unused hydrogen exits the Montemayor apparatus from the **outer region (tube 24)** in addition to the inner region (tube 22). [Figure 3.]

In response to the arguments in the preceding paragraph, the Examiner has taken the following positions:

The Office is interpreting the **arrow below the arrow 22 in Fig. 3 as the exhaust region** and thus, all of the byproducts and any unused reactants that exit the fuel cell assembly exit by way of the inner region.

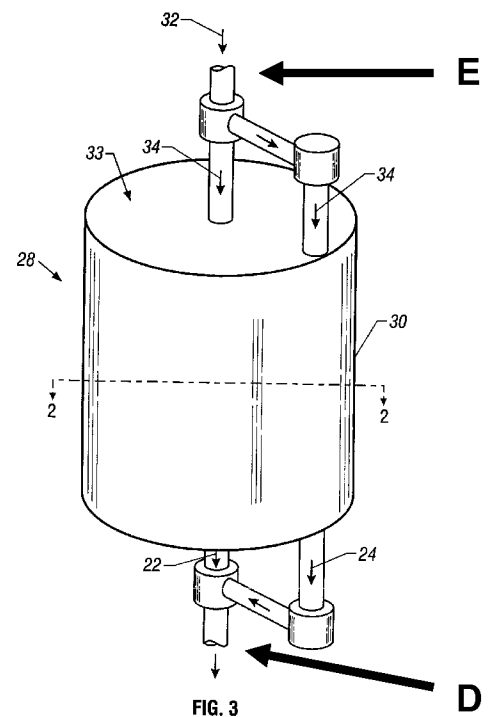
* * *

The Examiner notes that Montemayor as disclosed in Fig. 3 meets the limitation "such that all of the byproducts and any unused reactants that exit the fuel cell assembly exit by way of the inner region". The Examiner notes that Montemayor's configuration is **functionally equivalent** to Applicant's fuel cell assembly as claimed in claim 19.

[Office Action at pages 8 and 9.] Applicant respectfully submits that both of these positions are incorrect.

With respect to the first position, applicant has assumed that the Examiner intended to refer to "inner region," which is recited in claim 19, not "exhaust region." Applicant has also assumed that by "arrow below the arrow 22 in Fig. 3" the Examiner was referring to the outlet tube (labeled "D" in the reproduction of Figure 3 on the following page) that receives byproduct/unused reactant from both the center of the Montemayor casing 30 and the outer perimeter of the Montemayor casing, and is separated from Montemayor casing by two other outlet tubes (i.e. the tubes associated with arrows 22 and 24). **Should these assumptions be incorrect, clarification is hereby requested.**

There is simply no reasonable interpretation of “**all** of the byproducts and any unused reactants that exit the fuel cell assembly exit by way of the inner region [of the housing]” that would read on Montemayor device. Outlet tube D receives byproduct/unused reactant from both the center of the Montemayor casing 30 and the outer perimeter of the Montemayor casing, and is **separated from Montemayor casing by two other outlet tubes** (i.e. the tubes associated with arrows 22 and 24). In other words, the byproducts and any unused reactant exits by way of the tubes associated with arrows 22 and 24, and the tube associated with arrow 24 is not associated with the inner region.



It is also noteworthy that the Examiner’s interpretation of “**all** of the byproducts and any unused reactants that exit the fuel cell assembly exit by way of the inner region” appears to conflict with the Examiner’s interpretation of other portions of claim 19. More specifically, the functional statement in the means-plus-function element also includes “directing the reactants and byproducts **from the outer region** to the inner region.” If the Examiner is interpreting the claim such that outlet tube D corresponds to the claimed “inner region” of the housing, it would certainly follow that inlet tube E is also corresponds to the “inner region” and that the Montemayor device actually directs reactants **from the inner region** to the inner region.

Turning to the Examiner’s second position, applicant notes that **functional** equivalence is irrelevant in a means-plus-function analysis. The issues are (1) whether or not the **same function** is being performed and (2) whether the structure in the reference that performs the same function is the same as, or equivalent to, the structure that performs the function in the application at issue. See MPEP § 2182.

As illustrated above, the Montemayor ‘517 patent fails to teach or suggest each and every element of the combination recited in independent claim 19. Applicant

respectfully submits, therefore, that claims 19, 22 and 23 are patentable thereover and that the rejection under 35 U.S.C. § 102 should be withdrawn.

3. The Rejections Under 35 U.S.C. § 103

With respect to the alternative rejection of claims 19, 22 and 23 under 35 U.S.C. § 103, the Office Action provided the following basis for the conclusion of obviousness:

Should Montemayor not be anticipatory, the Examiner notes that it would have been obvious to one of ordinary skill in the art at the time the invention was made to modify the reactant outlet to solely the inner region for the benefit of simplifying the reactant exit flow.

[Office Action at page 12.] Applicant respectfully submits that this statement of Examiner opinion does not even come close to establishing a *prima facie* case of obviousness.

With respect to the legal standard upon which patentability under 35 U.S.C. § 103 is evaluated, *In re Kotzab*, 55 USPQ2d 1313, 1316-17 (Fed. Cir. 2000), provides a fairly succinct summary of the standard adhered to by the Federal Circuit:

A critical step in analyzing the patentability of claims pursuant to section 103(a) is casting the mind back to the time of invention, to consider the thinking of one of ordinary skill in the art, guided only by the prior art references and the then-accepted wisdom in the field. Close adherence to this methodology is especially important in cases where the very ease with which the invention can be understood may prompt one “to fall victim to the insidious effect of a hindsight syndrome wherein that which only the invention taught is used against its teacher.” Most if not all inventions arise from a combination of old elements. Thus, every element of a claimed invention may often be found in the prior art. However, identification in the prior art of each individual part claimed is insufficient to defeat patentability of the whole claimed invention. Rather, to establish obviousness based on a combination of the elements disclosed in the prior art, there must be some motivation, suggestion or teaching of the desirability of making the specific combination that was made by the applicant. ***Even when obviousness is based on a single prior art reference, there must be a showing of a suggestion or motivation to modify the teachings of that reference.***

[Citations emitted, emphasis added.] The *Kotzab* decision is also cited in Section 2143.01 of the MPEP.

“The motivation, suggestion or teaching may come explicitly from statements in the prior art, the knowledge of one of ordinary skill in the art, or, in some cases, the nature of the problem to be solved. In addition, the teaching, suggestion or motivation may be implicit from the prior art as a whole, rather than expressly stated.” *In re Kotzab*, 55 USPQ2d at 1317. Whether the showing is explicit or implicit, “rejections on obviousness grounds **cannot be sustained by mere conclusory statements**; instead, there must be some articulated reasoning with some rational underpinning to support the legal conclusion of obviousness.” *In re Kahn*, 78 USPQ2d 1329, 1336 (Fed. Cir. 2006), *citations omitted, emphasis added*. To that end, “particular findings must be made as to the reason the skilled artisan, with no knowledge of the claimed invention, would have selected [the] components for combination in the manner claimed.” *In re Kotzab*, 55 USPQ2d at 1317. “This factual question of motivation is material to patentability, and **[may] not be resolved on subjective belief and unknown authority**.” *In re Lee*, 61 USPQ2d 1430, 1434 (Fed. Cir. 2002), *emphasis added*.

The present rejection is based solely on a conclusory statement, subjective belief and unknown authority. As such, it is improper as a matter of law and must be withdrawn. It is also noteworthy that, in the Examiner’s opinion, eliminating the outlet tube associated with arrow 24 (Figure 3) would have “[simplified] the reactant exit flow.” Applicant respectfully submits that this statement ignores the fact that reactant is entering the Montemayor fuel cell from inward and outward ends at what appears to be equal pressure. Applicant hereby requests that the Examiner explain, based on her knowledge in the art, how the Montemayor device would function if all of the unused reactant and byproducts had to exit by way of the inward end of the fuel cell while, at the same time, reactants were being simultaneously supplied to the inward and outward ends of the fuel cell.

In view of the forgoing, applicant respectfully submits that the Montemayor ‘517 patent fails to render the invention defined by independent claim 19 obvious and that the alternative rejection of claims 19, 22 and 23 under 35 U.S.C. § 103 should be withdrawn.

Turning to claim 21, the Wattlelet '721 publication fails to remedy the above-identified deficiencies in the Montemayor '517 patent. Claim 21 is, therefore, patentable for at least the same reasons as independent claim 19 and the rejection of claim 21 under 35 U.S.C. § 103 should also be withdrawn.

V. CLOSING REMARKS

In view of the foregoing, it is respectfully submitted that the claims in the application are in condition for allowance. Reexamination and reconsideration of the application are respectfully requested. Allowance of the claims at an early date is courteously solicited.

If for any reason the Examiner finds the application other than in condition for allowance, the Examiner is respectfully requested to call applicant's undersigned representative at (310) 563-1458 to discuss the steps necessary for placing the application in condition for allowance.

The Commissioner is hereby authorized to charge any additional fees which may be required, or credit any overpayment to Deposit Account No. 08-2025. Should such fees be associated with an extension of time, applicant respectfully requests that this paper be considered a petition therefor.

Respectfully submitted,

April 18, 2007
Date

/Craig A. Slavin/
Craig A. Slavin
Reg. No. 35,362
Attorney for Applicant

Henricks, Slavin & Holmes LLP
840 Apollo Street, Suite 200
El Segundo, CA 90245
(310) 563-1458
(310) 563-1460 (Facsimile)

EXHIBIT 1

[54] **SOLID ELECTROLYTE
ELECTROCHEMICAL CELL**[75] Inventors: **George A. Louis**, West Hartford;
John M. Lee, Bloomfield; **Donald L. Maricle**; **John C. Trocciola**, both of
Glastonbury, all of Conn.[73] Assignee: **United Technologies Corp.**, Hartford,
Conn.[21] Appl. No.: **107,191**[22] Filed: **Dec. 26, 1979**[51] Int. Cl.³ **H01M 8/10**[52] U.S. Cl. **429/13; 429/30;**
204/195 S[58] **Field of Search** 429/30, 31, 32, 33,
429/191, 192, 193, 124, 13, 15; 204/1 S, 195 S[56] **References Cited****U.S. PATENT DOCUMENTS**

3,230,115	1/1966	Tamminen	429/124
3,525,646	8/1970	Tannenberger et al.	429/31
3,719,564	3/1973	Lilly et al.	204/1 S
3,974,054	8/1976	Poolman et al.	204/195 S
4,190,499	2/1980	Pebler	204/1 S

FOREIGN PATENT DOCUMENTS

2304464 8/1974 Fed. Rep. of Germany 204/195 S

Primary Examiner—Donald L. Walton*Attorney, Agent, or Firm*—Stephen E. Revis

[57]

ABSTRACT

A new type of electrochemical cell which can be used for generating electricity or in an electrolysis mode for producing gases such as hydrogen and oxygen comprises laterally spaced apart or side-by-side catalyst layers as electrodes with the gap between the catalyst layers being bridged by a solid electrolyte which provides an ion conductive path from one catalyst layer to the other. The catalyst layers and the electrolyte are preferably in the form of thin films or layers on the surface of an inert supporting substrate. A plurality of these cells may be disposed on the substrate and interconnected electrically forming a network of series and parallel connected cells. Means are provided to feed fuel and oxidant to the electrodes either as separate gases or mixed together if appropriate catalytic materials are selected.

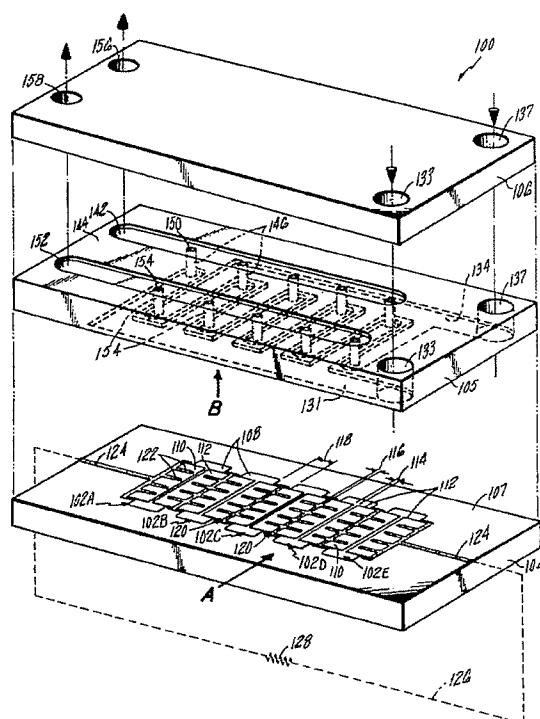
21 Claims, 14 Drawing Figures

FIG. 1

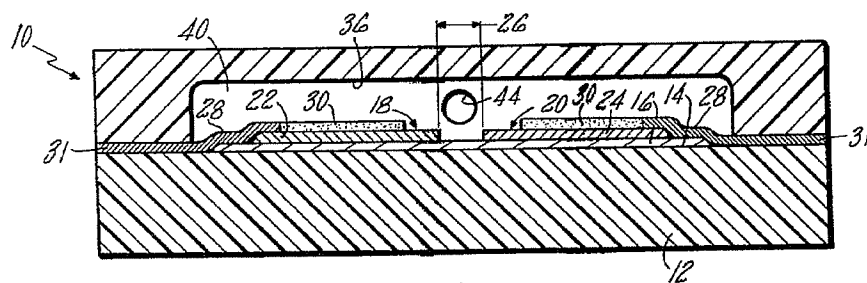
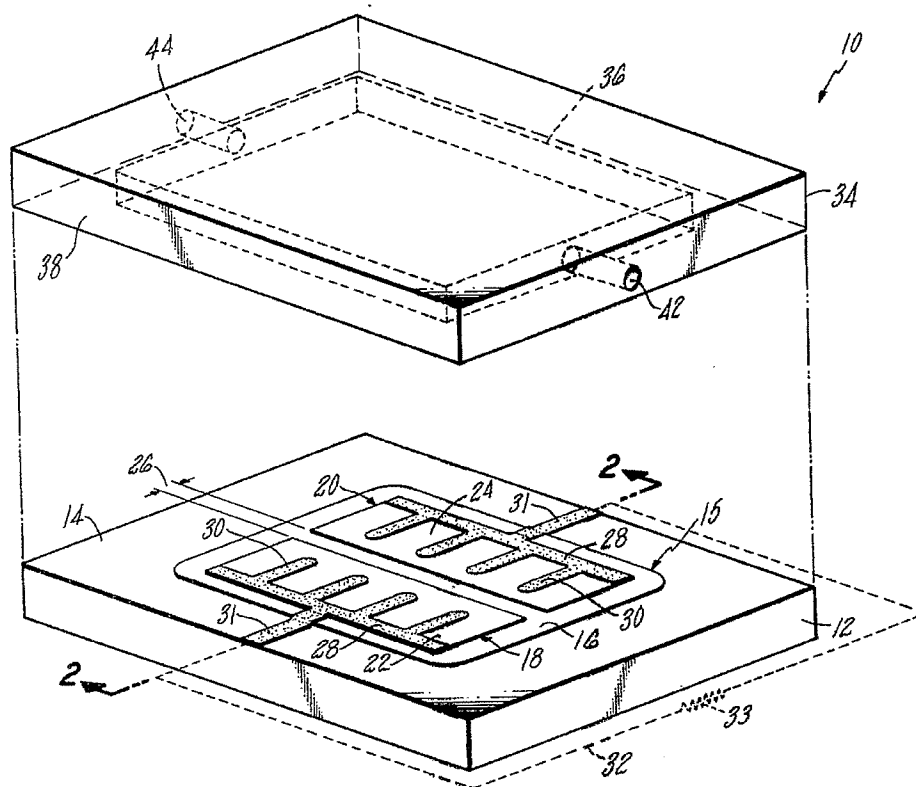
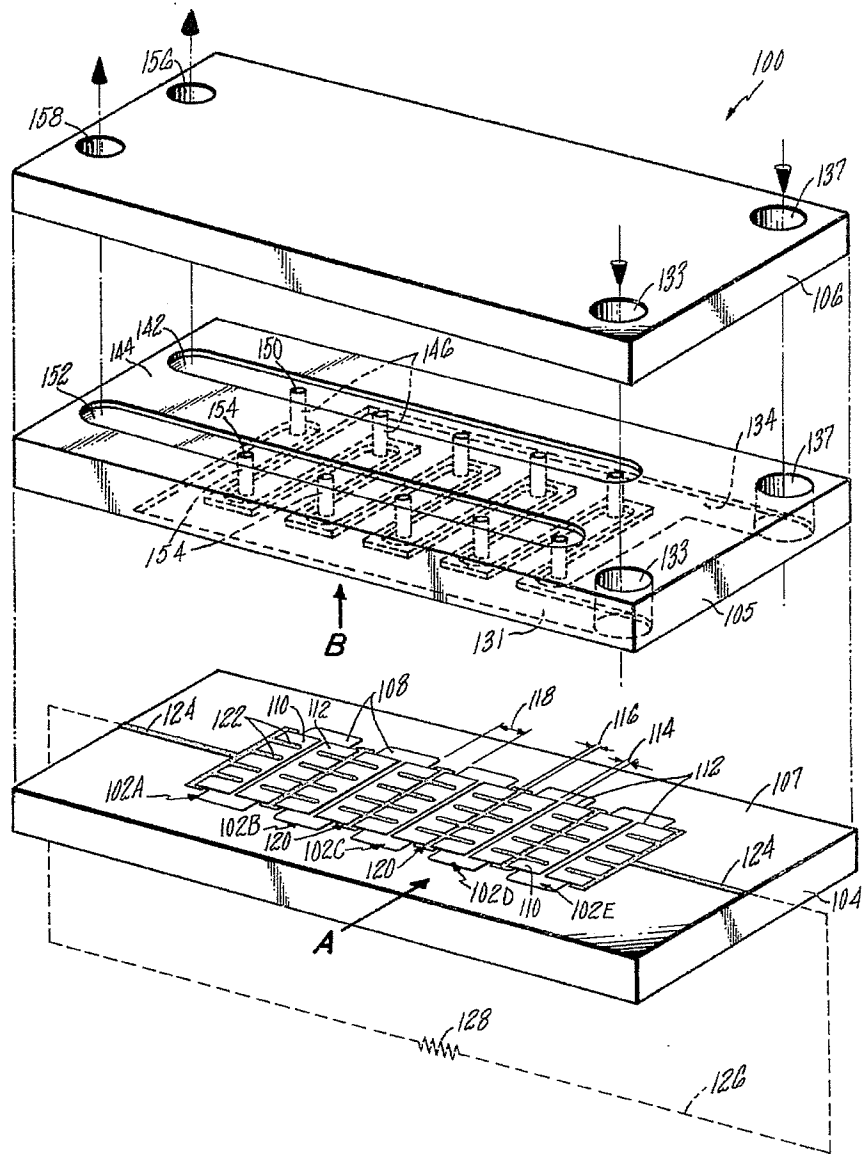


FIG. 2

FIG. 3



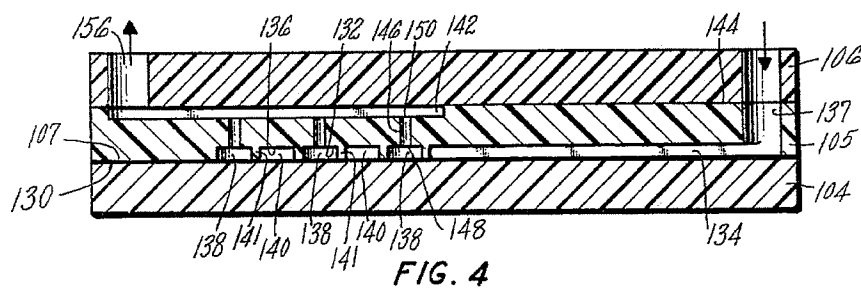
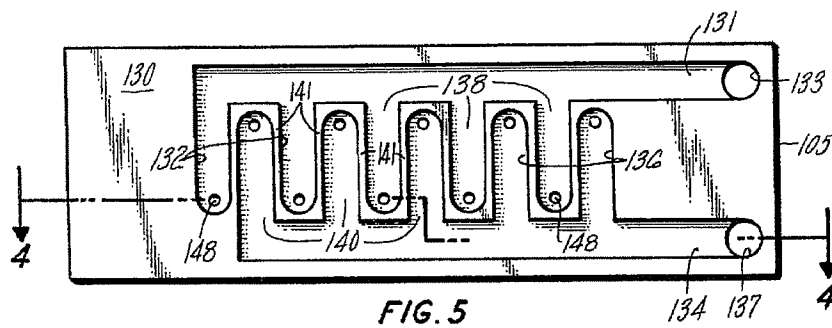
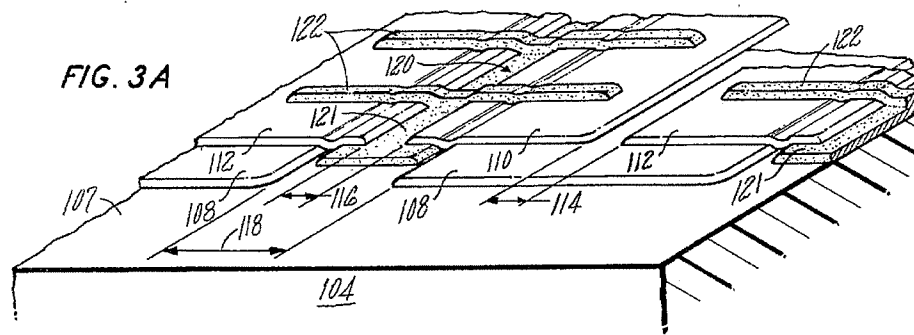
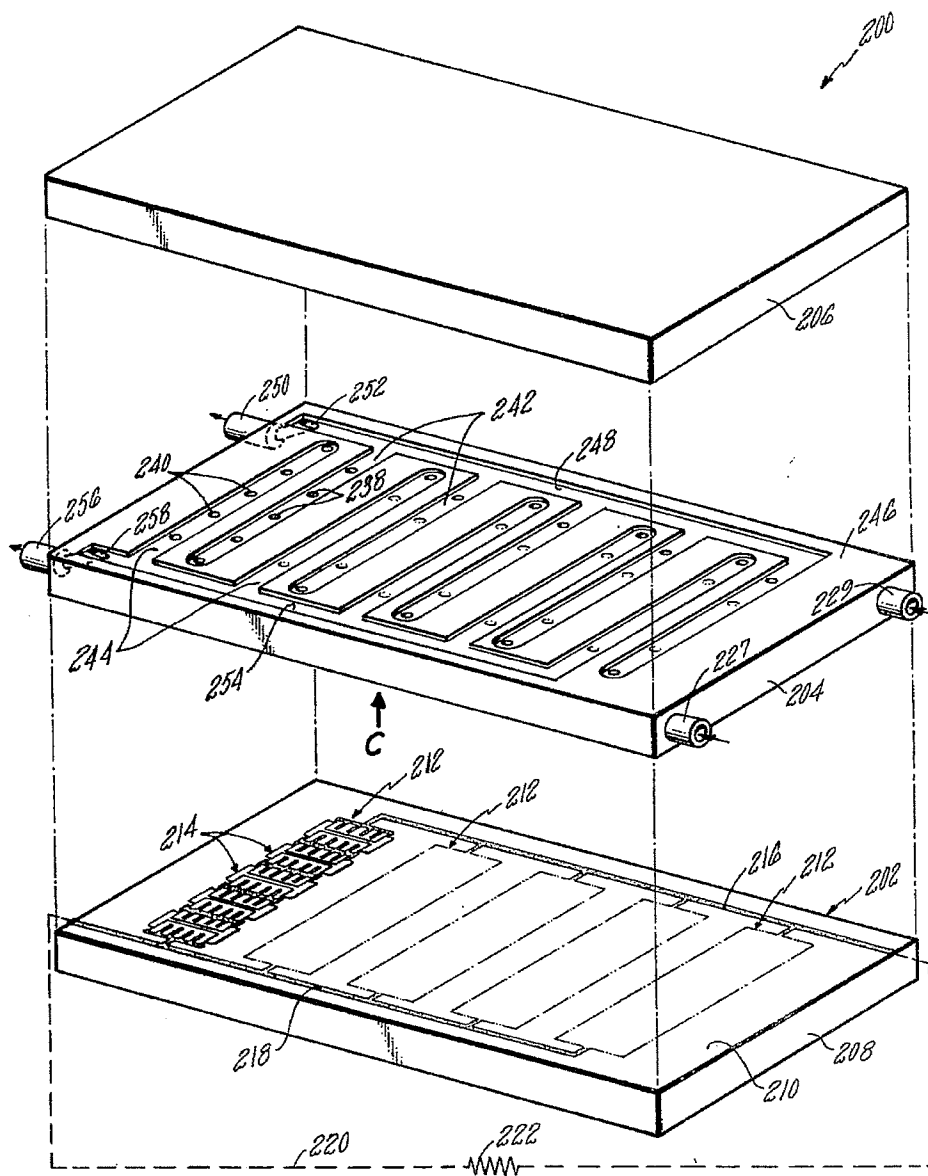
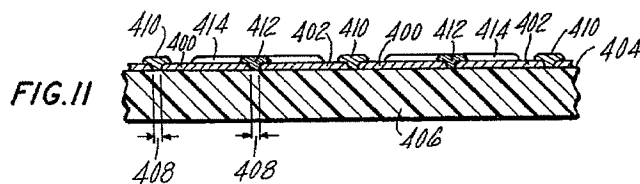
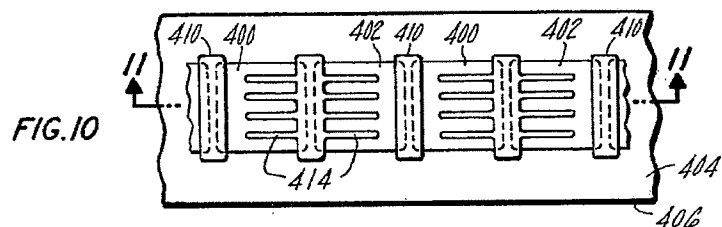
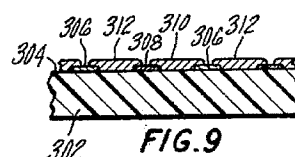
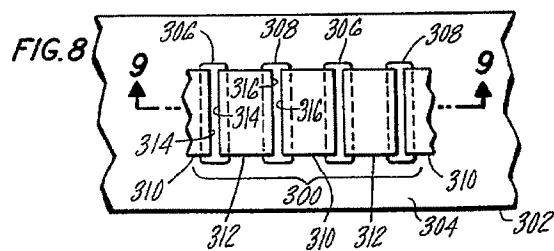
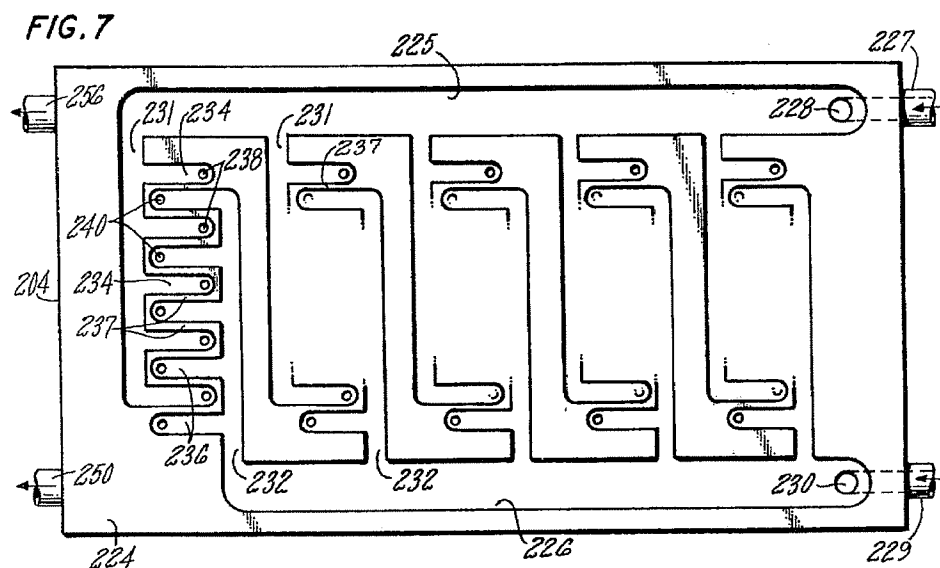
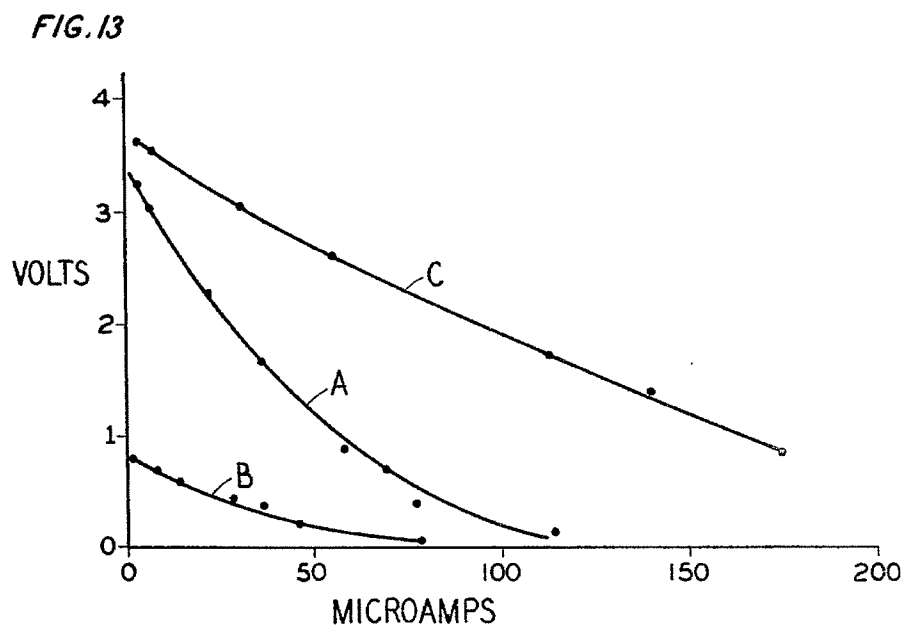
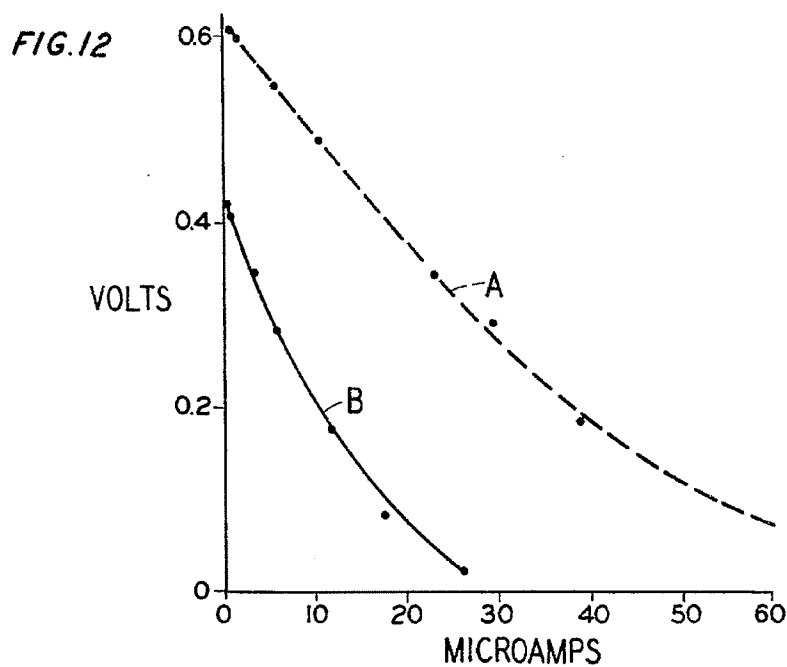


FIG. 6







SOLID ELECTROLYTE ELECTROCHEMICAL CELL

DESCRIPTION

1. TECHNICAL FIELD

The present invention relates to electrochemical cells, and, more particularly to electrochemical cells of simplified construction which utilize a solid electrolyte.

2. BACKGROUND ART

Electrochemical cells such as fuel cells are very old in the art. The basic components of an electrochemical cell are an anode electrode, a cathode electrode and an electrolyte. Using the fuel cell as an example, in the more conventional type fuel cell each electrode is a self-supporting sheet of electrically conducting material which includes a layer of catalytic material on one surface thereof or perhaps a catalytic material is distributed throughout the sheet. The surface of the anode and cathode electrode having the catalyst layer disposed thereon (or either surface if the electrode simply includes catalysts dispersed throughout) are arranged facing each other with the electrolyte disposed therebetween. The electrolyte may simply be a circulating liquid filling the space between the facing surfaces of the electrodes, or the liquid electrolyte may be disposed in a porous, nonelectrically conductive matrix which is sandwiched between the two electrodes. An example of the former type of fuel cell configuration is described in commonly owned U.S. Pat. No. 3,253,953. The latter type of cell is represented by commonly owned U.S. Pat. Nos. 4,017,664 and 4,129,685.

The electrolytes used in these types of cells may be either base electrolytes such as potassium hydroxide or acid electrolytes such as phosphoric acid. Other electrolytes which have been used are molten carbonate electrolytes, which are solid at room temperatures and liquid or molten at cell operating temperatures and materials (such as borophosphoric acid) which are gels at room temperature and at operating temperatures. For the most part, presently known good electrolytes of the types just described are very corrosive at cell operating temperatures, which severely limit the materials which can be used for other cell components.

Electrolytes which are solid at high temperatures have also been proposed and tested. They are described in detail in the book "Solid Electrolytes—General Principles, Characterization, Materials, Applications" edited by P. Hagenmuller and W. Van Gool, Academia Press, N.Y. (1978). One such electrolyte is doped zirconia ceramic. Zirconia is thermally and chemically stable at high temperatures and is not corrosive like many acid and base electrolytes. The book teaches that at temperatures greater than about 700° C. zirconia has excellent oxygen ion conductivity.

This same book also describes, at pages 447 and 448, a "thin-film" fuel cell concept, wherein a cell is constructed by overlaying, onto a porous substrate, a film of cathode catalyst material, followed by a film of doped zirconia electrolyte, followed by a film of anode catalyst material. Each film is stated as being 30–100 micrometers thick, forming a conventional sandwich type structure (with electrolyte in the middle) between 90–300 micrometers thick. The cell operates by feeding a gaseous fuel directly to the anode and by feeding the oxidant to the cathode catalyst layer through the porous substrate. As with other prior art cells, the electrolyte serves as a gas barrier between the oxidant on one side

of the cell and the fuel on the other side. The requirement that the electrolyte be a gas barrier also severely restricts the materials which can be used as the electrolyte.

DISCLOSURE OF THE INVENTION

One object of the present invention is an electrochemical cell stack of simplified construction.

An additional object of the present invention is a fuel cell which is operable on an oxidant and fuel reactant gas mixture.

Another object of the present invention is an improved cell utilizing a solid electrolyte.

Yet another object of the present invention is an electrochemical cell which is operable efficiently at low temperatures.

Another object of the present invention is an electrochemical cell configuration suitable for high speed production methods.

According to one aspect of the present invention an electrochemical cell comprises thin, laterally spaced apart anode and cathode catalyst layers in close proximity to each other with a solid electrolyte bridging the gap between the catalyst layers to provide an ion conductive path from one layer to the other. Another aspect of the present invention is a plurality of these cells laterally disposed relative to each other and connected electrically in series.

As used in the foregoing statement of the invention and in the remainder of the specification and claims, "laterally" means "to the side" such that elements "laterally spaced apart" or "laterally disposed relative to one another" do not have surfaces (other than edge surfaces) facing one another.

One important feature of the present invention is the lateral spacing of the catalyst layers of each cell with the solid electrolyte interconnection between these layers such that ion conduction between the catalyst layers is substantially parallel to the surfaces of the catalyst layers. This is in contrast to all known prior art cells wherein the electrodes have their catalyst surfaces facing each other with the electrolyte disposed therebetween forming a sandwich-like structure; and ion conduction between electrodes is substantially perpendicular to the surfaces of the catalyst layers.

In one exemplary embodiment the cell components are thin layers of appropriate materials. For example, the electrolyte may be a thin layer of solid material disposed on a supporting inert substrate, and the catalyst layers (i.e., electrodes) may be thin layers of catalytic material applied to the surface of the electrolyte layer with a small gap between adjacent edges of the catalyst layers. Appropriate means are provided to feed reactant gases to the catalyst layers. An electrochemical reaction then occurs where each catalyst layer contacts the electrolyte layer; and ions of a suitable species are formed and are conducted via the electrolyte layer across the gap between the catalyst layers while electrons are released and flow from one catalyst layer to the other via a suitable external electrical interconnection.

With the anode and cathode catalyst on the "same side" of the cell, the role of the electrolyte as reactant gas barrier between the fuel and oxidant is eliminated by the present invention. This may permit the use of some materials as electrolyte which otherwise would be unsuitable. Furthermore, this permits (although it does not

require) the use of extremely thin and perhaps even monolayer electrolyte films.

In this description of the invention and in the appended claims the phrase "solid electrolyte" is used in its broadest sense to include any electrolyte which exhibits the mechanical properties of a solid as opposed to a liquid. In other words, "solid" means a material which retains its shape without the benefit of a container or a porous supporting matrix. It, therefore, includes materials which are generally considered gels. Also, a material may still be considered a solid electrolyte even if its mechanism of ion conduction is through a liquid medium or is aided by a liquid medium disposed on its surface or within its pores.

For best efficiency cells of small dimensions are preferred with catalyst layers having projected surface areas on the order of a square centimeter or less and most preferably even orders of magnitude smaller. The gaps between anode and cathode catalyst layers of a cell are also, preferably, correspondingly small. The idea is to minimize cell resistance losses by reducing the distance the ions must travel. The low cell resistance resulting from the small cell dimensions expands the number of materials which may be suitable as solid electrolytes. Along these same lines, electrolytes which had sufficient ionic conductivity only at very high temperatures in prior art cell constructions, may have adequate ionic conductivity at much lower temperatures when used in accordance with the teachings of the present invention, thereby further opening up the field of candidate electrolyte materials.

From the foregoing it is apparent that a cell of the present invention is intended to produce only a small current, perhaps measured in microamps. High voltage and power output is obtained by connecting a large number of cells in series to form a group of cells, with the cells laterally disposed relative to each other on a common supporting surface. A large supporting surface, such as a thin wafer, could accommodate many groups of series connected cells; and the groups may be electrically connected in parallel and series to form a cell stack which further multiplies the power output. These wafers may be stacked together and electrically interconnected to form a cell stack capable of producing virtually any desired power output. Photolithographic thin film technology as used in the semiconductor integrated circuit art, is contemplated as being usable in the manufacture of cells, cell-groups and cell stacks according to the present invention.

If the individual cells of a cell stack are large enough, manifolding means could be provided to feed the cathodes with an oxidant such as air and the anodes with a fuel such as hydrogen, keeping the two reactants separate from each other as in conventional cells. If the individual cells in a network of series and parallel connected cells are very small, it may not be physically possible or practical to keep the fuel and oxidant separate over the individual anode and cathode catalyst layers. In that case the fuel and oxidant would be fed as a mixture over the catalyst layers of all the cells. It may be that the reactants would have to be diluted to prevent autoignition in the presence of the catalysts; or, instead, the catalysts may be appropriately selective to the oxidation of hydrogen or to the reduction of oxygen.

It is contemplated that cells of the present invention may be operable on fuels other than hydrogen (e.g., alcohols, hydrocarbons, and the like) and oxidants other

than oxygen (e.g., halogens, peroxides, oxides of nitrogen, and the like). Cells of the present invention may also be operated in the regenerative mode to accomplish energy storage.

BRIEF DESCRIPTION OF THE DRAWING

FIG. 1 is an exploded perspective view of a cell assembly in accordance with the present invention;

FIG. 2 is a cross-sectional view of the cell assembly of FIG. 1 taken along the line 2—2 of FIG. 1 and showing the cell elements with exaggerated thickness;

FIG. 3 is an exploded perspective view of a cell-group assembly in accordance with the present invention;

FIG. 3A is a perspective view taken in the direction A of FIG. 3 showing the cell elements with exaggerated thickness;

FIG. 4 is an offset cross-sectional view taken along the line 4—4 of FIG. 5;

FIG. 5 is a bottom view of the manifold plate of FIG. 3 taken in the direction B of FIG. 3;

FIG. 6 is an exploded perspective view of a fuel cell stack assembly according to the present invention;

FIG. 7 is a bottom view of the manifold plate of FIG. 6 taken in the direction C of FIG. 6;

FIG. 8 is a top, partial view of a cell-group disposed on a support according to an alternate embodiment of the present invention;

FIG. 9 is a cross-sectional view taken along the line 9—9 of FIG. 8 with the thickness of the cell elements being exaggerated;

FIG. 10 is a top, partial view of a cell-group disposed on a support according to yet another embodiment of the present invention;

FIG. 11 is a cross-sectional view taken along the line 11—11 of FIG. 10 with the thickness of the cell elements being exaggerated;

FIG. 12 is a graph showing performance curves for strontium ruthenate as an anode and then as a cathode catalyst, in each case the opposing electrode being a supported platinum catalyst; and

FIG. 13 is a graph showing performance curves for several different embodiments of the present invention.

BEST MODE FOR CARRYING OUT THE INVENTION

FIGS. 1 and 2 show a "mixed reactant" type fuel cell in accordance with an exemplary embodiment of the present invention. In a mixed reactant type cell, the fuel, such as hydrogen, and the oxidant, such as oxygen in the form of air, are mixed together and the mixture is fed to both the anode and cathode of the cell simultaneously via a common reactant gas space over the electrodes.

Referring to FIG. 1, a cell assembly 10 comprises a supporting plate 12 having a flat top surface 14. Disposed on and adhered to the surface 14 is a fuel cell 15 comprising a thin layer of solid electrolyte 16, and anode electrode 18, and a cathode electrode 20. The anode and cathode electrodes are disposed on and adhered to the surface of the electrolyte layer 16. The anode electrode 18 is simply a thin, gas porous, electrically conductive anode catalyst layer 22, and the cathode electrode 20 is simply a thin, gas porous, electrically conductive cathode catalyst layer 24. The anode and cathode catalyst layers are laterally spaced apart in close proximity to each other with a gap 26 being defined between the layers. A thin electrically conductive

layer 28 of metal paint is disposed along an edge of each catalyst layer 22, 24. Each electrically conductive layer 28 also includes fingers 30 of electrically conducting material extending over the surface of the catalyst layer and a narrow stripe 31 of electrically conducting material extending from the catalyst layer to the edge of the support plate 12. An external circuit 32 (shown dotted) including a load 33, electrically interconnects the two electrodes. A cover plate 34 mates with the top surface 14 of the support plate 12; and a cutout 36 in the bottom surface 38 of the cover plate defines a reactant gas space 40 (see FIG. 2) over the electrodes 18, 20. The cover plate 34 also includes a reactant gas inlet channel 42 and a reactant gas outlet channel 44, both in communication with the gas space 40.

FIG. 2 is a cross section through the cell assembly 10 of FIG. 1 with the electrolyte layer 16, the catalyst layers 22, 24, and the electrically conductive layers 28 drawn with greatly increased thickness for the purpose of clarity. In actuality these layers are like very thin layers of paint and may only be several micrometers thick, as will be hereinafter further described.

In operation the reactant gas mixture is passed through the cell assembly 10 in contact with the electrodes 18, 20, via the inlet channel 42, the gas space 40, and the outlet channel 44. Assuming that the electrolyte material is a proton conductor (although this need not be the case), at the anode electrode the fuel in the mixture (e.g., hydrogen) passes into the anode catalyst layer 18 and reacts electrochemically in the presence of the catalyst and electrolyte thereby generating electrons, protons, and heat. The electrons are conducted away from the anode electrode by the electrically conductive layer 28, and are conducted to the cathode electrode 20 via the external circuit 32. The ions are conducted to the cathode electrode 20 by the electrolyte layer 16 which provides an ion conductive path between the catalyst layers by bridging the gap 26 therebetween. At the cathode electrode 20 the oxidant in the reactant gas mixture (e.g., oxygen) electrochemically reacts with the ions and electrons from the anode electrode to produce water which leaves the cell as a vapor with the spent reactant gases via the outlet channel 44, the electron flow from one electrode to the other through the external circuit 32, is the useful electrical energy generated by the cell 15.

One advantage of the present invention, and the most obvious physical difference between the prior art and cells of the present invention, is that the anode and cathode electrodes are side by side with the electrolyte bridging the gap between adjacent electrode edges, rather than the electrodes being face to face with the electrolyte filling the volume between opposing surfaces of the electrode and acting as a reactant gas separator or barrier. The electrolyte in the present invention is truly only an ion conductor between the electrodes since its role as a reactant gas separator has been eliminated. This is also the case even if separate fuel and oxidant reactants are provided to the anode electrode and cathode electrode, as shown in other embodiments hereinafter to be described.

Another important feature and advantage of the present invention is the elimination of a "functional" substrate for the catalyst layers. In most cells of the prior art the catalyst layers of at least one and sometimes both electrodes are adhered to one side of a gas porous substrate. A reactant gas is fed to the other side of the substrate and must pass through it to react with the

catalyst layer and the electrolyte. In prior art cells using a liquid electrolyte there is the further complication of electrode flooding which requires the catalyst layer and perhaps the substrate to include wetproofing material, such as polytetrafluoroethylene. The result, in any case, is reduced effective surface area of the catalysts and increased difficulty in bringing the reactant gas into contact with both the catalyst and the electrolyte to effect the electrochemical reaction. These problems are eliminated by the present invention which uses a solid electrolyte, no wetproofing, and no porous catalyst supports. While the book "Solid Electrolytes" by Hagemuller et al referred to above describes, on pages 442 and 443, a solid electrolyte "sandwich" type cell with similar advantages, that cell is limited to a tubular configuration, which is an undesirable restriction and, more importantly, requires a structurally self-supporting electrolyte element which also must serve as a gas barrier.

One of the basic ideas behind the cell of the present invention is to minimize cell resistance and maximize catalyst effectiveness in a manner consistent with the ultimate objective (from a commercial point of view) of manufacturing a cost effective fuel cell stack having a useful power output. Reducing cell resistance is accomplished, in part, by minimizing the gap 26 between the electrodes, thereby reducing the distance the ions must travel to effect the electrochemical reaction. This makes the job of the electrolyte easier and permits the use of some materials as electrolytes which otherwise would not be considered to have sufficient ionic conductivity to be useful in fuel cells. In the alternative, some electrolytes which were only thought to have sufficiently high ion conductivity at high temperatures (e.g., zirconia at 700° C. and above) might now have sufficiently high ionic conductivity to be an effective fuel cell electrolyte at much lower temperatures and perhaps even at room temperature.

The present invention provides a unique opportunity to employ electrolytes which conduct primarily by surface ion conduction as opposed to the normal bulk ionic conduction. This is made possible by relieving the electrolyte of the gas separation requirement thus allowing the surface of a solid to interconnect the two electrodes. Ionic conduction in cells of the present invention is, however, not limited to surface ion conduction. Examples disclosed in this application may, in fact, function partially by bulk and partially by surface ionic conduction. It is not required that the exact type of conduction be known in order to practice this invention.

In the exemplary embodiment of FIGS. 1 & 2, the electrolyte is in the form of a thin layer. In that embodiment (and other embodiments using thin layers of electrolyte) it is preferred that the electrolyte layer be no greater than about 50 micrometers thick and most preferably less than 10 micrometers thick. It is not presently known what the lower limit of thickness is such that satisfactory ion conduction is still obtained. Satisfactory performance has been obtained with layers measured to be about 3 micrometers thick.

Notwithstanding the foregoing, a thick electrolyte layer, even thick enough to be self-supporting, could also be used in the present invention, but would not be expected to provide any improvement in cell performance (as compared to a thin film electrolyte) and is likely to be wasteful of material.

We have tested Baymal® alumina (a fibrillar boehmite alumina formerly manufactured by E. I. DuPont and more fully described in U.S. Pat. No. 2,915,475) as an electrolyte in fuel cells of the present invention and found it to work satisfactorily. Other materials which might make suitable electrolytes for use in the present invention are: hydronium β'' alumina, hydrogen uranyl phosphate, phosphomolybdic acid, and phosphotungstic acid. These other materials have been recently reported in the literature as being highly ion conductive in the solid state. Additional possible electrolyte materials are silica gel, alumina gel or the like.

Turning now to the electrodes, if the fuel and oxidant are separately manifolded to the anode and cathode electrodes, respectively, a conventional, electrically conductive fuel cell anode and cathode catalytic material, such as platinum or supported platinum, may be used for both catalyst layers. On the other hand, if mixed reactants are used, such as is the case in the embodiments shown in FIGS. 1 and 2, something must be done to cause an electrical potential to exist between the electrodes. For example, "selective" catalysts may be used for one or both electrodes. In this application a selective catalyst is one which, in the presence of mixed fuel and oxidant, will favor, to a significant extent, either the anode or cathode electrochemical reaction. Furthermore, as herein defined, to prevent ignition of the reactant mixture, a selective catalyst does not contribute to the direct chemical combination of the reactants.

Whether conventional or selective catalysts are utilized, it is preferred (although not required) that the catalyst layer be an intimate mixture of the catalytic material and the electrolyte material. This brings the electrolyte material and the catalyst material into intimate contact thereby improving the catalyst/electrolyte/reactant gas interaction during cell operation. The electrolyte may also serve as a binder for the catalyst layer. Some catalysts which may be used to selectively reduce oxygen are: strontium ruthenate (SrRuO_3) and lanthanum manganate (LaMnO_3). A catalyst which is selective to the oxidation of hydrogen is lanthanum cobalt ruthenate [$\text{La}(\text{CO}_{0.5}\text{Ru}_{0.5})\text{O}_3$].

Alternatively, a catalyst layer can be covered with a film or layer or material which is selective to (i.e., favors) the diffusion therethrough of the particular gas to be reacted at the electrode. A selective diffusion layer of this type does not have to be 100% selective to be effective. In other words, it does not have to completely exclude the other gases in the mixture. For example, some materials known to be selective to the diffusion of hydrogen are: nylon, polysulfone, polytrifluorochloroethylene and polypropylene.

A fuel cell like that shown in FIGS. 1 and 2 was built and tested. The support plate 12 and the cover plate 34 were made from 3.2 mm thick acrylic sheet. The electrolyte layer 16 was made from a fine powder of Baymal alumina. This fine powder disperses readily in water to form a colloidal dispersion. In this example we made a dispersion. In this example we made a dispersion comprising 5%, by weight, Baymal alumina in water. Using a small brush a film of this dispersion was applied to the surface 14 and was immediately exposed to ammonia vapor which caused the film to gel. This gel was allowed to dry at room temperature resulting in a solid film having a typical thickness of about 3.0 micrometers.

The catalyst layers 22, 24 were applied to the electrolyte layer 16 in such a manner that a long edge of one layer was parallel to a long edge of the other layer with a gap 26 therebetween on only 0.3–0.4 millimeter. The anode catalyst layer 22 was prepared by dispersing 1.0 gm platinum supported on carbon (a conventional fuel cell catalyst) and 0.5 gm Baymal alumina in 9.5 gm water. The solids were allowed to settle out for several hours and the clear liquid was decanted. The remaining wet paste, which had a consistency of poster paint, was painted onto the electrolyte layer 16 as a rectangle about 2.0 cm long, 0.5 cm wide and 5 micrometers thick (after drying). The finished anode catalyst layer was an intimate mixture of supported platinum and Baymal alumina electrolyte.

The cathode catalyst layer was prepared by dispersing 0.45 g strontium ruthenate in 30 ml of a 5% (by weight) aqueous solution of Baymal alumina. The solids were allowed to settle out for several hours and the clear liquid was decanted. The remaining wet paste was painted onto the electrolyte layer 16 as a rectangle 2.0 cm long, 0.5 cm wide, and 5 micrometers thick (after drying). The finished cathode catalyst layer was an intimate mixture of strontium ruthenate and Baymal alumina electrolyte.

Strontium ruthenate was chosen as the cathode catalyst because tests showed it to be selective to the reduction of oxygen. The selective catalytic performance of strontium ruthenate was determined by comparing it to the catalytic performance of a platinum catalyst layer in a cell of the type just described, except that the hydrogen and oxygen reactant gases over the catalyst layers were kept separate by suitable barrier means. First the strontium ruthenate was tested as a cathode by feeding 100% oxygen to it while feeding 100% hydrogen to the supported platinum catalyst layer. The curve A in the graph of FIG. 12 shows voltage versus current for varying resistive loads with strontium ruthenate as the cathode. The reactant flows were then reversed such that the strontium ruthenate was the anode. Curve B in FIG. 12 shows voltage versus current for varying resistive loads with strontium ruthenate as the anode. From the graph it can clearly be seen that strontium ruthenate has a significantly higher degree of catalytic activity as a cathode for the reduction of oxygen than it has as an anode for the oxidation of hydrogen.

The electrically conductive layer 28 was silver paint of the type generally used on printed circuit boards. It, too, was applied by hand using a small brush. The layer had a typical thickness of about 10 micrometers. It is estimated that the layer 28, including the fingers 30, covered about 10–15% of the surface area of each electrode. It is believed that this did not have a serious effect on cell performance. Note, however, that care must be taken not to cover too much of the catalyst surface area to assure that reactant gases have essentially complete access to catalyst areas.

To prevent reactant gas from leaking from the gas space 40 between the mating faces of the plates 12, 34, a thin layer of Fluorolube® grease (a fluorocarbon-based product having the consistency of petroleum jelly and manufactured by Hooker Chemical Corp.) was applied to the mating surfaces surrounding the electrolyte layer 16. Clamps were used to hold the plates in gas sealing relationship during the tests hereinafter described.

The foregoing cell was run at room temperature on a reactant gas mixture comprising air and an equal

amount (by volume) of 4% hydrogen in nitrogen. A diluted fuel gas was used to ensure the gas mixture could not ignite during the test. The reactant gas mixture was humidified to the extent of room temperature saturation prior to passing it through the cell by bubbling it through some water. It is believed that the surface ion conduction hereinbefore referred to takes the form of hydronium ion (H_3O^+) migration, and the water vapor enhances the ion current flow through the cell by combining with the hydrogen ions to form hydronium ions at the anode catalyst/electrolyte interface. The flow rate through the cell was maintained substantially constant at about 15 ml per minute. The results of the test, which continued for about 3 days, is displayed in Table 1 below. It took the cell about an hour to stabilize at an open circuit voltage of about 0.67 volts, and results prior to this time are not reflected in the table.

TABLE 1

Resistance (10000 Ω)	Voltage (volts)	Current (microamps)
1000.	0.507	0.51
470.	0.388	0.82
100.	0.166	1.66
47.	0.089	1.89
15.	0.031	2.1
10.	0.023	2.3
4.7	0.010	2.1
1.0	0.003	3.0

From Table 1 it is clear that a measurable amount of power was produced by the test cell despite the fact that only the cathode was a selective catalyst.

FIGS. 3 thru 5 show yet another embodiment of the present invention. The drawing depicts a cell-group assembly 99 comprising a cell stack component 100 and reactant manifold means 101. The cell stack component 100 comprises a "cell-group" of five cells labeled 102A thru 102E and a self-supporting substrate or support plate 104. A cell-group is a plurality of cells laterally disposed relative to each other and connected electrically in series. The manifold means 101 comprises a manifold plate 105 and a top plate 106. The five cells 102A thru 102E are disposed on the flat top surface 107 of the support plate 104. Each of the cells is similar in construction to the cell described with respect to FIGS. 1 and 2. Thus, referring to FIG. 3, each cell comprises an electrolyte layer 108, an anode catalyst layer 110, and a cathode catalyst layer 112. The catalyst layers within each cell are laterally spaced apart and in close proximity to each other on the surface of their respective electrolyte layers 108. A gap 114 separates the catalyst layers within a cell. Each cell 102A thru 102E is adjacent at least one other of the cells such that the cathode catalyst layer of one cell of each adjacent pair is in close proximity to but laterally spaced from the anode catalyst layer of the other cell of that pair. A space 116 (approximately the same width as the gap 114) is shown in the drawing as separating these catalyst layers. Gaps 118 separate the electrolyte layers 108 of adjacent cells to prevent ionic short circuits. The cells 102A thru 102E are connected electrically in series by bridging the spaces 116 with a layer 120 of electrically conductive material.

The spacial relationship between the various layers is best seen in FIG. 3A taken in the direction A of FIG. 3 wherein the thicknesses of the various cell layers are exaggerated for clarity. Note that each layer 120 includes a narrow stripe 121 of material under the adja-

cent catalyst edges and is somewhat wider than the gap between the catalyst edges. The stripes 121 are narrower than the gaps 118 such that the stripes 121 do not provide any electrical interconnection between adjacent electrolyte layers 108. A plurality of fingers 122 extend over the surfaces of the catalyst layers and interconnect with the stripes 121 along the gaps 116 for the purpose of providing improved electrical communication between the cells. The electrically conductive layers 120 of end cells 102A and 102E each include a narrow stripe 124 of electrically conductive material leading to an edge of the plate 104. These stripes 124 are interconnected by an external circuit 126 which includes a load 128.

Referring to FIGS. 4 and 5, machined into the bottom surface 130 of the manifold plate 105 is a fuel manifold channel 131 with a plurality of individual fuel channels 132 extending perpendicularly therefrom over each anode catalyst layer 110. A cylindrical fuel inlet passage 133 (FIG. 3 and FIG. 5) passes upwardly through both the plates 105 and 106 and communicates with the right-hand end of the fuel manifold channel 131. Also machined into the bottom surface 130 of the plate 105 is an oxidant manifold channel 134 with a plurality of individual oxidant channels 136 extending perpendicularly therefrom over each cathode catalyst layer 112. A cylindrical oxidant inlet passage 137 (FIG. 3 and FIG. 5) passes upwardly through both the plates 105 and 106 and communicates with the right-hand end of the oxidant manifold channel 134. The individual fuel channels 132 define separate fuel gas spaces 138 over each anode catalyst layer; and the individual oxidant channels 136 define separate oxidant gas spaces 140 over each cathode catalyst layer. Walls 141 in the plate 105 separate adjacent fuel and oxidant gas spaces and extend, alternately, along the gaps 114, 116 in sealing contact with the surfaces of the electrolyte layers 108 and the electrically conductive layers 120, respectively.

Associated with the individual fuel gas spaces 138, is a common fuel exhaust manifold channel 142 machined into the top surface 144 of the manifold plate 105. Cell fuel exhaust holes 146 drilled through the manifold plate 105 have their inlet ends 148 opening into their respective fuel gas spaces 138 and their outlet ends 150 opening into the exhaust manifold channel 142. Similarly, an oxidant exhaust manifold channel 152 (FIG. 3) in the top surface 144 of the manifold plate 105 communicates with the individual oxidant gas spaces 140 via cell oxidant exhaust holes 154 (FIG. 3) through the manifold plate 105. A cylindrical fuel outlet passage 156 and oxidant outlet passage 158 drilled through the top plate 106 communicate, respectively, with the left-hand end of the fuel exhaust manifold channel 142 and oxidant exhaust manifold channel 152. The three plates (shown in assembled relationship in the offset cross section of FIG. 4) are secured together by any suitable means such as bolts or clamps, not shown. As with the embodiment of FIGS. 1 and 2, a fluorocarbon base grease is applied to the mating surfaces of the plates to prevent gas leakage from the various manifolds and gas spaces formed between the plates.

A cell stack assembly comprising a five-cell cell-group like that shown in FIGS. 3 thru 5 was built and tested. Plates 104, 105, and 106 were made from acrylic sheet 3.2 mm thick. The electrolyte layers 108 were made from Baymal alumina, the same material as used in the single cell test described above and were applied in

the same manner. In this example the electrolyte layer had an estimated thickness of about 3 micrometers. Its area was large enough to accommodate the greater part of both catalyst layers hereinafter described. The gap 118 between adjacent electrolyte layers was about 3.2 mm wide. After applying the electrolyte layers to the support plate a stripe 121 of electrically conductive silver paint 1.5–2.0 mm wide and about 10 micrometers thick was painted along the gaps 118 between the electrolyte layers but not touching the electrolyte layers so as not to provide an electrical interconnection therebetween.

Since the fuel and oxidant were kept separated, the same material was used for both the anode and cathode catalyst layers 110, 112. In this embodiment they were made from the same material (i.e., an intimate mixture of Baymal alumina and carbon supported platinum) as the anode catalyst layer in the single cell example hereinabove described. The catalyst layers were also prepared and applied by the same method as described for that previous example. In this cell-group each catalyst layer was a rectangle about 8 mm long and 5 mm wide. Its thickness was about 5 micrometers. The catalyst layers were applied to the electrolyte layers in such a manner that each long edge of each catalyst layer was parallel to a long edge of the adjacent catalyst layer, and one edge of each catalyst layer overlaid one of the metallic paint stripes 121 which had been applied along the gaps between electrolyte layers. Within each cell the gap 114 was about 0.4 millimeter. The space 116 between the catalyst layers of adjacent cells was also about 0.4 millimeter. The silver paint fingers 122 were then painted onto the surface of the catalyst layers, interconnecting with the silver paint stripes 121 exposed between the catalyst layers. It is estimated that the fingers 122, covered about 10% of the surface area of each catalyst layer.

In a test the foregoing cell stack component was run at room temperature using pure hydrogen as the fuel and pure oxygen as the oxidant, both humidified to the extent of room temperature saturation. The hydrogen was introduced into the cells via the fuel inlet passage 133 at a flow rate of about 14 ml per minute, and was distributed to the fuel gas spaces 138 over the anode catalyst layers 110 via the fuel manifold channel 131. Spent fuel left each cell via the exhaust holes 146 leading to the fuel exhaust manifold channel 142, and from that channel left the cell stack component via the fuel outlet passage 156. Similarly, the oxygen was introduced into the cell stack component at a flow rate of about 3 ml per minute via the oxidant inlet passage 137, whereupon it was distributed to the oxidant gas spaces 140 over the cathode catalyst layers 112. Spent oxidant left the cells via the oxidant exhaust holes 154, and exited the cell stack component via the oxidant outlet passage 158.

The results of the test are shown in FIG. 13 as performance curve A.

A single cell of the same size and configuration as the cells of the five-cell cell-group was also tested under the same operating conditions. The results of that test are displayed in FIG. 13 as performance curve B. A comparison of curves A and B demonstrate the voltage additive effect of electrically connecting cells of the present invention in series.

Turning now to FIGS. 6 and 7, a fuel cell stack 200 is shown. The stack 200 includes a cell stack component 202, a manifold plate 204, and a top plate 206. The cell

stack component 202 comprises a support plate 208 having disposed on the top surface 210 thereof five cell-groups 212 each consisting of five cells 214. Each cell-group 212 is identical to the five-cell cell-group described with respect to FIGS. 3 thru 5. Reactant gas manifolding for feeding and removing reactant gases from each cell-group 212 is also very similar to that described with respect to the embodiment of FIGS. 3 thru 5. The cell-groups 212 are connected electrically in parallel by thin stripes 216, 218 of electrically conductive paint, and are connected to an external circuit 220 which includes a load 222.

Referring to FIG. 7 (which is a view taken in the direction C of FIG. 6), the bottom surface 224 of the manifold plate 204 includes a main fuel manifold channel 225 and a main oxidant manifold channel 226 machined therein. Fuel enters the stack 200 via a conduit 227 in communication with the main fuel manifold channel 225 via a passageway 228 through the manifold plate 204. Oxidant enters the stack 200 via a conduit 229 which is in communication with the main oxidant manifold channel 226 via a passageway 230 through the plate 204. The main fuel manifold channel 225 feeds fuel to a plurality of fuel header channels 231 which are functionally the same as the channel 131 of FIG. 5. The main oxidant manifold channel 226 feeds oxidant to oxidant header channels 232 which are functionally the same as the channel 134 of FIG. 5. Each header channel 231, 232 is associated with one of the cell-groups 212. Each fuel header channel 231 feeds fuel to individual fuel channels 234 which define separate fuel gas spaces over the anode catalyst layers of a cell-group 212. Similarly, oxidant header channels 232 feed oxidant to individual oxidant channels 236 which define separate oxidant gas spaces over the cathode catalyst layers of a cell-group. Walls 237 act as gas barriers or separators between the fuel and oxidant gas spaces. Spent reactant gases leave each cell via fuel exhaust holes 238 and oxidant exhaust holes 240 drilled through the manifold plate 204 and which lead, respectively, to fuel exhaust channels 242 and oxidant exhaust channels 244 machined into the top surface 246 of the manifold plate 204. The exhaust channels 242, 244 are functionally the same as the fuel exhaust manifold channel 142 and oxidant exhaust manifold channel 152, respectively, of the embodiment of FIGS. 3 thru 5. The fuel exhaust channels 242 empty into a fuel exhaust header channel 248 and leave the stack via a conduit 250 which is in communication with the header channel 248 via a passageway 252. The spent oxidant empties into an oxidant exhaust header channel 254 and leaves the stack via a conduit 256 which is in communication with the header channel 254 via a passageway 258.

A twenty-five cell stack virtually identical to that shown in FIGS. 6 and 7 was built and tested. Each cell-group and the individual cells therein were substantially identical in both materials, size, and method of construction as the single five-cell cell-group built and tested as described above. Test conditions, including reactant gas compositions and flow rates, were also the same as for the single five-cell cell-group test described above.

The results of that test are displayed in FIG. 13 as performance curve C. The amount of oxygen and hydrogen available to the cells using the same flow rates as indicated above for the single five-cell cell-group was determined to be well in excess of that required to generate the observed current. A comparison with curve A

clearly shows the current additive effect of connecting cell-groups in parallel.

Although not shown, it is contemplated that a larger cell stack with greater power output could be made by stacking together, one atop the other, and electrically interconnecting several stacks 200.

In the cells of all the foregoing examples the catalyst layers are disposed, in major part, on the surface of the electrolyte layer which, in turn, is disposed on the surface of a substrate or support plate. FIGS. 8 thru 11 show two other examples of cell-group configurations considered to be within the scope of the present invention. In FIGS. 8 and 9, part of a cell-group 300 is shown disposed on a nonconductive, inert support plate 302. The cell-group 300 is formed by applying narrow stripes or layers 306 of solid electrolyte to the surface 304 of the support plate, alternating with narrow stripes or layers 308 of electrically conductive material. Anode catalyst layers 310 and cathode catalyst layers 312 are then applied to the surface 304 of the support plate 302. Each catalyst layer is applied with one of its long edges 314 overlying a stripe 306 of electrolyte material, and its other long edge 316 overlying a stripe 308 of electrically conductive material. Note that the central portion or each catalyst layer is disposed directly on the surface 304.

In the embodiments of FIGS. 10 and 11, the anode and cathode catalyst layers 400, 402, respectively, are applied to the surface 404 of an inert support plate 406. Gaps 408 between adjacent catalyst layers are alternately bridged by stripes or thin layers of electrolyte material 410 and electrically conductive material 412. Fingers 414 of electrically conductive material extending outwardly from the electrically conductive stripes 412 are then applied to the surfaces of the catalyst layers to improve electrical conductivity.

The several embodiments shown in the drawing and described in the specification are only exemplary and should not be construed as limiting that which the inventors believe to be their invention. It should be understood by those skilled in the art that various changes and omissions in the form and detail of these embodiments may be made without departing from the spirit and the scope of the invention.

Having thus described typical embodiments of our invention, that which we claim as new and desire to secure by Letters Patent of the United States is:

1. A plurality of electrochemical cells for the production of electricity from a gaseous fuel and a gaseous oxidant, each cell comprising:
 - an anode electrode comprising a thin layer of anode catalyst adapted to electrochemically oxidize a gaseous fuel;
 - a cathode electrode comprising a thin layer of cathode catalyst adapted to electrochemically reduce a gaseous oxidant, said anode and cathode catalyst layers being laterally spaced apart and in close proximity to each other with a gap being defined between said layers;
 - means for feeding a gaseous fuel to said anode electrode and a gaseous oxidant to said cathode electrode and for removing spent fuel and oxidant from said cells; and
 - solid electrolyte means comprising electrolyte material bridging said gap between said anode and cathode catalyst layers to provide an ion conductive path therebetween, wherein said cells are laterally disposed relative to each other, each of said cells being

adjacent at least one other of said cells, the cathode catalyst layer on one cell of each adjacent pair of cells being in close proximity to the anode catalyst layer of the other cell of said same adjacent pair of cells with a space being defined between said last mentioned anode and cathode catalyst layers, and electrically conductive material bridging said spaces and connecting said plurality of cells electrically in series to form a cell-group.

2. The electrochemical cells according to claim 1 wherein said electrolyte means is a thin layer of solid electrolyte.

3. The electrochemical cells according to claim 2 wherein each of said cells includes a substrate having a surface, and said thin layer of electrolyte is disposed on said surface, said anode catalyst layer and said cathode catalyst layer each being at least partly disposed on said layer of electrolyte.

4. The electrochemical cells according to claim 3 wherein said anode and cathode catalyst layers each comprise an intimate mixture of catalytic material and said electrolyte material.

5. The electrochemical cells according to claim 2 wherein said thin layer of solid electrolyte is less than 50 micrometers thick.

6. The electrochemical cells according to claim 5 wherein said catalyst layers are less than 50 micrometers thick.

7. The electrochemical cells according to claim 2 wherein said thin layer of solid electrolyte and said thin anode and cathode catalyst layers are all less than 10 micrometers thick.

8. The electrochemical cells according to claim 7 wherein the projected surface area of each of said anode and cathode catalyst layers is less than about 1.0 cm².

9. The electrochemical cells according to claim 7 wherein said means for feeding said gases to said electrodes includes means defining a common reactant gas space over said electrodes for the feeding of a gaseous mixture of the fuel and oxidant to said electrodes.

10. The electrochemical cells according to claim 9 wherein said anode electrode comprises means for selectively oxidizing the fuel of the gaseous mixture, and said cathode electrode comprises means for selectively reducing the oxidant of the gaseous mixture.

11. The electrochemical cells according to claim 9 wherein said anode catalyst layer is selective to the reduction of hydrogen and said cathode catalyst layer is selective to the reduction of oxygen.

12. The electrochemical cells according to claim 9 wherein at least one of said electrodes of each of said cells includes a selective gas diffusion film covering said catalyst layer of said electrode, said film being selective to the diffusion of hydrogen if covering said anode catalyst layer and selective to the diffusion of oxygen if covering said cathode catalyst layer.

13. The electrochemical cells according to claim 1 wherein said electrolyte means is a surface conducting solid electrolyte.

14. The electrochemical cells according to claim 1 wherein said means for feeding a gaseous fuel and a gaseous oxidant to said electrodes includes means defining a fuel gas space over said anode catalyst layers and means defining an oxidant gas space over said cathode catalyst layers, said fuel gas spaces being separate from said oxidant gas spaces, said means for feeding gases to said electrodes also including means for introducing an

15

oxidant to said oxidant gas space and means for introducing a fuel to said fuel gas space.

15. A cell-group according to claims 1, 2, 3, 4, 8; 9, 10, 12, or 14 including self supporting substrate means having a surface, the cells of said cell-group being disposed on said surface, said substrate means and said cell-group defining a cell stack component.

16. A plurality of cell-groups according to claim 15 including means electrically connecting said cell-groups to form a network of parallel and series connected cell-groups defining a cell stack, wherein said means for feeding a gaseous fuel and a gaseous oxidant to said electrodes includes reactant manifold means for feeding the gases to said cells and for removing spent gases from said cells.

17. The cell stack according to claim 16 comprising a plurality of electrically interconnected cell stack components.

18. A method for producing electricity from an electrochemical cell comprising a thin anode catalyst layer, a thin cathode catalyst layer laterally spaced from said anode catalyst layer and in close proximity thereto with a gap being defined between said layers, and solid electrolyte means comprising electrolyte material bridging

16

said gap to provide an ion conductive path therebetween, including the steps of feeding a gaseous fuel to said anode catalyst layer and a gaseous oxidant to said cathode catalyst layer and removing spent fuel and oxidant from said cell;

electrochemically oxidizing said gaseous fuel at said anode catalyst layer and electrochemically reducing said gaseous oxidant at said cathode catalyst layer.

19. The method for producing electricity according to claim 18 wherein said gaseous fuel and gaseous oxidant are fed as a gaseous mixture to a common reactant gas space over said anode and cathode catalyst layers, and said step of oxidizing includes selectively oxidizing said gaseous fuel, and said step of reducing includes selectively reducing said gaseous oxidant.

20. The method for producing electricity according to claims 18 or 19 wherein said gaseous fuel is hydrogen and said gaseous oxidant is oxygen.

21. The method for producing electricity according to claims 18 or 19 wherein said solid electrolyte is in the form of a layer less than 10 micrometers thick and said layers of anode catalyst and cathode catalyst are each less than 10 micrometers thick.

* * * * *

25

30

35

40

45

50

55

60

65

UNITED STATES PATENT AND TRADEMARK OFFICE
CERTIFICATE OF CORRECTION

PATENT NO. : 4,248,941

DATED : February 3, 1981

INVENTOR(S) : GEORGE A. LOUIS ET AL

It is certified that error appears in the above-identified patent and that said Letters Patent are hereby corrected as shown below:

Column 7, lines 60-61: Delete the sentence "In this example we made a dispersion."

Column 9, Table 1, first column: "Resistance (10000 Ω)"
should be --Resistance
(1000 Ω)--.

Column 12, line 58: "snple" should be --single--.

Claim 1, Column 14, line 2: "on" should be --of--.

Claim 18, Column 16, line 1: "providean" should be --provide
an--.

Signed and Sealed this

Seventh Day of July 1981

[SEAL]

Attest:

RENE D. TEGTMEYER

Attesting Officer

Acting Commissioner of Patents and Trademarks

EXHIBIT 2



US005102750A

United States Patent [19][11] **Patent Number:** **5,102,750****Taylor**[45] **Date of Patent:** **Apr. 7, 1992**[54] **EFFICIENCY ENHANCEMENT FOR
SOLID-ELECTROLYTE FUEL CELL**[75] **Inventor:** **Thomas M. Taylor, Flanders, N.J.**[73] **Assignee:** **Bell Communications Research, Inc.,
Livingston, N.J.**[21] **Appl. No.:** **629,220**[22] **Filed:** **Dec. 18, 1990**[51] **Int. Cl.⁵** **H01M 8/10**[52] **U.S. Cl.** **429/30; 429/44**[58] **Field of Search** **429/30, 34, 40, 44,
429/12**[56] **References Cited****U.S. PATENT DOCUMENTS**

4,248,941	2/1981	Louis et al.	429/13
4,863,813	9/1989	Dyer	429/33
4,894,301	1/1990	Dyer	429/193

4,988,582 1/1991 Dyer 429/30

Primary Examiner—Anthony Skapars*Attorney, Agent, or Firm*—Leonard Charles Suchyta;
Lionel N. White[57] **ABSTRACT**

In a solid-electrolyte fuel cell of the type described in U.S. Pat. No. 4,863,813, a permeable catalytic electrode in contact with the solid electrolyte is ordinarily exposed to a mixture comprising an oxidizer and a hydrogen-containing fuel. To increase the fuel efficiency of the cell, the permeable electrode is patterned and coated with a material that is permeable to the fuel but relatively impermeable to the oxidizer. The oxidizer enters the electrolyte through channels where the surface of the electrolyte is not covered by the patterned and coated electrode.

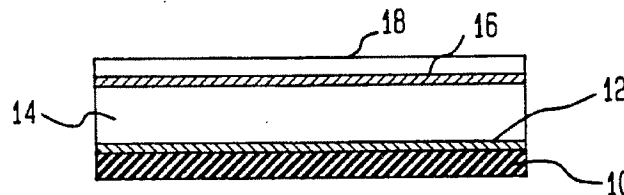
20 Claims, 2 Drawing Sheets

FIG. 1

(PRIOR ART)

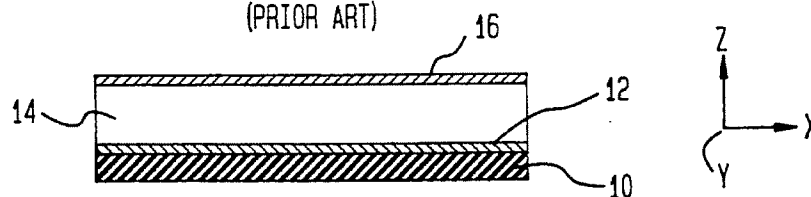


FIG. 2

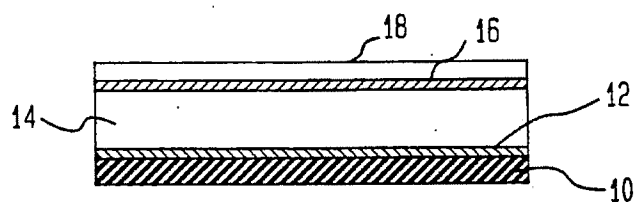


FIG. 3

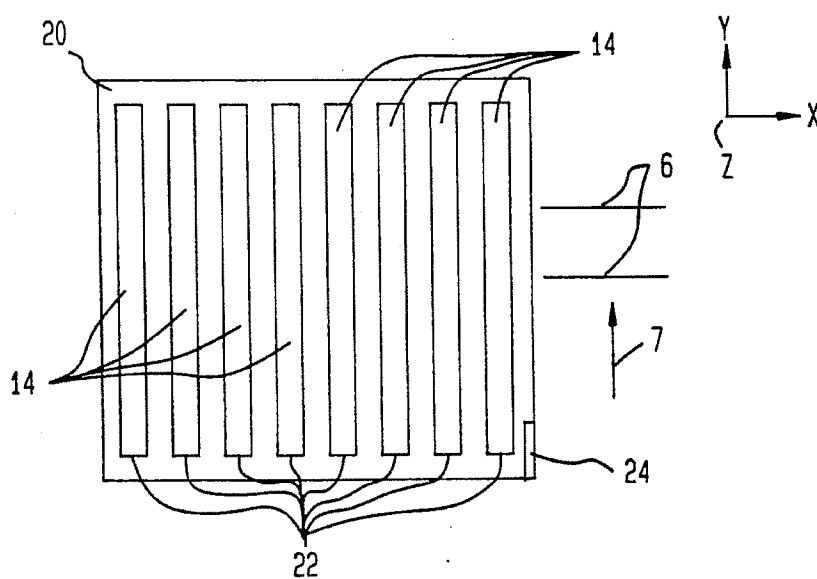


FIG. 4

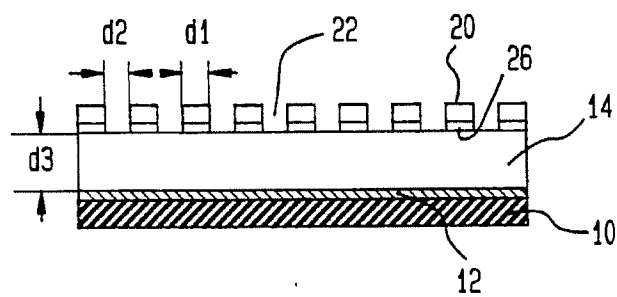
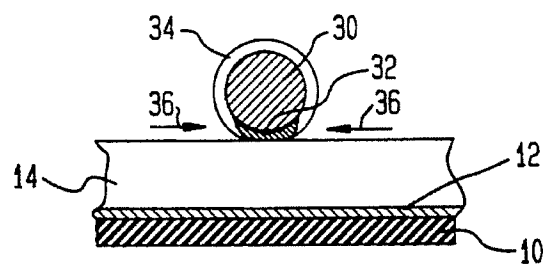


FIG. 5



EFFICIENCY ENHANCEMENT FOR SOLID-ELECTROLYTE FUEL CELL

BACKGROUND OF THE INVENTION

This invention relates to fuel cells and, more particularly, to cells which consume gaseous or liquid fuels and produce electrical energy.

An advantageous fuel cell for energy conversion is described in U.S. Pat. No. 4,863,813 (for which a reissue application, Ser. No. 552,800, was filed on July 13, 1990). In a cell of the type described therein, a hydrogen-containing material at room temperature, such as a gaseous mixture of hydrogen and oxygen, is directly converted to direct-current electrical energy and the only reaction product is water.

In one specific illustrative such cell, a submicrometer-thick gas-permeable ionically conducting membrane made of pseudoboehmite is deposited on an electrode that comprises a platinized impermeable substrate. This membrane constitutes the solid electrolyte of the cell. A layer, of platinum for example, is deposited on the top surface of the membrane to form the second electrode of the cell. The entirety of the second electrode is sufficiently porous (permeable) to allow the gas mixture to pass therethrough.

For a hydrogen/air mixture, such a cell provides useful current at an output voltage as large as about one volt, independent of the ratio of hydrogen to air for hydrogen > 50%. In practice, the efficiency of such a cell in converting the fuel mixture to electrical energy is impaired by a side reaction that occurs on the permeable electrode. In this side reaction, which accounts for about 90% of the fuel inefficiency of the cell, hydrogen and oxygen combine to form water. Only heat is produced in this side reaction. Nothing is thereby contributed to the electrical output of the cell.

Fuel efficiency is the single most important parameter that must be improved to upscale a basic cell of the aforespecified type to higher power levels. Such improvement would of course significantly increase the applications for which the cell would be regarded as an attractive energy source.

SUMMARY OF THE INVENTION

In accordance with the principles of the present invention, a fuel cell of the type specified above is modified to substantially reduce the amount of oxidizer in a fuel/oxidizer mixture that can contact the permeable electrode. At the same time, access is provided for the oxidizer to enter the solid electrolyte and migrate to the impermeable electrode. In this way, a fuel-consuming side reaction at the permeable electrode is substantially reduced and the fuel efficiency of the cell is consequently increased.

In a particular embodiment of the invention, the permeable electrode comprises multiple spaced-apart portions that are electrically connected together. These portions are coated with a material that is relatively permeable to the fuel but relatively impermeable to the oxidizer. The oxidizer enters the surface of the solid electrolyte mainly via the spaces between the electrode portions.

BRIEF DESCRIPTION OF THE DRAWING

A complete understanding of the present invention and of the above and other features and advantages thereof will be apparent from a consideration of the

detailed description below taken in conjunction with the accompanying drawing, not drawn to scale, in which:

FIG. 1 is a simplified schematic depiction in cross-section of a conventional fuel cell of the type described in the aforesaid Dyer patent;

FIG. 2, which shows a coating overlying the top electrode of the FIG. 1 cell, represents the initial step of a fabrication sequence designed to modify the FIG. 1 cell to form a specific illustrative embodiment of the principles of the present invention,

FIG. 3 is a top view of the FIG. 2 arrangement as further processed in accordance with the principles of the present invention to form a modified version of the FIG. 1 cell;

FIG. 4 is a side view of a section of the FIG. 3 cell between X-Z planes 6 as viewed in the direction of arrow 7;

and FIG. 5 is a simplified representation of a portion of another specific illustrative cell made in accordance with the principles of the invention.

DETAILED DESCRIPTION

In accordance with the principles of the present invention a basic fuel cell of the type described in U.S. Pat. No. 4,863,813 is modified to increase its fuel efficiency. A typical prior known such basic cell is depicted in FIG. 1.

A hydrogen-containing fuel/oxidizer mixture is utilized to power the cell shown in FIG. 1. Suitable fuels that are consumed by the FIG. 1 cell to produce electrical energy are hydrogen-containing materials such as hydrogen, methane and methanol. The fuel can be supplied to the cell in liquid or gaseous form.

Further, many suitable oxidizers or oxidizer species are available for combining with the fuel to provide a mixture suitable for powering the FIG. 1 cell. In practice, the most common oxidizers are gaseous oxygen and air.

The specific illustrative prior known cell shown in FIG. 1 comprises a substrate 10 that is designed to be impermeable to the mixture of fuel and oxidizer materials that is utilized to power the cell. By way of example, the substrate is made of quartz and is about 0.32 centimeters (cm) thick in the indicated Z direction.

A catalyst layer 12 (FIG. 1) overlies the top planar surface of the substrate 10. As described in U.S. Pat. No. 4,863,813, various materials are suitable for forming such a catalyst layer. Suitable materials include platinum, palladium, gold, nickel and various alloys of these materials. Other suitable catalyst materials include non-metals such as electronically conducting mixed oxides with a spinel or perovskite structure.

The catalyst layer 12 of FIG. 1 is, for example, about 1000-to-5000 nanometers (nm) thick. Due to the aforementioned impermeability of the substrate 10, none of the fuel/oxidizer mixture supplied to the depicted cell is able to pass through the layer 12 from the bottom side thereof. Thus, together the substrate 10 and the layer 12 constitute an impermeable electrode assembly. Alternatively, as described in U.S. Pat. No. 4,863,813, the layer 12 can be made sufficiently thick that it by itself is impermeable to the fuel/oxidizer mixture. In any case, the catalyst layer 12 of FIG. 1 constitutes one electrode of the depicted fuel cell.

As shown in FIG. 1, a layer 14 that comprises a solid electrolyte overlies the top surface of the catalyst layer

12. As described in detail in U.S. Pat. No. 4,863,813, the layer 14 is made of a material that is characterized by a usefully high conductivity for hydrogen ions (H^+) or hydronium ions (H_3O^+). Additionally, the layer 14 is permeable to the fuel, to the oxidizer and to products of the reaction between the fuel and oxidizer. Further, the layer 14 constitutes an electron insulator, with a resistivity of at least about 10^6 ohm-centimeters. Also, in preferred embodiments the solid electrolyte is capable of being made in very thin layers. Herein, for illustrative purposes, the Z-direction thickness of the layer 14 will be assumed to be about 0.5 micrometers (μm).

Two classes of solid-electrolyte materials are suitable for forming the layer shown in FIG. 1. One class consists of selected hydrated aluminum oxides. The other class consists of selected polymeric materials.

The physical properties and conditions for forming layers of hydrated aluminum oxide have been extensively studied. A review of many of these studies appears as Chapter 3 of "Oxides and Oxide Films", edited by J. W. Diggle and N. K. Vijh, volume 4, Marcer Dekker, New York, 1976, pages 169-253. Depending on the particular conditions, the product of the reaction between aluminum and water includes bohemite, pseudoboehmite, bayerite, gibbsite and combinations of these materials. One of these materials, pseudoboehmite, has been found to be particularly appropriate for inclusion in devices made in accordance with the invention. Layers including at least 50% pseudoboehmite are preferred, layers including at least 95% pseudoboehmite being most preferred.

Suitable permeable solid-electrolyte layers of hydrated aluminum oxide can be produced by several methods. For example, such a layer forms on a clean metallic aluminum surface exposed to water in liquid form in a container or exposed to water in vapor form in a chamber in a temperature range of about 20-to-374 degrees Celsius. Pseudoboehmite is predominant in layers produced in the temperature range from approximately 90-to-100 degrees Celsius. Solid-electrolyte layers can also be produced by exposing aluminum oxide to water and/or liquid vapor phases. The pseudoboehmite form is predominant in layers produced in the temperature range of about 90-to-100 degrees Celsius.

Suitable aluminum oxide layers can also be produced by anodization of metallic aluminum. Thicker layers can be produced by a multi-layer process that includes alternate steps of aluminum deposition and exposure of the aluminum or anodized aluminum surface to water. Radio-frequency backsputtering can be used during deposition of the metallic aluminum prior to water exposure. Such backsputtering can improve the uniformity of coverage of the aluminum and therefore also of the permeable solid-electrolyte layer.

The production of a hydrated aluminum oxide layer from an anodically formed aluminum oxide layer has the advantage that such a layer is characteristically of a very uniform thickness and can be grown precisely to a specified thickness. In the multilayer process comprising sequential aluminum depositions, solid-electrolyte layers of approximately 500 nm thickness have been produced with 3-to-5 sequential processing steps. More generally, hydrated aluminum oxide layers about 300 nm-to-10 μm thick are suitable for forming the solid-electrolyte layer 14 shown in FIG. 1.

Additionally, carbon-based polymeric materials are known which possess the required hydrogen ion conductivity, electronic resistivity and permeability to fuel,

oxidizer and products of the reaction between them. Perfluorinated sulfonic acid is an example of a polymer in which ionic hydrogen species can be readily mobilized. This supplies the necessary hydrogen ion mobility. Such polymers commonly have sufficient gas permeability and electronic resistance to be useful as solid electrolytes in assemblies made in accordance with the principles of the present invention.

One specific illustrative polymeric material suitable for forming the solid-electrolyte layer 14 (FIG. 1) is the commercially available perfluorinated sulfonic acid polymer known as Nafion. In practice, this material is much easier to use than pseudoboehmite because Nafion can be solution-cast to form thin layers in the range of about 1-to-10 μm .

Layers 16 shown in FIG. 1 overlies the top surface of the solid electrolyte 14. The layer 16 comprises a permeable catalyst made of a material such as, for example, platinum, palladium, gold, nickel or alloys of these materials. Other suitable catalytic materials include non-metals such as electronically conducting mixed oxides with a spinel or pervskite structure.

The layer 16 of FIG. 1 is permeable in the sense that it permits the fuel/oxidizer mixture to pass through it. Illustratively, this can be realized by sputtering a thin inherently porous layer, up to, for example, a thickness of about 100 nm, on the surface of the layer 14. For thicker layers that do not inherently exhibit the required porosity to the fuel/oxidizer mixture, the layer 16 can be rendered permeable by forming therein a pattern of through-apertures. The permeable layer 16 constitutes the other electrode of the depicted fuel cell.

Due to the fact that the topmost layer 16 of the priorly known cell shown in FIG. 1 is exposed to the fuel/oxidizer mixture, constituents of that mixture combine on the catalyst layer 16 to form water and produce heat. In this side reaction, fuel which otherwise would be available to contribute to the electrical output of the cell is consumed. This result and the heat that is produced in the process are undesirable consequences of the noted side reaction.

In accordance with the principles of the present invention, a more fuel-efficient cell that operates at lower temperatures than the FIG. 1 cell is provided. This is done by eliminating or substantially reducing the afore-described side reaction that occurs on the catalyst layer 16 shown in FIG. 1.

For illustrative purposes, parts of the cell depicted in FIG. 2 will be assumed herein to be identical to corresponding parts of the FIG. 1 cell. These parts are identified in FIG. 2 by the same respective reference numerals employed therefor in FIG. 1. Thus, the FIG. 2 cell also includes a substrate 10, a bottom catalyst layer 12, a solid-electrolyte layer 14 and a top catalyst layer 16.

One specific illustrative way of modifying the FIG. 1 cell to form an embodiment of the present invention involves the initial step of coating the entire top surface of the permeable electrode 16 with a layer 18, as indicated in FIG. 2. In accordance with the invention, the layer 18 is made of a material that is relatively permeable to the hydrogen-containing fuel contained in the fuel/oxidizer mixture supplied to the cell but relatively impermeable to the oxidizer in the mixture. Many materials exhibiting such selectivity are known.

Illustratively, the layer 18 shown in FIG. 2 comprises a coating about 0.1 μm thick made of a polymer material such as nylon, polysulfone, polytrifluorochloroethylene or polypropylene. Such materials are known to be

relatively permeable to hydrogen but relatively impermeable to oxygen.

Many conventional ways are known for forming the layer 18 of FIG. 2. Thus, for example, the layer 18 can be formed simply by dipping the electrode 16 in a solution containing one of the aforespecified polymers in suspension. Or the layer 18 can be formed in a standard plasma polymerization step.

Next, in accordance with the principles of the present invention, spaced-apart channels are formed in the FIG. 2 structure. The channels, which extend through both the polymer layer 18 and the electrode layer 16, are formed, for example, by conventional oblation, etching or microscratching techniques. A top view of the structure after formation of the channels is shown in FIG. 3.

In FIG. 3, the remaining portion of the layer 18 constituting a patterned coating having channels there-through is designated by reference numeral 20. Multiple channels 22 formed in the patterned layer 20 are shown in FIG. 3. As indicated earlier above, the channels 22 extend through both the layer 20 and the underlying electrode 16 (FIG. 2). Thus, the surfaces seen through the channels 22 of FIG. 3 are portions of the top surface of the solid-electrolyte layer 14.

In a fuel cell structure of the type described herein, electrical connections are made between the electrodes 12 and 16 and an external circuit. To facilitate making such a connection to the top electrode 16 of the FIG. 3 cell, it is advantageous to remove a portion of the patterned coating 20 to expose a surface region of the underlying electrode layer 16. Such an exposed region of the top surface of the layer 16 is shown in the lower right-hand corner of FIG. 3 and is designated by reference numeral 24.

In one specific illustrative embodiment of the principles of the present invention, the area of the top surface of the patterned coating 20 shown in FIG. 3 is approximately 55% of the area of the top surface of the unpatterned layer 18 (FIG. 2). Since the underlying electrode 16 is patterned identically to the coating 20 (except for the contact pad 24 defined in the lower right-hand corner of the coating 20), the area of the top surface of the patterned top electrode of FIG. 3 is also about 55% of the area of the top surface of the unpatterned electrode 16 represented in FIG. 2.

FIG. 4 is a side view of a section of FIG. 3 between planes 6 as viewed in the direction of arrow 7 of FIG. 3. The aforementioned patterned coating 20 and a correspondingly patterned electrode layer 26 are shown in FIG. 4, as are the channels 22.

Since the coating 20 of FIG. 4 is relatively permeable to hydrogen, hydrogen will pass through the coating 20 and reach the permeable electrode layer 26, as it does under normal operation of a priorly known uncoated cell. However, since the coating 20 is relatively impermeable to oxygen, little oxygen will pass through the coating 20 and reach the electrode layer 26. Hence, only a relatively small amount of oxygen is available at that catalytic surface, the layer 26, to combine with the fuel in a fuel-consuming side reaction to form water. Accordingly, most of the fuel that reaches the electrode layer 26 is available to be converted to hydrogen ions or hydronium ions which, in turn, propagate towards the bottom electrode 12.

The channels 22 shown in FIGS. 3 and 4 allow oxygen to enter and pass through the solid-electrolyte layer 14, thereby to be available at the lower electrode 12. Such availability of oxygen at the electrode 12 is essen-

tial. Oxygen combines with hydrogen ions or hydronium ions and electrons at the bottom electrode to form water, thereby completing the electrical-energy-producing electrochemical reaction that is characteristic of the depicted cell.

It is evident from FIG. 4 that both hydrogen and oxygen can pass into the solid-electrolyte layer 14 via the channels 22. As a result, some hydrogen fuel and oxygen will pass through the layer 14 and be available at the bottom electrode 12 to combine to form water in a side reaction. But in practice it has been determined that the fuel consumed in this side reaction is considerably less than that consumed at the top electrode of a priorly known cell of the type shown in FIG. 1.

In a specific illustrative embodiment of the present invention, the width d1 (FIG. 4) of the spaced-apart portions of the patterned coating 20 and the width d2 of the channels 22 are about equal to each other and are each approximately 0.1 μ m. In practice, for such dimensions and for a thickness d3 of the layer 14 of about 0.5 μ m, most of the surface area of the bottom electrode 12 is effective to catalyze the desired electrochemical reaction between hydrogen ions or hydronium ions and oxygen to produce water. Ideally, the dimensions d1 and d2 should be very small compared to the electrolyte thickness d3.

The particular fabrication sequence described above for making the correspondingly patterned layers 20 and 26 shown in FIG. 4 is illustrative only. Another feasible sequence for making such a structure involves first patterning the electrode layer 16 of FIG. 1 by conventional photolithographic techniques. The patterned layer 16 can then be coated with a polymer by standard electrophoresis to form the overlying layer 20 whose pattern will be identical to that of the layer 20.

FIG. 5 shows a portion of another specific illustrative embodiment of the principles of the present invention. In the FIG. 5 embodiment, a fine-gauge gauze mesh is utilized to form the top electrode assembly overlying the surface of the solid-electrolyte layer 14. A cross-section of one strand of such a mesh is shown in FIG. 5.

Illustratively, the strand shown in FIG. 5 comprises a wire 30 made of a material such as copper. One side of the wire 30 is coated with a layer 32 made of a catalytic material such as platinum. The entire surface of the wire 30, except for the portion on which the layer 32 is coated, is covered with a polymer 34. As in the previously described embodiments, the polymer 34 is designed to be relatively permeable to the fuel but relatively impermeable to the oxidizer supplied to the cell. Thus, fuel but only a relatively small amount of oxidizer directed at the mesh wire in the direction of arrows 36 will pass through the polymer 34 and be available on the layer 32. In that way, the amount of oxygen available to combine with fuel at the top electrode (layer 32) to form water in a non-electrical-energy producing side reaction is significantly reduced relative to that of priorly known cells.

Finally, it is to be understood that the various specific arrangements described herein are only illustrative of the application of the principles of the present invention. In accordance with these principles, numerous alternatives and modifications may easily be made by those skilled in the art without departing from the spirit and scope of the invention. For example, although emphasis above has been directed to uniform linear channels formed in the coating 18 and the electrode 16, it is apparent that a variety of other patterns are feasible.

Thus, the channels could be curved and non-uniform. Further, other patterns such as an array of holes would have the same effect. In any case, an essential property of the pattern formed in the electrode 16 is that it not disrupt the connectivity of all remaining area of the electrode to the contact pad 24 (FIG. 3).

Additionally, the coating 18 may be patterned to overlap the underlying patterned electrode. In that way, the sides as well as the tops of the patterned electrode portions can be protected from oxidizer impingement, thereby further reducing the aforespecified undesired side reaction.

What is claimed is:

1. A fuel cell comprising a first electrode assembly and a second electrode assembly separated by and in contact with a solid electrolyte body, wherein the first electrode assembly is permeable to a fuel and an oxidizer, the second electrode assembly is impermeable to the fuel and the oxidizer, and the solid electrolyte body consists essentially of an electron-insulating material which is also ionically conducting to at least a first ionic species and which material is permeable to the fuel, the oxidizer and products of electrochemical reactions of the fuel and the oxidizer,

wherein the improvement resides in that the first electrode assembly comprises spaced-apart portions that expose surface regions of said solid electrolyte body,

and a coating is disposed on the spaced-apart portions of said first electrode assembly, said coating comprising a material that is relatively permeable to the fuel but relatively impermeable to the oxidizer.

2. A cell as in claim 1 wherein said coating comprises a polymer material.

3. A cell as in claim 2 wherein said polymer material is selected from the group consisting of nylon, polysulfone, polytrifluorochloroethylene and polypropylene.

4. A cell as in claim 1 wherein the spaced-apart portions of said first electrode assembly comprise elongated portions that are parallel to each other.

5. A cell as in claim 4 wherein the widths of said elongated portions are approximately equal to each other.

6. A cell as in claim 5 wherein the widths of the channels between said elongated portions are approximately equal to each other.

7. A cell as in claim 6 wherein the widths of said elongated portions and the widths of said channels are approximately the same.

8. A cell as in claim 7 wherein the widths of said elongated portions and said channels are each approximately 0.1 μm .

9. A cell as in claim 8 wherein the thickness of said solid electrolyte body is approximately 0.5 μm .

10. A cell as in claim 1 wherein said species is ionic hydrogen.

11. A cell as in claim 10 wherein each of said first and second electrode assemblies comprises a material selected from the group consisting of platinum, palladium and alloys of platinum and palladium.

12. A cell as in claim 1 wherein said fuel and oxidizer are gaseous.

13. A cell as in claim 1 wherein said first-mentioned material consists essentially of a hydrated oxide of aluminum consisting primarily of the pseudoboehmite structure.

14. A cell as in claim 12 wherein said first-mentioned material is at least 50% of the pseudoboehmite structure.

15. A cell as in claim 12 in which the solid electrolyte body is from 30 Angstrom units to 10 μm in thickness.

16. A cell as in claim 1 wherein said first-mentioned material consists essentially of a carbon-based polymer.

17. A cell as in claim 15 wherein said carbon-based polymer comprises perfluorinated sulfonic acid.

18. A cell as in claim 1 wherein said oxidizer comprises a gas selected from the group consisting of oxygen and air, and said fuel comprises at least one member selected from the group consisting of hydrogen, methane and methanol.

19. A cell as in claim 1 wherein said first electrode assembly comprises a wire mesh having a catalytic material deposited on one side of said wire mesh in contact with said solid electrolyte body, the remainder of said wire mesh being covered with the coating that is relatively permeable to the fuel but relatively impermeable to the oxidizer.

20. A cell as in claim 1 wherein said second electrode assembly is a composite structure that comprises a layer of catalytic material that is permeable to the fuel and the oxidizer deposited on a substrate that is impermeable to the fuel and the oxidizer.

* * * * *

EXHIBIT 3

Single Chamber Solid Oxide Fuel Cell Constructed from an Yttria-Stabilized Zirconia Electrolyte

Takashi Hibino,^{a,z} Shuqiang Wang,^b Shiro Kakimoto,^c and Mitsuru Sano^c

^aNational Industrial Research Institute of Nagoya, Nagoya 462, Japan

^bNew Energy and Industrial Technology Development Organization, Nagoya 462, Japan

^cNagoya University, Nagoya 464, Japan

A single chamber cell constructed from an yttria-stabilized zirconia solid electrolyte with a nickel anode and a strontium-doped lanthanum manganese oxide ($\text{La}_{0.8}\text{Sr}_{0.2}\text{MnO}_3$) cathode can generate an electromotive force (emf) of 795 mV and a power density of 121 mW cm⁻² in a mixture of methane and air at a flow rate of 300 mL min⁻¹ and 950°C. The simultaneous additions of 25 wt % gadolinium-doped cerium oxide ($\text{Ce}_{0.8}\text{Gd}_{0.2}\text{O}_{1.9}$) and 15 wt % manganese oxide (MnO_2) to the anode and cathode, respectively, further increased the emf to 833 mV and the power density to 162 mW cm⁻².

© 1999 The Electrochemical Society. S1099-0062(99)03-023-0. All rights reserved.

Manuscript submitted March 2, 1999; revised manuscript received March 30, 1999. Available electronically May 6, 1999.

Conventional fuel cells consist of two gas chambers partitioned by gastight electrolytes. The working principle of such cells is based on the separate supply of fuel and air to the anode and cathode, respectively. Another type of fuel cell based on a different principle has been suggested by many researchers.¹⁻⁶ This type of fuel cell consists of only one gas chamber, where both the anode and the cathode are exposed to the same mixture of fuel and air. According to the working principle most commonly mentioned,^{1,2,5,6} one electrode has a higher electrocatalytic activity for the anodic oxidation of the fuel, whereas the other electrode has a higher electrocatalytic activity for the cathodic reduction of oxygen, thus resulting in an electromotive force (emf) between the two electrodes even in a uniform atmosphere. The construction of this type of cell is simpler than for conventional fuel cells, because there is no need for separating the supply of fuel and air. However, all one-chamber fuel cells proposed so far employ impractical electrode and/or electrolyte materials, which are expensive or unstable under the proposed operating conditions. For example, the $\text{Pt}/\text{BaCe}_{0.8}\text{Y}_{0.2}\text{O}_{3-\alpha}/\text{Au}$ cell reported by our research group showed a short lifetime of ca. 5 h in a flowing mixture of methane and air at 950°C, because $\text{BaCe}_{0.8}\text{Y}_{0.2}\text{O}_{3-\alpha}$ reacted with carbon dioxide to form barium carbonate and/or the Au electrode was gradually sintered.⁷ Subsequently, although yttria-stabilized zirconia (YSZ) and YSZ-doped by some metal cations, were examined as the solid electrolytes, these cells showed very low power densities, because of the large overpotentials at both the Pt and Au electrodes.⁸

A cell consisting of $\text{Ni}/\text{YSZ}/\text{La}_{0.8}\text{Sr}_{0.2}\text{MnO}_3$ (LSM) is widely used as a conventional solid oxide fuel cell (SOFC). All of the component parts of this cell are inexpensive and very stable at high temperatures. Therefore, we applied this cell as a single chamber SOFC working in a flowing mixture of methane and air. This paper demonstrates that the Ni and LSM electrodes can be used in place of the Pt and Au electrodes, respectively, for a single chamber SOFC. In addition, the simultaneous additions of $\text{Ce}_{0.8}\text{Gd}_{0.2}\text{O}_{1.9}$ (GDC) and MnO_2 to the Ni and LSM electrodes, respectively, make it possible for this cell to exhibit high performance.

Experimental

Figure 1a shows a two-chamber cell constructed from a YSZ solid electrolyte with three electrodes for measurement of the anodic and cathodic polarization properties of the Ni- and LSM-based working electrodes, respectively, and their catalytic activities for the oxidation of methane. The sintered YSZ disk (8 mol % yttria, 14 mm diam, 1 mm thick) was purchased from Nikkato Co., Ltd. The Ni- and LSM-based working electrodes were deposited on the YSZ surface as follows: NiO powder (Kojundo Chemical Laboratory Co., Ltd.) or LSM powder (Anan Kasei Co., Ltd.) was mixed with various metal oxides (CeO_2 , GDC, CoO , Fe_2O_3 , IrO_2 , MnO_2 , Pr_6O_{11} ,

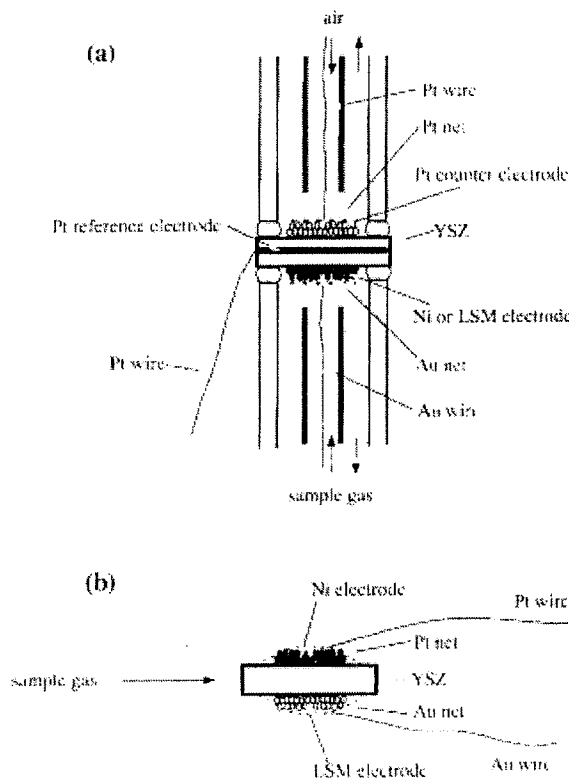


Figure 1. Schematic of (a) dual-chamber cell and (b) single-chamber cell.

RuO_2 , Ta_4O_7 , TiO_2 , YSZ, and WO_3) (Kojundo Chemical Laboratory Co., Ltd.), with a weight ratio of NiO or LSM to the metal oxide of 90/10, in ethyl Carbitol and then ground using a planetary mill (Fritsch P-5) with a zirconia mill container and zirconia grinding balls for 1 h. The as-formed paste was smeared on the bottom surface (0.5 cm² area) of the YSZ disk as thinly as possible with a brush.

After the smeared paste was dried at 130°C for 10-20 min in air, it was calcined at 1250°C for 3 h in air. The Pt and Au working electrodes for comparison with the Ni- and LSM-based working electrodes, respectively, were prepared as described in previous papers.^{7,8} The Pt counter and reference electrodes were deposited by smearing Pt paste (Tokuriki Co., Ltd.) on the top surface (0.5 cm² area) and the side surface of the YSZ disk, respectively, and then calcining at 900°C for 1 h in air.

^z E-mail: thibino@nirin.go.jp

Two gas chambers were set up by placing the cell between two alumina tubes (9 and 13 mm inner and outer diam, respectively). Each chamber was sealed by melting a glass ring gasket at 900°C. The working chamber was supplied with a mixture of methane and air having a volume ratio of methane:oxygen = 1:1 at a flow rate of 300 mL min⁻¹ and an operating temperature of 950°C.

The counter and reference electrodes were exposed to atmospheric air. The anodic and cathodic overpotentials corrected for ohmic losses of the Ni- and LSM-based working electrodes, respectively, were measured by the current-interrupt technique using a current-pulse generator (Nikko Keisoku NCPG-101). The analysis of the outlet gases from the Ni- and LSM-based working chambers was performed on a dry basis using on-line gas chromatography (Shimadzu GC-8A). The separation of methane, oxygen, hydrogen, and carbon monoxide was performed using a molecular sieve 5A column at 50°C, and carbon dioxide was analyzed using a Porapak Q column at 50°C.

Figure 1b shows a single chamber cell constructed from the YSZ solid electrolyte with the Ni-based anode and the LSM-based cathode. These electrodes were deposited on opposite surfaces (0.5 cm² area) of the YSZ disk (14 mm diam and 0.5 mm thick) in the same way as previously described. The cell was placed in an alumina tube (15 and 19 mm inner and outer diam, respectively) which was heated to 950°C. The same mixture of methane and air as previously described was supplied to the cell at a flow rate of 300 mL min⁻¹. The performance of this cell was examined by measuring the terminal voltage between the two electrodes during discharge of the cell.

Results and Discussion

The anodic polarization curve of the Ni working electrode in the two-chamber cell is shown in Fig. 2, where a typical result for the Pt working electrode is also included for comparison. The potential of the Ni working electrode at zero current was more negative than that of the Pt working electrode at zero current. Table I summarizes the compositions of the outlet gases from the Ni and Pt working chambers of the dual-chamber cell. Oxygen and methane were consumed more completely at the Ni working electrode than at the Pt working electrode. In addition, more hydrogen and carbon monoxide were formed at the Ni working electrode than at the Pt working electrode, although the opposite was observed for carbon dioxide. It is generally reported that reaction 1 takes place through reactions 2, 3, and 4. Assuming that this also applies to the present case, the Ni working electrode must have higher catalytic activities, especially for reactions 3 and 4, than the Pt working electrode

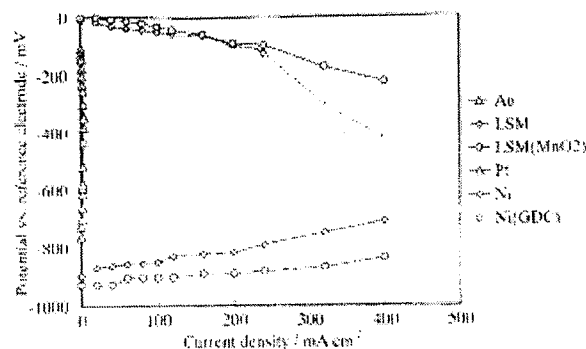
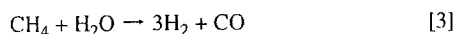
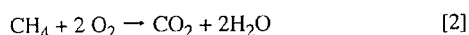
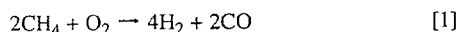
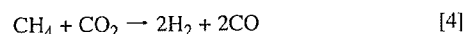


Figure 2. Anodic and cathodic polarization curves of Ni-based and LSM-based working electrodes, respectively, in a dual-chamber cell: sample gas is 22 vol % methane and 22 vol % oxygen in nitrogen; flow rate is 300 mL min⁻¹; operating temperature is 950°C; all overpotentials are free from ohmic loss.



Another difference between the two working electrodes is visible in Fig. 2; the anodic overpotential of the Ni working electrode was much smaller than that of the Pt working electrode. A significant amount of carbon was confirmed to be deposited on the Pt surface after the experiment. This coking may be a reason for the large overpotential and the low catalytic activity of the Pt working electrode.

A comparison of the cathodic polarization at the LSM working electrode with that at the Au working electrode is also shown in Fig. 2. The potential of the Au working electrode at zero current changed gradually from -8 to -100 mV with time. However, as can be seen from Table I, the oxidation of methane proceeded at a slow rate at the Au working electrode. This discrepancy is believed to be based on the preferential adsorption of methane molecule on the Au surface as discussed in a previous paper.⁸ On the other hand, the potential of the LSM working electrode at zero current was found to be a constant value of -16 mV. In addition, the oxidation of methane did not proceed at a significant rate at the LSM working electrode as shown in Table I. This result is particularly surprising, because it is well known that LSM powder shows moderate catalytic activity for the oxidation of hydrocarbons.⁹⁻¹³ However, it is also reported that LSM powder exhibits significantly decreasing catalytic activity with increasing particle size.^{12,13} A scanning electron microscope image of the LSM working electrode after its calcination at 1250°C showed that the mean particle size was ca. 2.5 μm. Another striking characteristic of the LSM working electrode is its small cathodic overpotential, indicating that it has high electrocatalytic activity in spite of having low catalytic activity.

Table I. Compositions of inlet and outlet gases from working chamber and potentials of working electrodes against reference electrode at zero current.

Electrode	Inlet gas ^a (%)		Outlet gas ^a (%)				Potential ^b (mV)	
	CH ₄	O ₂	CH ₄	O ₂	H ₂	CO	CO ₂	(Carbon balance)
Pt	19.5	15.9	11.6	0.2	0.8	5.4	6.1	+18
Ni	19.6	16.3	9.3	0.1	5.9	9.5	4.0	+16
Ni (GDC)	20.5	16.1	8.1	0.0	8.2	10.7	3.8	+10
Au	19.5	16.2	17.5	13.2	0.0	1.1	0.8	-0.5
LSM	19.4	16.3	15.7	7.2	0.0	2.6	3.6	+13
LSM (MnO ₂)	18.6	16.5	16.4	13.6	0.0	1.2	0.6	-2.2

^a The balance gas is nitrogen.

^b This is the potential against the reference electrode of the dual-chamber cell.

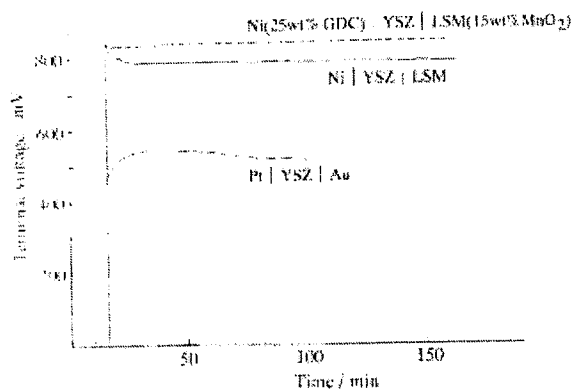


Figure 3. Transient changes of emfs generated from various single chamber cells: sample gas is 22 vol % methane and 22 vol % oxygen in nitrogen; flow rate is 300 mL min⁻¹; operating temperature is 950°C.

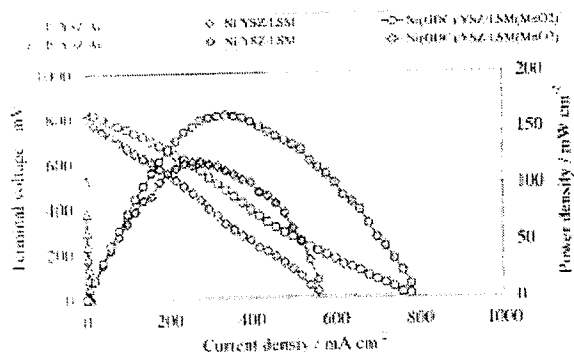


Figure 4. SOFC performance of various single chamber cells: experimental conditions are the same as in Fig. 3.

Figure 3 shows the transient changes in the emfs generated from the single chamber cells, Pt/YSZ/Au and Ni/YSZ/LSM. The emf of the Pt/YSZ/Au cell increased to 542 mV and then gradually decreased to 508 mV. This behavior is in good agreement with that found in a previous paper.⁸ On the other hand, the emf of the Ni/YSZ/LSM cell decreased somewhat and then reached a constant value of 795 mV. Preliminary experiments showed that emfs of more

than 750 mV were always generated from a Ni/YSZ/LSM cell when the flow rate of the methane and air mixture was more than 150 mL min⁻¹, the operating temperature was higher than 800°C, and the volume ratio of methane to oxygen was more than 0.8. Figure 4 shows the discharge properties of these single chamber cells. The Ni/YSZ/LSM cell showed much better performance than the Pt/YSZ/Au cell. The maximum power densities of the Ni/YSZ/LSM and Pt/YSZ/Au cells were 121 and 0.57 mW cm⁻², respectively.

In order to further improve the performance of the single chamber cell, various metal oxides were added to the Ni and LSM electrodes. As a result, GDC and MnO₂ were found to be the most suitable additives for the Ni and LSM electrodes, respectively, their effects being maximized at 25 wt % GDC and 15 wt % MnO₂. The addition of GDC shifted the potential of the Ni electrode at zero current to a more negative value and reduced its anodic overpotential (Fig. 2). The catalytic activity of the GDC-added Ni electrode was higher than that of the parent Ni electrode (Table I). On the other hand, the addition of MnO₂ shifted the potential of the LSM electrode at zero current to 0 mV and reduced its cathodic overpotential, especially at high current densities (Fig. 2). The catalytic activity of the MnO₂-containing LSM electrode was lower than that of the parent LSM electrode (Table I). Therefore, the combined addition effects enhanced the emf of the single chamber cell (Fig. 3) and resulted in better performance (Fig. 4), where the maximum power density was 162 mW cm⁻². It was confirmed that a current could be drawn from this cell for at least 5 h. The long-term stability of this cell is now under investigation.

The National Industrial Research Institute assisted in meeting the publication costs of this article.

References

1. W. van Gool, *Philips Res. Rep.*, **20**, 81 (1965).
2. G. A. Lousi, J. M. Lee, D. L. Maricle, and J. C. Trocicola, U.S. Pat. 4,248,941 (1981).
3. C. K. Dyer, *Nature*, **343**, 547 (1990).
4. P. Moseley and D. Williams, *Nature*, **346**, 23 (1990).
5. T. Hibino, K. Asano, and H. Iwahara, *Chem. Lett.*, 1131 (1993).
6. I. Riess, P. J. van der Put, and J. Schoonman, *Solid State Ionics*, **82**, 1 (1995).
7. T. Hibino, K. Ushiki, and Y. Kuwahara, *Solid State Ionics*, **91**, 69 (1995).
8. K. Asano, T. Hibino, and H. Iwahara, *Denki Kagaku oyobi Kogyo Butsuri Kagaku*, **64**, 649 (1996).
9. Y. F. Y. Yao, *J. Catal.*, **36**, 266 (1975).
10. H. Arai, T. Yamada, K. Eguchi, and T. Seiyama, *Appl. Catal.*, **26**, 265 (1986).
11. J. E. France, A. Shamsi, and M. Q. Ahsan, *Energy Fuels*, **2**, 235 (1988).
12. N. Yamazoe and Y. Teraoka, *Catal. Today*, **8**, 175 (1990).
13. T. Hibino, K. Suzuki, K. Ushiki, Y. Kuwahara, and M. Mizuno, *Appl. Catal.*, **145**, 297 (1996).

EXHIBIT 4

REPORTS

ration, in this case, variations in the ratio of photo/dark respiration may cause some changes in Δ_{\max} , especially in conditions of inorganic carbon limitation favorable to photorespiration such as in terrestrial C_3 vegetation. However, aquatic plants developed mechanisms to concentrate CO_2 and suppress photorespiration [A. Kaplan and L. Reinhold, *Annu. Rev. Plant Physiol. Plant Mol. Biol.* **50**, 539 (1999)]. As a result, photorespiration is not likely to affect oceanic Δ_{\max} .

11. H. Craig and L. I. Gordon, in *Conference on Stable Isotopes in Oceanographic Studies and Paleotemperatures*, E. Tongiorgi, Ed. (Laboratory of Geology and Nuclear Science, Pisa, Italy, 1965), pp. 9–130.
12. Air-water equilibrium was attained in less than 24 hours by bubbling outside air into seawater (25°C). The Δ_{eq} value was determined in five separate experiments. Its average value was 16 per meg with a standard error of ± 2 per meg. For simplicity in calculations we assumed that the deviation of Δ_{eq} from zero is the result of isotopic fractionation occurring only during O_2 invasion. In the cases discussed here, errors due to this assumption are negligible.
13. J. F. Clark *et al.*, in *Air-Water Gas Transfer*, B. Jaehne and E. C. Monahan, Eds. (Aeon Verlag & Studio, Hanau, Germany, 1995), pp. 785–800.
14. P. D. Nightingale *et al.*, *Global Biogeochem. Cycles* **14**, 373 (2000).
15. H. Craig and T. Hayward, *Science* **235**, 199 (1987).
16. W. J. Jenkins and J. C. Goldman, *J. Mar. Res.* **43**, 465 (1985); W. S. Spitzer and W. S. Jenkins, *J. Mar. Res.* **47**, 169 (1989).
17. B. Luz and E. Barkan, data not shown.
18. A. F. Michaels and A. H. Knap, *Deep-Sea Res. II* **43**, 157 (1996); S. C. Doney, D. M. Glover, R. G. Najjar, *Deep-Sea Res. II* **43**, 591 (1996).
19. B. B. Benson and D. Krause Jr., *Limnol. Oceanogr.* **29**, 620 (1984).
20. Data is found at www.bbsr.edu/Weather/climatology.html; R. Wanninkhof, *J. Geophys. Res.* **97**, 7373 (1992).
21. We are grateful to M. Bender for numerous discussions on all aspects of this research. Comments by A. Kaplan, Y. Kolodny, and three anonymous reviewers significantly improved the manuscript. We appreciate the help of the Bermuda Biological Station in sampling at BATS and extend special thanks to S. Bell. The support of the Kinneret National Laboratory is appreciated. Y. Yacobi and Y. Sagi helped in gross-production measurements in the Sea of Galilee, and J. Erez and K. Schneider helped with the coral experiment. The support of the U.S.-Israel Binational Science Foundation, The Israeli Science Foundation, MARS-2, and the Moshe-Shilo Minerva Center is greatly appreciated.

6 December 1999; accepted 11 May 2000

A Low-Operating-Temperature Solid Oxide Fuel Cell in Hydrocarbon-Air Mixtures

Takashi Hibino,^{1*} Atsuko Hashimoto,¹ Takao Inoue,² Jun-ichi Tokuno,² Shin-ichiro Yoshida,² Mitsuru Sano²

The performance of a single-chamber solid oxide fuel cell was studied using a ceria-based solid electrolyte at temperatures below 773 kelvin. Electromotive forces of ~900 millivolts were generated from the cell in a flowing mixture of ethane or propane and air, where the solid electrolyte functioned as a purely ionic conductor. The electrode-reaction resistance was negligibly small in the total internal resistances of the cell. The resulting peak power density reached 403 and 101 milliwatts per square centimeter at 773 and 623 kelvin, respectively.

Fuel cells are widely viewed as a promising source of low-emission power generation for vehicles. There is great controversy over which fuel should be used. Polymer electrolyte fuel cells (PEFCs) exhibit high power densities at low temperatures (~353 K), but they require hydrogen as the fuel, which is impractical in terms of storage and handling. An external reformer can be used to convert alcohols and hydrocarbons into hydrogen, but their portability is inferior. There have been recent successes with solid oxide fuel cells (SOFCs), which perform well between 823 and 973 K using methane (1) and *n*-butane (2) directly as the fuels. A further reduction in the operating temperature of SOFCs and an enhancement in their thermal and mechanical shock resistance would make this technology a promising alternative to PEFCs.

A type of fuel cell that consists of only one gas chamber, where both the anode and the cathode are exposed to the same mixture of fuel and air, has been proposed by many

researchers (3–8). This design is more shock resistant than conventional fuel cells, both thermally and mechanically. We have recently succeeded in applying this single-chamber cell design to a SOFC constructed from yttria-stabilized zirconia (YSZ), which is commonly used as a solid electrolyte in SOFCs, with a Ni-based anode and a perovskite cathode (9). This SOFC, however, must operate at the high temperature of 1223 K to achieve sufficient ionic conduction in the solid electrolyte.

Different cation-doped ceria, notably samaria-doped ceria (SDC), have much higher ionic conduction than YSZ in an oxidizing atmosphere, whereas they show *n*-type semiconduction in a reducing atmosphere (10, 11). Because the resulting electromotive force (EMF) of the SOFC is lower than the theoretical value, the SDC electrolyte has so far been regarded as unsuitable for such applications. However, the partial pressure of oxygen at the boundary of the two atmospheres becomes gradually lower as the operating temperature decreases (12), which suggests that the SDC electrolyte can be used even under fuel cell conditions, provided it operates at extremely low temperatures. In this report, we demonstrate a low-temperature SOFC by combining the advantages of the SDC electrolyte with the single-chamber cell design.

The SDC electrolyte we used here was prepared by pressing a commercial ceramic powder, $Ce_{0.8}Sm_{0.2}O_{1.9}$ (Anan Kasei Co. Ltd.), hydrostatically into a pellet at 2×10^3 kg cm⁻² and then sintering in air at 1773 K for 10 hours. After the pellet was cut into a disk (diameter 14 mm, thickness ~1 mm), the SDC disk surface was polished to a given thickness (0.15 to 0.50 mm) with an abrasive paper. YSZ (8 mol% yttria) and $La_{0.9}Sr_{0.1}Gd_{0.8}Mg_{0.2}O_3$ (LSGM) were used as solid electrolytes for comparison. Preliminary experiments revealed that 10 weight % SDC-containing Ni and $Sm_{0.5}Sr_{0.5}CoO_3$ electrodes best functioned as the anode and the cathode, respectively. These pastes were smeared on the opposite surfaces (area 0.5 cm²) of the SDC disk, followed by calcining in air at 1223 K for 4 hours. The cell thus fabricated was placed in an alumina tube (inner and outer diameters 15 and 19 mm, respectively). Methane, ethane, and propane were mixed with air for each of the respective concentrations—30 volume % for methane, 18 volume % for ethane, and 14 volume % for propane—so that the oxidation would proceed safely without exploding (the explosive limits of methane, ethane, and propane in air are 15.0, 12.5, and 9.5 volume %, respectively). The gas mixture was supplied to the cell at flow rates of 300 ml min⁻¹ between 623 and 773 K (Fig. 1).

When the single-chamber SOFCs using SDC, YSZ, and LSGM with a thickness of 0.50 mm were supplied with a mixture of ethane and air at 773 K, all three cells generated stable EMFs of ~920 mV, where the

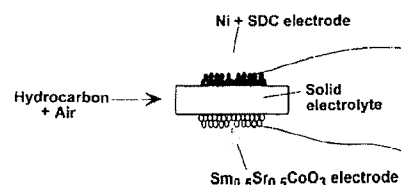


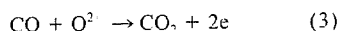
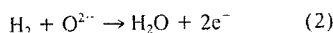
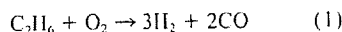
Fig. 1. A schematic illustration of single-chamber SOFC in a flowing mixture of hydrocarbon and air.

¹Department of Structure Formation Process, National Industrial Research Institute of Nagoya, Nagoya 462-8510, Japan. ²Graduate School of Human Information, Nagoya University, Nagoya 466-0804, Japan.

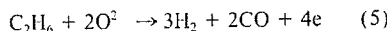
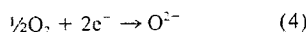
*To whom correspondence should be addressed. E-mail: thibino@nirino.go.jp

REPORTS

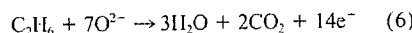
potential of the 10 weight % SDC-containing Ni electrode was negative versus the $\text{Sm}_{0.5}\text{Sr}_{0.5}\text{CoO}_3$ electrode (Fig. 2). From the analysis of the outlet gas from the cell having only the 10 weight % SDC-containing Ni or $\text{Sm}_{0.5}\text{Sr}_{0.5}\text{CoO}_3$ electrode, it was found that the partial oxidation of ethane by oxygen proceeded to form a large amount of hydrogen and carbon monoxide over the 10 weight % SDC-containing Ni electrodes, whereas such an oxidation proceeded at a very slow rate over the $\text{Sm}_{0.5}\text{Sr}_{0.5}\text{CoO}_3$ electrode. Therefore, it can be predicted that the potential of the 10 weight % SDC-containing Ni electrode is determined by the partial pressure of oxygen in its vicinity after the following reactions attain equilibrium:



[For details on Eq. 1, see (13).] Hence, this electrode will show a significantly negative potential. On the other hand, the potential of the $\text{Sm}_{0.5}\text{Sr}_{0.5}\text{CoO}_3$ electrode is a mixed potential based on the following reactions:



or



The large EMF values stated above, however,

suggest that this electrode favors Eq. 4 rather than Eqs. 5 or 6, because the potential determined by Eq. 4 is much less negative than those determined by Eqs. 5 and 6.

The similarity in EMF values among the three cells (Fig. 2) means that the SDC behaved as a purely ionic conductor during operation in a similar manner to the other solid electrolytes [the equilibrium partial pressure of oxygen in the gas mixture under the present conditions, $\sim 10^{-19}$ atm, is in the range of the electrolytic domain at 773 K (12)]. Although current could be drawn from the three cells, the voltage drop was the least in the cell using the SDC. The impedance spectra of the three cells further clarified this point (Fig. 3). The order of the ohmic resistance was $\text{SDC} < \text{LSGM} < \text{YSZ}$, which can be predicted from their ionic conductivities at 773 K. More important was the extremely small electrode-reaction resistance of 0.24 ohms observed on the cell using the SDC, suggesting that the cell performance would be improved using an even thinner SDC film. It has been reported that when the charge transfer reaction at the three-phase (gas-electrode-electrolyte) boundary is a rate-determining step in the electrode reaction, the anodic or cathodic reactions (or both) are promoted as the ionic conductivity of the solid electrolyte increases (14), which best explains why the cell using the SDC exhibited the smallest electrode-reaction resistance.

Evidence for the above suggestion is provided by the discharge properties of the single-chamber SOFC using SDC of different thicknesses in a flowing mixture of ethane and air at 773 K (Fig. 4). The voltage drop during cell discharge was strongly dependent on the thickness of the SDC, which resulted in an increasing power density with decreasing thickness of the SDC. In the cells using LSGM and YSZ, there was little correlation between the power density and the thickness of the solid electrolyte, because of their large electrode-reaction resistances. For example, the power density of the cell using LSGM increased

Fig. 2. Terminal voltage–current density curves of single-chamber SOFCs using SDC, YSZ, and LSGM with a thickness of 0.50 mm in a flowing mixture of ethane and air at 773 K. The gas mixture consisted of 52 ml min⁻¹ ethane, 52 ml min⁻¹ oxygen, and 196 ml min⁻¹ nitrogen.

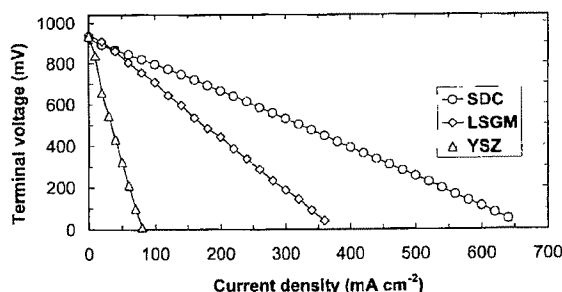


Fig. 3. Impedance spectra of single-chamber SOFCs using SDC, YSZ, and LSGM with a thickness of 0.50 mm in a flowing mixture of ethane and air at 773 K. These spectra were measured under open-circuit conditions by changing the frequency from 0.1 to 10⁴ Hz. The impedance arcs correspond to the total electrode-reaction resistance in the cell.

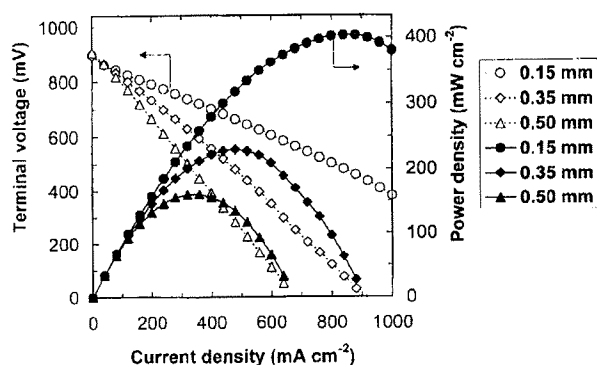
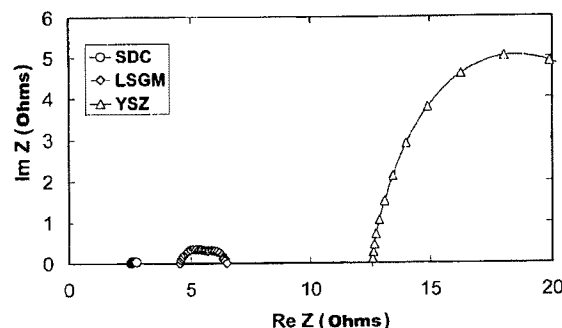
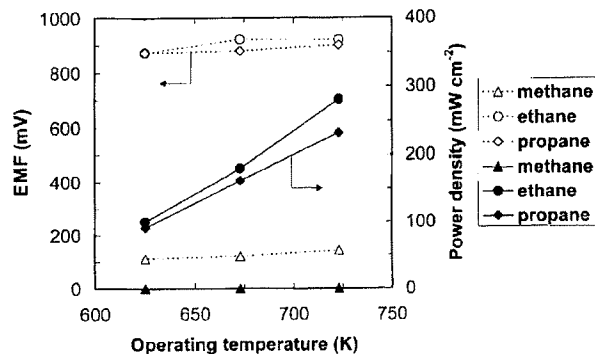


Fig. 4 (left). Discharge properties of single-chamber SOFCs using SDC of different thicknesses in a flowing mixture of ethane and air at 773 K. Experimental conditions are the same as in Fig. 2. **Fig. 5 (right).** EMF and power density of single-chamber SOFCs using SDC with a thickness of 0.15 mm in a mixture of different hydrocarbons and air between 623

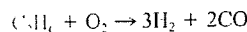


and 723 K. The mixture of methane and air consisted of 89 ml min⁻¹ methane, 44 ml min⁻¹ oxygen, and 167 ml min⁻¹ nitrogen. The mixture of propane and air consisted of 41 ml min⁻¹ propane, 54 ml min⁻¹ oxygen, and 205 ml min⁻¹ nitrogen.

REPORTS

from 90 to no more than 140 mW cm⁻² as thickness decreased from 0.5 to 0.15 mm.

The partial oxidation of ethane represented by Eq. 1 is thermodynamically possible even below 773 K:



$$\Delta G^\circ(773 \text{ K}) = -383 \text{ kJ mol}^{-1} \quad (7)$$

where ΔG° is Gibbs free energy. We therefore studied the performance of the single-chamber SOFC using SDC with a thickness of 0.15 mm under such conditions (Fig. 5). In the range of 623 to 723 K, the cell generated EMFs of ~900 mV, and the discharge properties were stable and reproducible. No carbon deposition was observed on the anode after operation. In addition, the impedance spectra of the cell showed small electrode-reaction resistances: 0.34 ohms for 723 K, 0.79 ohms for 673 K, and 1.64 ohms for 623 K. It appears that such fast electrode kinetics clean the precursors for carbon formation on the anode.

Figure 5 also shows the corresponding results for the other hydrocarbons. The cell performance in a mixture of propane and air was similar to that in a mixture of ethane and air, except at 723 K, where the $\text{Sm}_{0.5}\text{Sr}_{0.5}\text{CoO}_3$ electrode could not function well as the cathode, because this material was no longer inert to the oxidation of propane. On the other hand, the EMFs generated from the cell in a mixture of methane and air were only ~120 mV throughout the tested temperature range, where the oxidation rate of methane was too slow to form hydrogen and carbon monoxide over the 10 weight % SDC-containing Ni anode, probably causing a depression in Eqs. 2 and 3. We thus conclude that ethane and propane can be successfully used in the present SOFC at an operating temperature of 773 K or less. Because of their similar properties, we can assume that liquefied petroleum gas (LPG) or even butane would perform equally well.

The present SOFC has several additional advantages over PEFCs: (i) The anode is not subject to poisoning by carbon monoxide, whereas it is a critical problem for PEFCs (15, 16). (ii) There is no noble metal, such as Pt, in our SOFC, so fabrication costs are low. (iii) Although PEFCs themselves can operate at low temperatures, the hydrocarbon reformer (17) must operate at a higher temperature than our SOFC. (iv) The single-chamber cell design provides a more compact cell stack. These advantages, as well as the above results, greatly enhance the position of SOFCs as the preferred electric power generation technique for vehicles in the foreseeable future.

References

1. E. P. Murray, T. Tsai, S. A. Barnett, *Nature* **400**, 649 (1999).
2. S. Park, J. M. Vohs, R. J. Gorte, *Nature* **404**, 265 (2000).
3. W. van Gool, *Philips Res. Rep.* **20**, 81 (1965).

4. G. A. Lousi, J. M. Lee, D. L. Maricle, J. C. Trociola, U.S. Patent 4,248,941 (1981).
5. C. K. Dyer, *Nature* **343**, 547 (1990).
6. T. Hibino and H. Iwahara, *Chem. Lett.*, 1131 (1993).
7. C. A. Cavalca, G. Larsen, C. G. Vayenas, G. L. Haller, *J. Phys. Chem.* **97**, 6115 (1993).
8. I. Riess, P. J. van der Put, J. Schoonman, *Solid State Ionics* **82**, 1 (1995).
9. T. Hibino, S. Wang, S. Kakimoto, M. Sano, *Electrochem. Solid-State Lett.* **2**, 317 (1999).
10. B. C. H. Steele, *J. Power Source* **49**, 1 (1994).
11. C. Milliken, S. Guruswamy, A. Khandkar, *J. Electrochem. Soc.* **146**, 872 (1999).

12. H. L. Tuller and A. W. Nowick, *J. Electrochem. Soc.* **122**, 255 (1975).
13. A. T. Ashcroft et al., *Nature* **344**, 319 (1990).
14. H. Uchida, M. Yoshida, M. Watanabe, *J. Phys. Chem.* **99**, 3282 (1995).
15. S. Mukerjee et al., *Electrochem. Solid-State Lett.* **2**, 12 (1999).
16. M. Ciureanu and H. Wang, *J. Electrochem. Soc.* **146**, 4031 (1999).
17. N. Hashimoto, *Chem. Chem. Ind.* **50**, 1324 (1997).

28 February 2000; accepted 1 May 2000

Discovery of a Basaltic Asteroid in the Outer Main Belt

D. Lazzaro,^{1*} T. Michtchenko,² J. M. Carvano,¹ R. P. Binzel,³
S. J. Bus,³ T. H. Burbine,³ T. Mothé-Diniz,¹ M. Florczak,⁴
C. A. Angeli,¹ Alan W. Harris⁵

Visible and near-infrared spectroscopic observations of the asteroid 1459 Magnya indicate that it has a basaltic surface. Magnya is at 3.15 astronomical units (AU) from the sun and has no known dynamical link to any family, to any nearby large asteroid, or to asteroid 4 Vesta at 2.36 AU, which is the only other known large basaltic asteroid. We show that the region of the belt around Magnya is densely filled by mean-motion resonances, generating slow orbital diffusion processes and providing a potential mechanism for removing other basaltic fragments that may have been created on the same parent body as Magnya. Magnya may represent a rare surviving fragment from a larger, differentiated planetesimal that was disrupted long ago.

The diversity of compositions of iron meteorites and nonchondritic stony meteorites (1) suggests an early period of heating, melting, and differentiation of planetesimals that were later disrupted and became asteroids in the main belt rather than accreting to form planets. In the main belt today, only the large (525-km diameter) asteroid Vesta (2–4) and its associated family of impact excavated fragments (5–9) have been considered to be basaltic remnants (representing the crust of a differentiated planetesimal) from this early epoch of solar system history. We report observations of a 30-km outer main-belt asteroid, 1459 Magnya, that also shows the characteristic signature of a basaltic surface.

In September 1998, we performed spectroscopic observations of Magnya that indicated its possible basaltic composition (10) at the European Southern Observatory at La Silla (ESO-Chile) (11). Additional observations of

this asteroid were obtained in November 1999 and January 2000 with the double spectrograph on the 5-m Hale telescope at Palomar Observatory and in December 1999 with NSFCAM on the 3-m NASA Infrared Telescope Facility (IRTF) at Mauna Kea, Hawaii (12).

The ESO, Palomar, and Mauna Kea spectra of Magnya compared with the spectra of Vesta (Fig. 1) show similar absorptions near 1 and 2 μm , indicating a basaltic composition for Magnya. The basaltic nature of these surfaces is further confirmed by their match to basaltic achondrite meteorites, such as meteorites from the howardite, eucrite, and diogenite (HED) classes. Although Vesta has been suggested as a source for HED meteorites (7–9, 13), the implied ejection velocity (7, 8) for a fragment the size of Magnya being ejected from Vesta (at semimajor axis, a , of 2.36 AU) to Magnya's present location ($a = 3.14$ AU, $e = 0.24$, and $i = 17^\circ$, where e and i are the orbit eccentricity and inclination, respectively) is in excess of 5 km/s. We consider this high velocity to exceed any plausible limit for linking Magnya as a fragment directly ejected from Vesta. The orbits of Magnya and Vesta do overlap (the perihelion distance of Magnya is less than the aphelion distance of Vesta), leaving open some possibility that Magnya is an ejected and dynamically evolved fragment from Vesta. However, the lack of other evidence for such a dynamical evolution of the Vesta family (5–8) makes this link unlikely. Therefore, we consid-

¹Observatório Nacional, Departamento de Astrofísica, Rua Gal. José Cristino 77, 20921-400 Rio de Janeiro, Brazil. ²Instituto Astronômico e Geofísico, Universidade de São Paulo, Av. Miguel Stéfano 4200, 04301-904 São Paulo, Brazil. ³Department of Earth, Atmospheric, and Planetary Sciences, Massachusetts Institute of Technology, 77 Massachusetts Avenue, Cambridge, MA 02139–4301, USA. ⁴Centro Federal de Educação Tecnológica do Paraná, Departamento de Física, Av. Sete de Setembro 3165, 80230-901 Curitiba, Brazil. ⁵Jet Propulsion Laboratory, MS 183-501, 4800 Oak Grove Drive, Pasadena, CA 91109, USA.

*To whom correspondence should be addressed.

EXHIBIT 5

Improvement of a Single-Chamber Solid-Oxide Fuel Cell and Evaluation of New Cell Designs

Takashi Hibino,^{a,*} Hajime Tsunekawa,^b Satoshi Tanimoto,^b and Mitsuru Sano^b

^aNational Industrial Research Institute of Nagoya, Nagoya 462, Japan

^bNagoya University, Nagoya 464, Japan

The performance of a single-chamber solid-oxide fuel cell (SOFC) made from an yttria-stabilized zirconia solid electrolyte with a 25 wt % Ce_{0.8}Gd_{0.2}O_{1.9} (GDC)-containing Ni anode and a 15 wt % MnO₂-containing La_{0.8}Sr_{0.2}MnO₃ cathode was found to be significantly enhanced by the deposition of Mn, Ga, Cr, Ce, and Lu oxide layers on the YSZ surface. In particular, the deposition of the Mn oxide layer increased the maximum power density from 161 to 213 mW cm⁻² in a mixture of methane and air having a volume ratio of methane to oxygen of 1/1 at a flow rate of 300 mL min⁻¹ (methane 52 mL min⁻¹, oxygen 52 mL min⁻¹, nitrogen 196 mL min⁻¹), and at an operating temperature of 950°C. This effect was the result of the promoted anodic and cathodic reactions. Two types of cell designs were examined for the single-chamber SOFC; the two electrodes were deposited on opposite surfaces (A-type cell) and on the same face (B-type cell) of the solid electrolyte. The A-type cell showed an increasing power density with decreasing thickness of the solid electrolyte. The maximum power density was 256 mW cm⁻² at a solid electrolyte thickness of 0.3 mm. The B-type cell showed an increased power density for a decreased gap between the two electrodes. The maximum power density was 143 mW cm⁻² for a gap of 0.5 mm between the two electrodes. In addition, the long-term stability of the single-chamber SOFC was also studied and found to have a direct relationship with the carbon deposition on the GDC-containing Ni electrode.

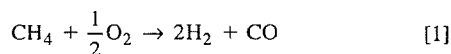
© 2000 The Electrochemical Society. S0013-4651(99)10-044-2. All rights reserved.

Manuscript submitted October 12, 1999; revised manuscript received December 13, 1999.

Solid-oxide fuel cells (SOFCs) have been under development for about 30 years. In this period, many design concepts have been considered. Current development efforts focus on two types of cell designs, tubular and planar cell designs. The tubular SOFC is developed more than the planar SOFC, but high fabrication costs, especially for the electrochemical vapor deposition (EVD) process of yttria-stabilized zirconia (YSZ), are considered one of its major problems.¹ The planar SOFC offers low-cost fabrication of the cell system, but this design makes it difficult to maintain high-temperature gastight seals.² Although these problems are solved by developing materials with higher conductivities than YSZ or lowering the operating temperature, the approach will require very time-consuming studies and high material costs.

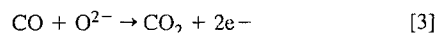
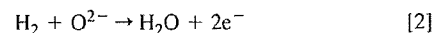
A novel type of SOFC distinguished from the tubular and planar SOFCs in principle and cell design has been suggested by a few researchers.³⁻⁵ This type of SOFC consists of only one gas chamber, where both the anode and the cathode are exposed to the same mixture of fuel and air, thus resulting in two advantages compared to conventional SOFCs, *i.e.*, (i) the single-chamber SOFC does not require high-temperature leakproof seals, because there is no need for separating the supply of fuel and air and (ii) if both the anode and the cathode are attached on the same face of the solid electrolyte, the ohmic resistance of the single-chamber SOFC decreases by reducing the gap between the two electrodes instead of using a thinner electrolyte film. Similar studies have also been conducted at room temperature on polymer membrane fuel cells.⁶⁻⁹

We recently reported a single-chamber SOFC using a YSZ solid electrolyte with a Ni-based anode and a strontium-doped lanthanum manganite (LSM)-based cathode, most commonly used in conventional SOFCs, in a flowing mixture of methane and air at high temperatures.¹⁰ The working principle of this cell is based on the difference in catalytic activity between the two electrodes for the partial oxidation of methane by oxygen to form hydrogen and carbon monoxide¹¹

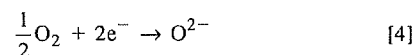


A large amount of hydrogen and carbon monoxide is formed over the Ni-based electrode due to its high catalytic activity for Reaction 1.

This allows the Ni-based electrode to work as the anode for the following reactions



On the other hand, most of the oxygen supplied remains unreacted over the LSM-based electrode due to its inactivity for Reaction 1. The LSM-based electrode thus can act as the cathode for the following reaction



However, the resulting maximum power density is still an insufficient value of 161 mW cm⁻² at a YSZ thickness of 0.5 mm. This is attributable not only to the very large electrolyte thickness but also to the large overpotentials at both electrodes.

It is often said that electrode reactions in conventional SOFCs are promoted by the location of catalytic layers having mixed conducting or redox properties between the YSZ solid electrolyte and the electrode.¹²⁻¹⁶ The promotional effect can also be applied to the electrode reactions in the single-chamber SOFC. In this study, we thus deposited 15 different metal oxides at the electrode-electrolyte interface and evaluated their electrocatalytic activities. As a result, it was found that a Mn oxide layer most enhanced both the anodic and cathodic reactions. Two types of cell designs were used to examine the performance of the improved single-chamber SOFC; the two electrodes were deposited on opposite surfaces (A-type cell) and on the same face (B-type cell) of the solid electrolyte. Finally, the long-term stability of the single-chamber SOFC was tested with respect to the relationship between the stability of the cell and carbon deposition on the Ni surface.

Experimental

Figures 1a and b show two types of single-chamber cells used in this study. The sintered YSZ disk (8 mol % yttria, 14 mm diam, 1 mm thickness) was purchased from Nikkato Co., Ltd. The different metal oxide layers were deposited on the YSZ surface as follows. The YSZ surface was polished with an abrasive paper and then washed with distilled water in an ultrasonic cleaner. After the YSZ disk was dried at 130°C in air, it was dipped in an aqueous solution of the corresponding metal nitrate at a concentration of 0.5 mol L⁻¹

* Electrochemical Society Active Member.

E-mail: thibino@nirin.go.jp

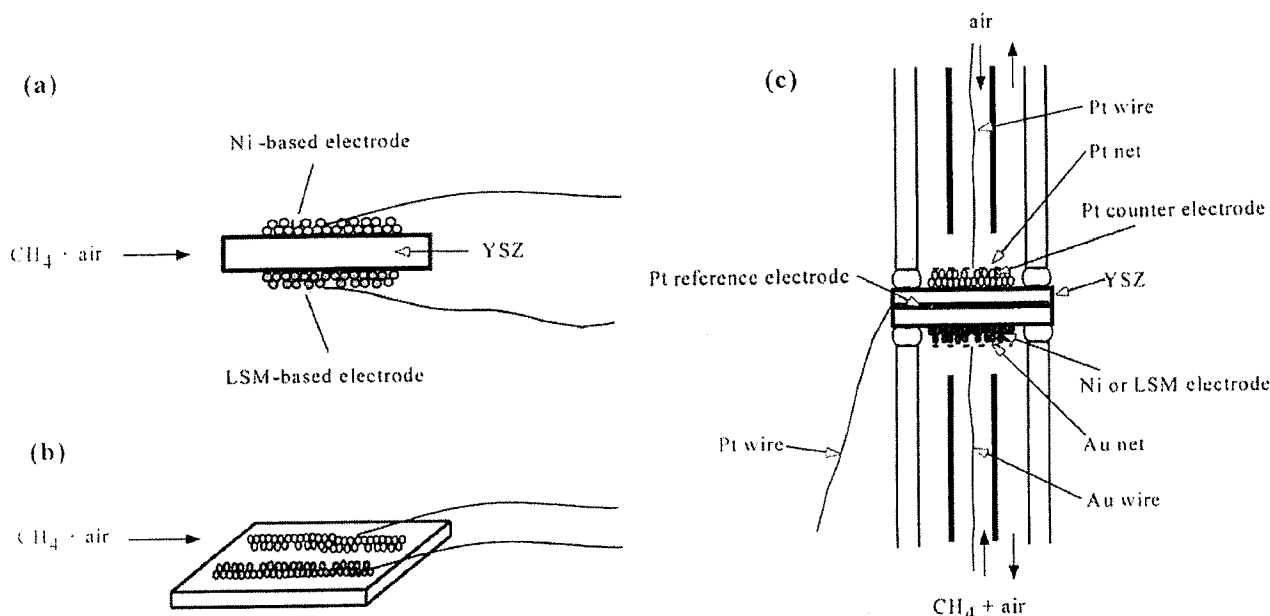


Figure 1. Schematic illustrations of (a) A-type one-chamber cell, (b) B-type one-chamber cell, and (c) a two-chamber cell.

for ca. 1 min. Subsequently, the YSZ disk was calcined at 1300°C for 1 h in air. The process was repeated several times, if necessary. The crystal structures of the metal oxide layers were studied by X-ray diffraction (XRD) (Rigaku Rotaflex). The preparation of 25 wt % $\text{Ce}_{0.8}\text{Gd}_{0.2}\text{O}_{1.9}$ -containing Ni [Ni(GDC)] and 15 wt % MnO_2 -containing $\text{La}_{0.8}\text{Sr}_{0.2}\text{MnO}_3$ [LSM(MnO_2)] pastes was described in a previous paper.¹⁰ The two pastes were smeared on opposite surfaces (0.5 cm² area) of the metal oxide-deposited YSZ disk for the A-type single-chamber cell shown in Fig. 1a and on the same face (0.05 cm² area) of the metal oxide-deposited YSZ disk for the B-type single-chamber cell shown in Fig. 1b. In the case of the A-type single-chamber cell, the thickness of the YSZ disk was changed from 0.3 to 0.6 mm. In the case of the B-type single-chamber cell, the shortest gap between the two electrodes was changed from 0.5 to 3 mm. After the smeared paste was dried at 130°C in air, it was calcined at 1250°C for 3 h in air. A Pt wire and a Pt mesh were used as the output terminal and the electrical collector, respectively, for the Ni(GDC) electrode, and an Au wire and an Au mesh were similarly used for the LSM(MnO_2) electrode. The cell was placed in an alumina tube (15 and 19 mm id and od diameters, respectively) which was heated to 950°C. A mixture of methane and air having volume ratios of methane to oxygen of 0.5/1 to 2.5/1 was supplied to the cell at flow rates from 50 to 500 mL min⁻¹ between 800 and 950°C. The discharge properties of the cell were examined by measuring the cell potential between the two electrodes during the discharge of the cell using a galvanostat (Hokuto Denko HA-501) and by monitoring the impedance between the two electrodes under open-circuit conditions using an impedance analyzer (Solartron SI 1260 and SI 1287).

Figure 1c shows a two-chamber cell constructed for measurement of the anodic and cathodic polarization properties of the Ni(GDC) and LSM(MnO_2) working electrodes, respectively, and their catalytic activities for the oxidation of methane. The two working electrodes were deposited on the bottom surface (0.5 cm² area) of the YSZ disk (1 mm thickness) in the same manner as previously described. Pt counter and reference electrodes were deposited by smearing Pt paste (Tokuriki Co., Ltd.) on the top surface (0.5 cm² area) and the side surface of the YSZ disk, respectively, and then calcining at 900°C for 1 h in air. Two gas chambers were set up by placing the cell between two alumina tubes (9 and 13 mm id and od diameters, respectively). Each chamber was sealed by melting a glass ring gasket at 950°C. The working chamber was supplied with a mixture of methane and air having a volume ratio of methane to oxygen of 1/1 at a flow rate of

300 mL min⁻¹ and at an operating temperature of 950°C. The counter and reference electrodes were exposed to atmospheric air. The anodic and cathodic reactions of the Ni(GDC) and LSM(MnO_2) working electrodes, respectively, were studied using their overpotentials measured by a current-pulse generator (Nikko Keisoku NCPG-101) and their impedance spectra monitored as described above. The analysis of the outlet gases from the Ni(GDC) and LSM(MnO_2) working chambers was performed on a dry basis using on-line gas chromatography (Shimadzu GC-8A). The separation of methane, oxygen, hydrogen, and carbon monoxide was performed using a molecular sieve 5 A column at 50°C, and carbon dioxide was analyzed using a Porapak Q column at 50°C.

Results and Discussion

Electrocatalytic activities of metal oxide layers.—The discharge properties of the A-type single-chamber SOFCs with the YSZ surfaces deposited by different metal oxide layers are summarized in Table I, where the open-circuit potential, maximum power density, ohmic resistance, and electrode resistance of each cell are shown. As reported in a previous paper,¹⁰ the open-circuit potential and maximum power density of the Ni|YSZ|LSM cell were enhanced by the addition of 25 wt % GDC and 15 wt % MnO_2 to the Ni anode and the LSM cathode, respectively. The further enhancement of the discharge properties of the single-chamber cell was caused by the deposition of Mn, Ga, Cr, Ce, and Lu oxide layers on the YSZ surface. In particular, the deposition of the Mn oxide layer increased the maximum power density to 213 mW cm⁻², the mean of 204, 206, 208, 217, and 231 mW cm⁻² obtained from five identically prepared samples. In addition, the deposition of the Mn oxide layer decreased the electrode resistance rather than the ohmic resistance. It was thus found that the effect of the deposited Mn oxide layer on the discharge properties of the single-chamber cell is attributable to the improved anodic and/or cathodic polarization.

Table II shows the corresponding results for the A-type single-chamber SOFC with the YSZ surface deposited by a Mn oxide layer several times. The discharge properties of the single-chamber cell were unaffected by the deposition repeated between one and three times, but they were gradually lowered when the deposition was repeated more than three times. Table II also shows that only the Mn oxide layer deposited five times was identified to be $\gamma\text{-Mn}_2\text{O}_3$, suggesting that a very small amount of the Mn oxide, which cannot be identified by the XRD measurement, effectively reduced the anodic

Table I. Performance of single-chamber SOFCs^a with YSZ surface deposited by various metal oxide layers.

Anode	Cathode	Metal oxide	Open-circuit potential (mV)	Power density (mW cm ⁻²)	R_{ohm}^b (Ω)	R_c^c (Ω)
Ni	LSM	None	795	121	1.4	1.8
Ni(GDC)	LSM(MnO ₂)	None	833	161	1.6	0.9
Ni(GDC)	LSM(MnO ₂)	Mn	845	213 ^d	1.6	0.4
Ni(GDC)	LSM(MnO ₂)	Ga	840	179	1.7	0.5
Ni(GDC)	LSM(MnO ₂)	Cr	845	176	1.8	0.5
Ni(GDC)	LSM(MnO ₂)	Ce	824	176	1.6	0.7
Ni(GDC)	LSM(MnO ₂)	Lu	850	166	2.2	0.6
Ni(GDC)	LSM(MnO ₂)	Pb	848	160	1.9	0.7
Ni(GDC)	LSM(MnO ₂)	Y	835	158	1.9	0.5
Ni(GDC)	LSM(MnO ₂)	Zn	845	139	1.9	0.8
Ni(GDC)	LSM(MnO ₂)	Pr	812	139	1.8	0.8
Ni(GDC)	LSM(MnO ₂)	Cu	808	136	1.8	0.9
Ni(GDC)	LSM(MnO ₂)	Co	831	117	2.1	0.7
Ni(GDC)	LSM(MnO ₂)	Sm	833	114	2.5	0.7
Ni(GDC)	LSM(MnO ₂)	Nd	835	83	3.6	1.1
Ni(GDC)	LSM(MnO ₂)	Yb	851	76	4.4	1.3
Ni(GDC)	LSM(MnO ₂)	Er	823	53	5.3	1.8
Ni(GDC)	LSM(MnO ₂)	Sr	785	43	4.2	2.3

^a YSZ thickness = 0.5 mm; operating temperature = 950°C; volume ratio of methane to air = 1; flow rate = 300 mL min⁻¹.^b R_{ohm} is the ohmic resistance of the cell measured by an impedance analyzer at 10 kHz.^c R_c is the total electrode resistance of the cell measured by an impedance analyzer in the region of 10 kHz to 0.1 Hz.^d This is the mean obtained from four identically prepared samples.

and/or cathodic polarization. We thus used the single-chamber SOFC with the YSZ surface deposited by the single-Mn oxide layer in subsequent experiments.

To understand better the effect of the deposited Mn oxide layer on the electrode reactions, the Ni-based and LSM-based electrodes were separated using the two-chamber cell shown in Fig. 1c. In Fig. 2, the overpotentials of the Ni-based and LSM-based electrodes are shown as a function of the current density. Linear relationships between the overpotential and current density were observed at all the electrodes, their slopes being reduced by the deposition of the Mn oxide layer. This indicates that the deposited Mn oxide layer enhances both the anodic and cathodic reactions. Similar results were observed for their impedance spectra shown in Fig. 3, where the electrode resistance was in the order Ni(GDC)/Mn < Ni(GDC) < Ni electrodes (Fig. 3a) and LSM(MnO₂)/Mn < LSM(MnO₂) < LSM electrodes (Fig. 3b). Furthermore, the apparent electrode capacitance obtained from the impedance arc according to Eq. 5 increased from 7000 to 10610 μF cm⁻² for the Ni(GDC) electrode and 4975 to 5303 μF cm⁻² for the LSM(MnO₂) electrode

$$C_e = 1/2\pi AR_e f_T \quad [5]$$

where A is the electrode area, R_e is the electrode resistance obtained from the impedance arc, and f_T is the frequency at the top of the impedance arc.

Table II. Performance of single-chamber SOFCs with YSZ surface deposited by Mn oxide layer several times.^a

Number	Open-circuit potential (mV)	Power density (mW cm ⁻²)	R_{ohm} (Ω)	R_c (Ω)	Crystal structure
0	833	161	1.6	0.9	—
1	845	213	1.6	0.4	—
2	835	222	1.3	0.5	—
3	834	222	1.5	0.4	—
4	815	168	1.9	0.7	—
5	826	113	1.9	1.4	γ-Mn ₂ O ₃

^a Experimental conditions are the same as in Table I.

In Table III, the compositions of the outlet gases from the Ni-based and LSM-based electrodes under open-circuit conditions are shown together with their potentials vs. the reference electrode. Over the Ni-based electrodes, oxygen was almost completely consumed by reacting with methane to form hydrogen, carbon monoxide, and carbon dioxide. The amounts of the formed hydrogen and carbon monoxide increased in the order Ni < Ni(GDC) < Ni(GDC)/Mn electrodes, which was the same as the order observed in the potential, suggesting Reactions 2 and 3 shown above as the anodic reactions. On the other hand, over the LSM-based electrode, methane reacted with oxygen at a very slow rate. The amount of the unreacted oxygen was in the order LSM < LSM(MnO₂) < LSM(MnO₂)/Mn electrodes, which corresponded well to that of the electrode potential, suggesting Reaction 4 shown above as the cathodic reaction. Therefore, the data in Table III together with those in Fig. 2 and 3 indicate that the deposited Mn oxide layer effectively promotes Reactions 2, 3, and 4. Many researchers have observed the promotional effects of metal oxides such as Mn, Ce, or Fe oxide on the anodic and/or cathodic reactions in conventional SOFCs. There are various explanations for this effect in the literature.¹²⁻¹⁶ As a general view, the mixed valence state of the metal oxide decreases the contact resistance at the electrolyte-electrode interface. However, this does not apply to the present case because the impedances at high frequencies

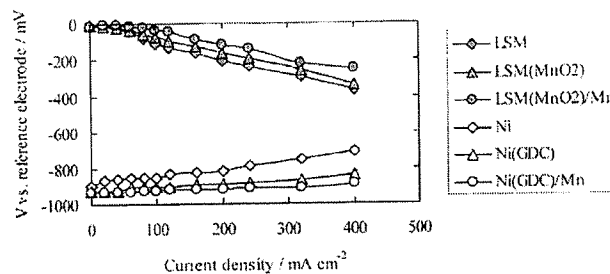


Figure 2. Anodic and cathodic polarization curves of Ni-based and LSM-based working electrodes, respectively, in a two-chamber cell. All overpotentials are free from ohmic loss. Volume ratio of methane to air = 1/1; flow rate = 300 mL min⁻¹; operating temperature = 950°C.

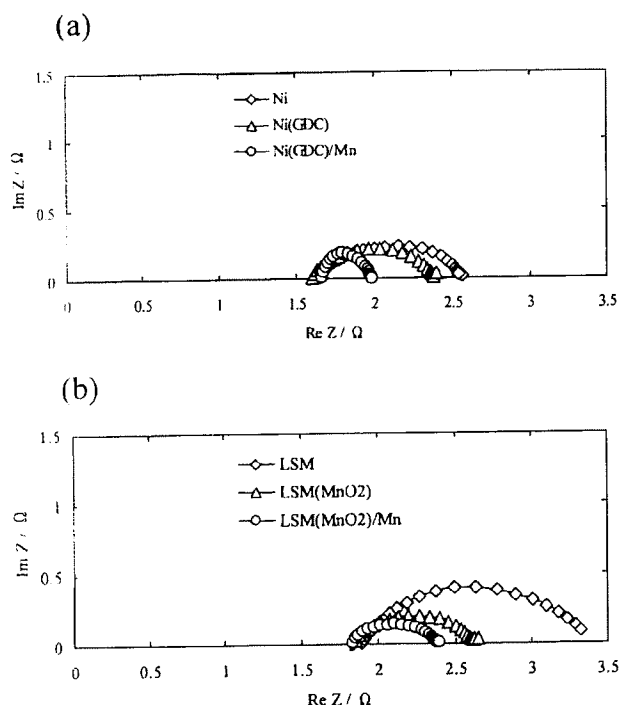


Figure 3. Impedance spectra of Ni-based and LSM-based working electrodes in a two-chamber cell. These data were measured under open-circuit conditions. Experimental conditions are the same as in Fig. 2.

shown in Fig. 3a and b were only slightly affected by the deposition of the Mn oxide layer. The mixed valence state of the metal oxide is also reported to allow an accumulation of charge, such as electrons and holes at the interface.¹³ Schouler¹² and Thampi *et al.*¹⁶ propose that the presence of mobile electrons and holes in the vicinity of oxide ion vacancies at the interface results in an increase in the reaction zone and triple-phase boundary. As described above, the Ni(GDC)/Mn and LSM(MnO₂)/Mn electrodes exhibited larger capacitances than the Ni(GDC) and LSM(MnO₂) electrodes, respectively, suggesting that the charge at the interface is increased by the deposition of the Mn oxide layer. Therefore, it is assumed that the present Mn oxide layer can also function as such a charge collector in the vicinity of oxide ion vacancies and increase the reaction zone for both anodic Reactions 2 and 3 and cathodic Reaction 4. However, an excess of the Mn oxide layer inhibited these reactions as shown in Table II. This will result from the formation of the insulating γ -Mn₂O₃ at the YSZ-electrode interface.

Performance of two types of single-chamber SOFC.—The discharge property of the A-type single-chamber SOFC, Ni(GDC)/Mn deposited YSZ/LSM(MnO₂), was measured under various conditions. Figure 4a shows that the discharge properties of the cell are gradually enhanced as the operating temperature increases from 800 to 950°C. However, the discharge properties at 1000°C were found to be somewhat worse than those at 950°C, because the Au electrical collector began to soften. One should use an electrical collector having a higher melting point instead of the Au mesh. As shown in Fig. 4b, the open-circuit potential of the cell was very small at a flow rate of 50 mL min⁻¹, whereas steady potentials near 800 mV were obtained at more than 50 mL min⁻¹. The potential drop of the cell during the discharge decreased with increasing flow rate of the mixture. These results can be explained by the fact that Reaction 1 over the LSM(MnO₂) electrode is enhanced by the decrease in flow rate of the mixture, thus resulting in a decrease in the amount of the unreacted oxygen in the neighborhood of the LSM(MnO₂) electrode. Therefore, the open-circuit potential of the single-chamber SOFC decreases, and its cathodic polarization increases. As shown in Fig. 4c, the increase in volume ratio of methane to oxygen resulted in an enhancement of the open-circuit potential of the cell, but the best discharge properties of the cell were observed at a volume ratio of methane to oxygen of 1/1. A significant amount of carbon was confirmed to be deposited at volume ratios of methane to oxygen of more than 1/1 on the Ni(GDC) electrode after the experiment. This coking is a reason for the lower discharge properties of the cell at volume ratios of methane to oxygen more than 1/1. Further details of the carbon deposition are discussed later. On the other hand, the reaction of methane with oxygen over the Ni(GDC) electrode is considered to shift from partial to complete oxidation, which forms water vapor and carbon dioxide in place of hydrogen and carbon dioxide, respectively, as the volume ratio of methane to oxygen decreases. This shift will be a reason for the lower discharge properties at volume ratios of methane to oxygen of less than 1/1. Subsequent experiments were carried out at an operating temperature of 950°C, a flow rate of 300 mL min⁻¹, and a volume ratio of methane to oxygen of 1/1.

In the A-type single-chamber SOFC, the Ni(GDC) and LSM(MnO₂) electrodes are attached on opposite surfaces of the YSZ solid electrolyte. If the potential drop of the cell during the discharge shown in Fig. 4 is mainly due to the ohmic resistance of the solid electrolyte, the power density of the cell will be enhanced using a thinner solid electrolyte. Figure 5 shows the effect of the thickness of the solid electrolyte on the discharge properties of the cell. The power density becomes higher as the thickness of the solid electrolyte decreases from 0.6 to 0.3 mm. The maximum power density is 256 mW cm⁻² at a solid-electrolyte thickness of 0.3 mm (376 mV at 680 mA cm⁻²).

In the B-type single-chamber SOFC, the two electrodes are attached on the same face of the YSZ solid electrolyte. There is a possibility that the power density of the cell is enhanced by moving

Table III. Compositions of inlet and outlet gases from working chamber and potentials of working electrodes against reference electrode under open-circuit condition.

Electrode	Inlet gas ^a (%)		Outlet gas ^a (%)						Potential ³ (mV)
	CH ₄	O ₂	CH ₄	O ₂	H ₂	CO	CO ₂	H ₂ O ^b	
Ni	19.6	16.3	9.3	0.1	5.9	9.5	4.0	14.7	-879
Ni(GDC)	20.5	16.1	8.1	0.0	8.2	10.7	3.8	16.6	-913
Ni(GDC)/Mn	21.8	15.6	6.7	0.2	12.4	12.0	3.3	17.8	-936
LSM	19.4	16.3	15.7	7.2	0.0	2.6	3.6	7.4	-16
LSM(MnO ₂)	18.6	16.5	16.4	13.6	0.0	1.2	0.6	4.4	-3
LSM(MnO ₂)/Mn	16.9	16.5	15.9	14.5	0.0	0.6	0.3	2.0	-2

^a The balance gas is nitrogen.

^b This is estimated by balancing the inlet and outlet gas compositions.

^c This is the potential against the reference electrode of the two-chamber cell.

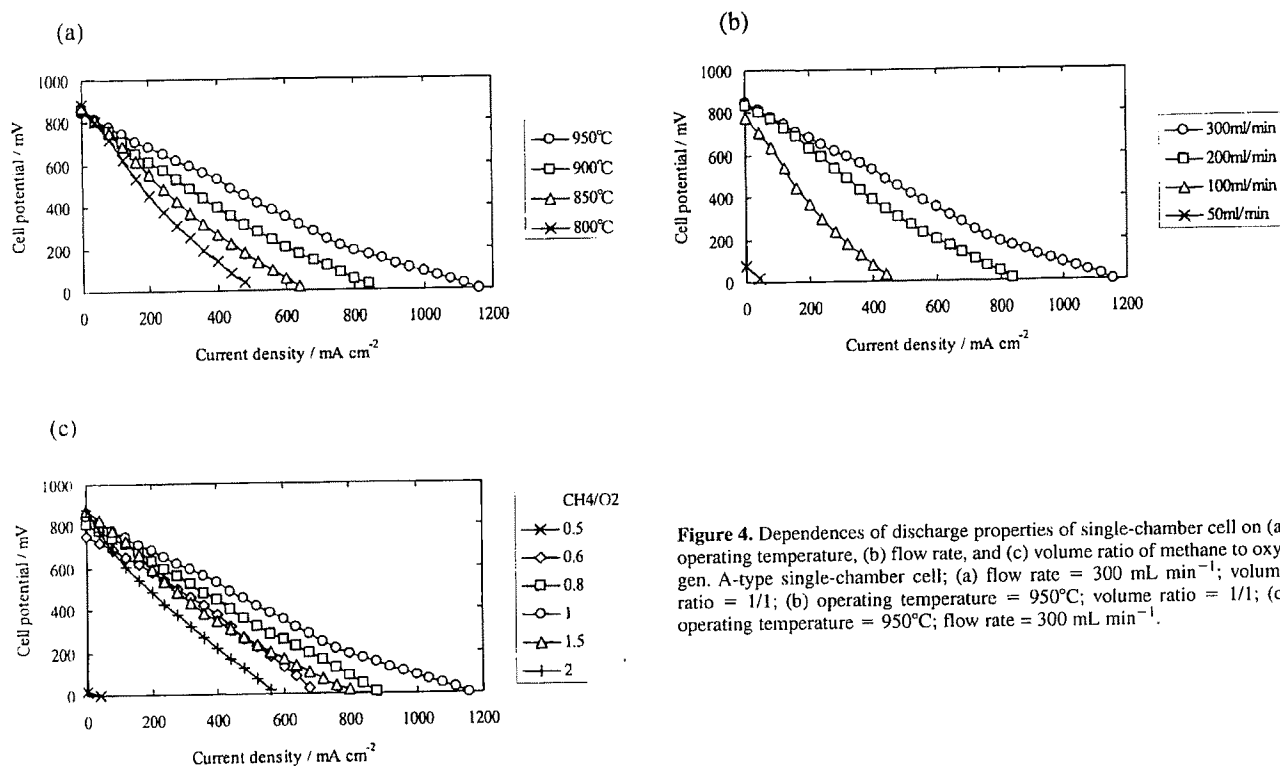


Figure 4. Dependences of discharge properties of single-chamber cell on (a) operating temperature, (b) flow rate, and (c) volume ratio of methane to oxygen. A-type single-chamber cell; (a) flow rate = 300 mL min⁻¹; volume ratio = 1/1; (b) operating temperature = 950°C; volume ratio = 1/1; (c) operating temperature = 950°C; flow rate = 300 mL min⁻¹.

the two electrodes closer to each other. Figure 6 shows the effect of the gap between the two electrodes on the discharge properties of the B-type single-chamber SOFC. The decrease in gap between the two electrodes resulted in a reduction of the potential drop and thus an enhancement in the power density. The maximum power density was 143 mW cm⁻² (396 mV at 360 mA cm⁻²) at a gap of 0.5 mm between the two electrodes. However, the power density was much smaller compared to that of the A-type single-chamber cell at a solid electrolyte thickness of 0.5 mm shown in Fig. 5. As described above, the gap between the two electrodes shown in Fig. 6 means the shortest conduction path of oxide ion between them. Each electrode is 1 mm wide; therefore, the longest conduction path of oxide ion between the two electrode is 2.5 (= 1 + 1 + 0.5) mm. As a result, the ohmic resistance of the B-type single-chamber cell at a gap of 0.5 mm between the two electrodes was 1.8 Ω cm⁻², in contrast to 0.8 Ω cm⁻² for the A-type single-chamber cell at a solid-electrolyte thickness of 0.5 mm. Therefore, if the two electrodes are in a comb-shape array, facing each other in close proximity, it will reduce effectively the electrode width, maintaining a large electrode area.

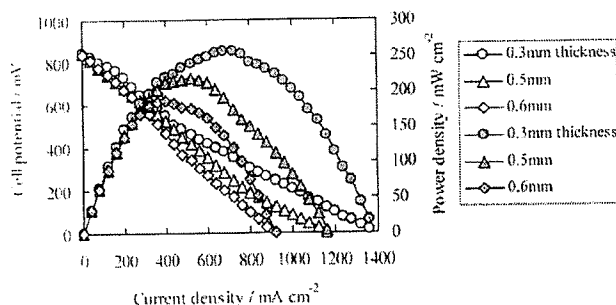


Figure 5. Effect of thickness of YSZ solid electrolyte on discharge properties of A-type single-chamber cell. Experimental conditions are the same as in Fig. 2.

Figure 7 shows the continuous discharge properties of the A-type single-chamber SOFC at a constant current density of 320 mA cm⁻². The potential of the cell gradually decreased with time during the discharge. Carbon deposition was confirmed on the Ni(GDC) electrode after the experiment. It is generally known that carbon is formed by the cracking of methane in the case of an insufficient supply of steam or the Boudouard reaction in the case of excess carbon monoxide¹⁷



Since methane is thermodynamically more unstable than carbon monoxide above 600°C,¹⁸ the carbon deposition will be mainly based on Reaction 6 under the present conditions. Therefore, the mixture of methane and air was saturated with water vapor by passing it through a water bath at room temperature. As shown in Fig. 7, the potential of the cell was maintained at a constant value of ca. 570 mV during the discharge. In addition, the carbon deposition was not at all observed after the experiment. For a future long-term stability test of the single-chamber cell, one should determine a more accurate ratio of steam to

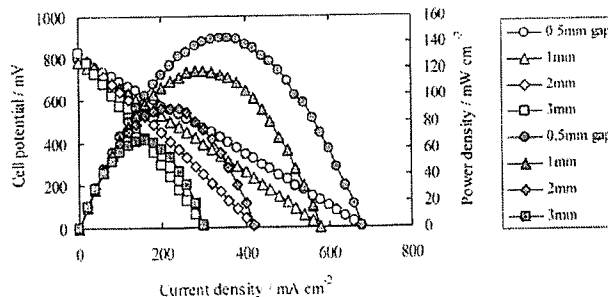


Figure 6. Effect of gap between two electrodes on discharge properties of B-type single-chamber cell. Experimental conditions are the same as in Fig. 2.

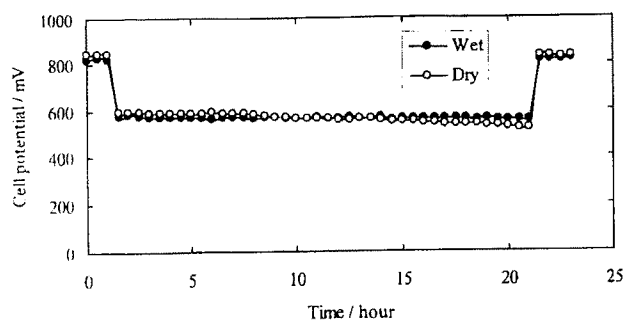


Figure 7. Continuous discharge property of single-chamber SOFC at a constant current density of 320 mA cm^{-2} . A-type single-chamber cell. Experimental conditions are the same as in Fig. 2.

carbon in the mixture of methane and air where the carbon deposition does not thermodynamically take place.

Conclusions

The performance of a single-chamber SOFC constructed from a YSZ solid electrolyte with a Ni(GDC) anode and a LSM(MnO_2) cathode can be effectively improved by the deposition of a Mn oxide layer between the solid electrolyte and the electrode. The improvement is the result of the promoted anodic and cathodic reactions, which is based on the mixed valence state of the Mn oxide. The performance of the present SOFC can be further enhanced by different processes for the reduction of the ohmic resistance of the cell. One process is the use of a thinner YSZ film when the two electrodes are arranged on opposite surfaces of the solid electrolyte. This is similar to the process for conventional SOFCs. Another process is the transfer of the two electrodes closer to each other when they are arranged on the same surface of the solid electrolyte. This offers low-cost

fabrication of the cell system in contrast to conventional SOFCs. The long-term stability of the present SOFC is also studied and found to have a direct relationship with the carbon deposition on the Ni(GDC) electrode.

National Industrial Research Institute of Nagoya assisted in meeting the publication costs of this article.

References

1. G. R. Heath and R. F. Singer, in *Proceedings of the 2nd International Symposium on Solid Oxide Fuel Cell*, F. Grosz, P. Zegers, S. C. Singhal, and O. Yamamoto, Editors, Commission of the European Communities, Brussels, Belgium (1991).
2. K. Krist and J. D. Wright, in *Proceedings of the 3rd International Symposium on Solid Oxide Fuel Cell*, S. C. Singhal and H. Iwahara, Editors, PV 93-4, p. 782, The Electrochemical Society Proceedings Series, Pennington, NJ (1993).
3. G. A. Lousi, J. M. Lee, D. L. Maricle, and J. C. Trocciola, U.S. Pat. 4,248,941 (1981).
4. T. Hibino and H. Iwahara, *Chem. Lett.*, 1131 (1993).
5. I. Riess, P. J. van der Put, and J. Schoonman, *Solid State Ionics*, **82**, 1 (1995).
6. C. Eyraud, J. Lenoir, and M. Gery, *C. R. Acad. Sci. Paris*, **252**, 1599 (1961).
7. W. van Gool, *Philips Res. Rep.*, **20**, 81 (1965).
8. C. K. Dyer, *Nature*, **343**, 547 (1990).
9. P. Moseley and D. Williams, *Nature*, **346**, 23 (1990).
10. T. Hibino, S. Wang, S. Kakimoto, and M. Sano, *Electrochem. Solid-State Lett.*, **2**, 317 (1999).
11. A. T. Ashcroft, A. K. Cheetham, J. S. Foord, M. L. H. Green, C. P. Grey, A. J. Murrell, and P. D. F. Vernon, *Nature*, **344**, 319 (1990).
12. E. J. L. Schouler, *Solid State Ionics*, **9-10**, 945 (1983).
13. B. A. Van Hassel, B. A. Boukamp, and A. J. Burggraaf, *Solid State Ionics*, **51**, 175 (1992).
14. T. Kawada, N. Sakai, H. Yokogawa, M. Dokiya, and I. Anzai, *Solid State Ionics*, **50**, 189 (1992).
15. R. F. Reidy and G. Simkovich, *Solid State Ionics*, **62**, 85 (1993).
16. K. R. Thampi, A. J. McEvoy, and J. Van herle, *J. Electrochem. Soc.*, **142**, 506 (1995).
17. Y. C. Hsiao and J. R. Selman, in *Proceedings of the 3rd International Symposium on Solid Oxide Fuel Cell*, S. C. Singhal and H. Iwahara, Editors, PV 93-4, p. 895, The Electrochemical Society Proceedings Series, Pennington, NJ (1993).
18. A. Andersen and I. M. Dahl, in *SOFC Reforming Chemistry*, p. 65, IEA Workshop on Mathematical Modeling, Charmey, Switzerland, July 2-8, 1989.

EXHIBIT 6



A Solid Oxide Fuel Cell Using an Exothermic Reaction as the Heat Source

Takashi Hibino,^{a,*} Atsuko Hashimoto,^a Takao Inoue,^b Jun-ichi Tokuno,^b Shin-ichiro Yoshida,^b and Mitsuru Sano^b

^aNational Industrial Research Institute of Nagoya, Nagoya 462-8510, Japan

^bNagoya University, Nagoya 466-0804, Japan

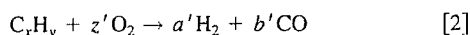
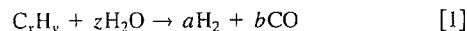
Performance of a single-chamber solid oxide fuel cell was evaluated using a 0.15 mm thick Sm-doped ceria (SDC) electrolyte together with a 30 wt % SDC-Ni anode and a $\text{Sm}_{0.5}\text{Sr}_{0.5}\text{CoO}_3$ cathode at heating temperatures below 500°C in a flowing mixture of butane and air. A large quantity of reaction heat, which was evolved by the partial oxidation of butane by oxygen at the anode, caused a temperature rise of more than 100°C at the anode, followed by thermal conduction to the cathode through the electrolyte. Simultaneously, the cell generated a large electromotive force of ca. 900 mV between the two electrodes. The resulting peak power density reached 245, 180, 105, and 38 mW cm^{-2} at heating temperatures of 450, 400, 350, and 300°C, respectively. The comparison of the butane fuel with the other hydrocarbon fuels showed that the fuel cell performance became enhanced, especially at reducing temperatures, as the carbon number of the hydrocarbon increased, and the chain structure was branched.

© 2001 The Electrochemical Society. [DOI: 10.1149/1.1368098] All rights reserved.

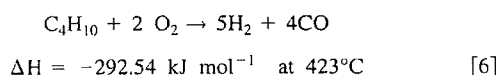
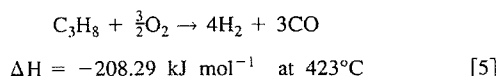
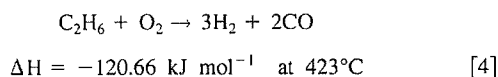
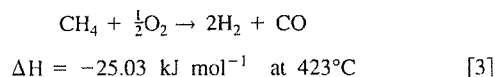
Manuscript submitted October 26, 2000; revised manuscript received February 2, 2001.

Currently, there is great interest in the development of solid oxide fuel cells (SOFCs) capable of starting up at low temperatures for vehicular applications.¹⁻⁶ A key subject for this development is the use of a highly conductive electrolyte with a highly active anode and cathode, because the operation of SOFCs under such conditions causes excessive ohmic and polarization losses in the cell. Ceria-based oxides are promising electrolytes which exhibit much higher ionic conductivities than that of yttria-stabilized zirconia (YSZ).⁷⁻¹³ In addition, metal-ceria cermets¹⁴⁻¹⁶ and Co-based perovskite oxides¹⁷⁻¹⁹ have been generally regarded as suitable anodes and cathodes, respectively, at reduced temperatures. It is, however, difficult for these materials to exhibit high performance below 400°C. For example, even a 5 μm thick Sm-doped ceria (SDC) electrolyte is calculated to show a large ohmic resistance of 7 $\Omega \text{ cm}^{-2}$ at 300°C from its ionic conductivity.

In this study, we demonstrate a novel technique enabling the SOFC to meet rapid low temperature startup criteria for electric vehicles. The conversion of hydrocarbon fuels into hydrogen and carbon monoxide is mainly achieved by two reactions: the steam reforming of hydrocarbons²⁰⁻²³ and their partial oxidation by oxygen²⁴⁻²⁷



Reaction 1 is endothermic, so that it requires a large amount of heat to sustain an adequate reaction rate. In contrast, Reaction 2 is exothermic, thus evolving reaction heat according to the carbon number of the hydrocarbons



If Reaction 2 of a higher hydrocarbon, such as butane, is used as the internal reforming reaction in the SOFC, the anode temperature can effectively increase due to the evolution of a large quantity of reaction heat. A similar increase in the temperature can also be expected for the electrolyte and the cathode by thermal conduction to the cathode through the electrolyte. A serious problem, however, arises whereby the cell cannot hold a quick temperature rise of several tens of degrees Celsius or more. In particular, the tightly stacked cells in conventional SOFCs are easily damaged by such a thermal shock. A novel single-chamber fuel cell has been proposed by many research groups.^{6,28-32} This cell consists of only one gas chamber, where the

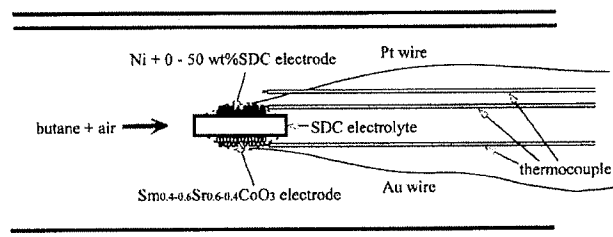


Figure 1. A schematic illustration of a single-chamber SOFC with three attached thermocouples.

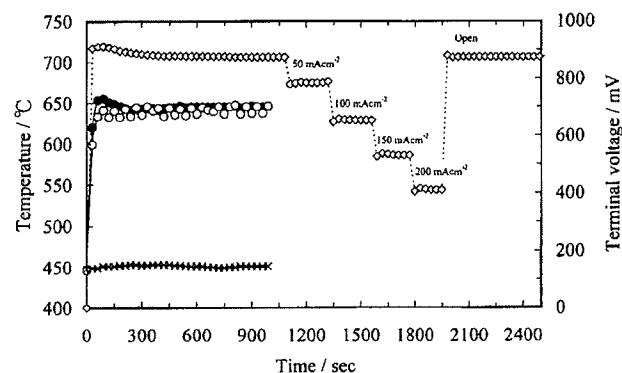


Figure 2. Transient changes in temperature at three places and EMF of a single-chamber SOFC in a mixture of butane and air at a heating temperature of 450°C. ● Anode, ○ cathode, × gas phase, ◇ EMF, anode = 30 wt % SDC-Ni, cathode = $\text{Sm}_{0.5}\text{Sr}_{0.5}\text{CoO}_3$, SDC thickness = 0.5 mm, electrode area = 0.5 cm^2 .

* Electrochemical Society Active Member.

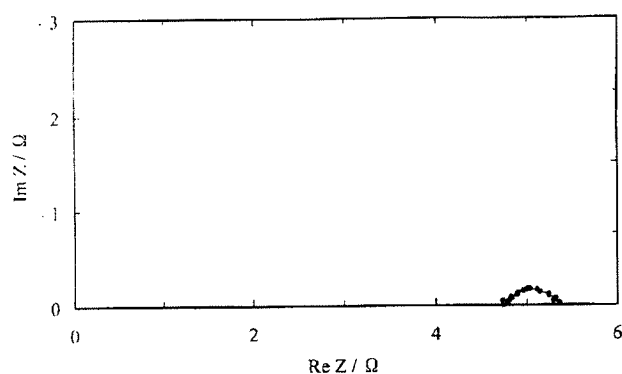


Figure 3. Impedance spectrum of a single-chamber SOFC measured by changing frequency from 0.1 to 10^5 Hz under open-circuit conditions. Experimental conditions are the same as in Fig. 2.

anode and the cathode are exposed to the same mixture of fuel and air. The resulting stacked cells are simple and loose, thus making the cell less damageable for the thermal shock than the conventional SOFCs. Therefore, we combine the advantages of using Reaction 2 of butane with the single-chamber fuel cell design.

Experimental

The SDC electrolyte used in this study was prepared by pressing a commercial ceramic powder, $\text{Ce}_{0.8}\text{Sm}_{0.2}\text{O}_{1.9}$, (Anan Kasei Co., Ltd.) hydrostatically into a pellet form at $2 \times 10^3 \text{ kg cm}^{-2}$ and then sintering in air at 1500°C for 10 h. After the pellet was cut into a disk (14 mm diam, ca. 1 mm thick), the surface was polished to a given thickness (0.15–0.50 mm) with an abrasive paper. 0–50 wt % SDC–Ni metals were used as the anodes. NiO powder was mixed with the SDC powder and then ground in ethyl carbitol using a planetary ball mill with a zirconia mill container and zirconia grinding balls at 180 revolutions per minute (rpm) for 14 h. The paste was smeared on one surface (4–8 mm diam, 0.13–0.50 cm^2 area) of the electrolyte disk as thinly as possible with a brush, then was calcined in air at 1450°C for 1 h. $\text{Sm}_{0.4-0.6}\text{Sr}_{0.6-0.4}\text{CoO}_3$ oxides were used as the cathodes. The desired amounts of Sm_2O_3 , SrCO_3 and Co_3O_4 powders were mixed in ethanol with a mortar and a pestle and then calcined in air at 1200°C for 6 h. The formed oxide was ground in ethyl carbitol using the planetary ball mill at 180 rpm for 4 h. The paste was applied on another face of the electrolyte disk in a manner similar to that stated above and then calcined in air at 965°C for 4 h.

The cell thus fabricated was set up in an alumina tube (15 and 19 mm inner and outer diam, respectively) as shown in Fig. 1. Butane was mixed with air at a concentration of 10 vol %, which deviated from the explosive limit between 1.86 and 8.41 vol %, so that the oxidation would safely proceed without exploding. Methane, ethane, propane, isobutane, and butene were also tested as the fuels for comparison. The gas mixture was supplied to the cell at flow rates of 300 mL min^{-1} between 300 and 450°C . For the measurement of the cell temperature, two thermocouples were attached on the anode and cathode surfaces, respectively, and a thermocouple was placed ca. 5 mm apart from the anode surface, where the precision was 0.1°C between 0 and 800°C . For the evaluation of the fuel-cell performance, a Pt wire and a Pt mesh were used as the output terminal and

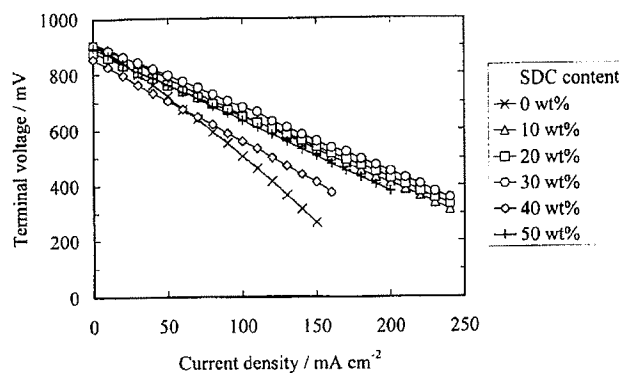


Figure 4. Discharge properties of single-chamber SOFCs using 0–50 wt % SDC–Ni anodes in a flowing mixture of butane and air at a heating temperature of 450°C . Cathode = $\text{Sm}_{0.5}\text{Sr}_{0.5}\text{CoO}_3$, SDC thickness = 0.5 mm, electrode area = 0.5 cm^2 .

the electrical collector, respectively, for the anode, and an Au wire and an Au mesh were similarly used for the cathode. The fuel-cell tests were conducted by measuring the terminal voltage between the two electrodes during cell discharge using a galvanostat (Hokuto Denko HA-501) and by measuring the impedance spectrum under open-circuit conditions using an impedance analyzer (Solartron SI-1260). The outlet gas from the cell having only the anode or the cathode was also analyzed on a dry basis using on-line gas chromatography (Shimadzu GC-8A). Hydrogen, oxygen, nitrogen, methane, and carbon monoxide were separated using a molecular sieve 5A column at 50°C , and the others were measured using a Porapak Q column between 80 and 140°C .

Results and Discussion

Fuel-cell performance at a heating temperature of 450°C .—The single-chamber SOFC using a 0.5 mm thick SDC electrolyte with 30 wt % SDC–Ni and $\text{Sm}_{0.5}\text{Sr}_{0.5}\text{CoO}_3$ electrodes was supplied with a mixture of butane and air at a heating temperature of 450°C . Figure 2 shows the transient changes in temperature at the three places stated above and the electromotive force (EMF) of the cell. Both electrode temperatures quickly rose to $\sim 600^\circ\text{C}$ and then attained respective equilibrium values of 645°C for the anode and 640°C for the cathode, although the temperature in the gas mixture was maintained at almost 450°C . Simultaneously, the cell generated a large EMF of 874 mV, where the potential of the SDC–Ni electrode was negative vs. the $\text{Sm}_{0.5}\text{Sr}_{0.5}\text{CoO}_3$ electrode. Current could be stably drawn from the cell, and the terminal voltage returned again to the initial EMF value on opening the circuit. As shown in Fig. 3, the impedance spectrum of the cell under open-circuit conditions consisted of a small and single arc, which was contributed by the impedance at the electrode-electrolyte interface, because the arc was observed between 100 and 0.1 Hz.

The temperature rise in the single-chamber SOFC and the generation of the EMF from it shown in Fig. 2 can be explained by the difference in catalytic activity between the two electrodes for the partial oxidation of butane by oxygen as shown in Table I. A large amount of hydrogen and carbon monoxide was formed over the SDC–Ni electrode, while most of the oxygen supplied remained un-

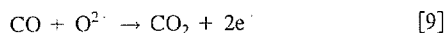
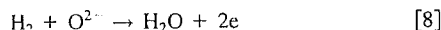
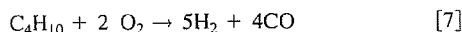
Table I. Inlet and outlet gases from cell having only Ni + 30 wt % SDC or $\text{Sm}_{0.5}\text{Sr}_{0.5}\text{CoO}_3$ electrode at 450°C . The balance gas is nitrogen.

Electrode	Inlet gas %					Outlet gas %				
	C_4H_{10}	O_2	CH_4	C_2H_6	C_3H_8	C_4H_{10}	O_2	H_2	CO	CO_2
Ni + 30 wt % SDC	10.1	20.1	0	0.1	0.1	5.9	8.1	8.1	6.5	7.7
$\text{Sm}_{0.5}\text{Sr}_{0.5}\text{CoO}_3$	9.2	21.2	0	0.1	0	8.7	20.8	0	0.3	0.3

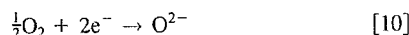
Table II. Ohmic and electrode-reaction resistances estimated from impedance spectra of single-chamber SOFCs with various anodes and cathodes at 450°C.

Electrode	Ohmic resistance (Ω)	Electrode-reaction resistance (Ω)
Ni	5.5	1.9
Ni + 10 wt % SDC	4.7	0.7
Ni + 20 wt % SDC	5.2	0.5
Ni + 30 wt % SDC	4.8	0.4
Ni + 40 wt % SDC	4.9	1.2
Ni + 50 wt % SDC	4.2	1.4
$\text{Sm}_{0.40}\text{Sr}_{0.60}\text{CoO}_3$	5.2	2.3
$\text{Sm}_{0.45}\text{Sr}_{0.55}\text{CoO}_3$	5.3	1.1
$\text{Sm}_{0.50}\text{Sr}_{0.50}\text{CoO}_3$	4.8	0.4
$\text{Sm}_{0.55}\text{Sr}_{0.45}\text{CoO}_3$	5.9	1.6
$\text{Sm}_{0.60}\text{Sr}_{0.40}\text{CoO}_3$	6.3	1.9

reacted over the $\text{Sm}_{0.5}\text{Sr}_{0.5}\text{CoO}_3$ electrode. This suggests that the reaction heat which evolved at the SDC-Ni electrode was conducted to the $\text{Sm}_{0.5}\text{Sr}_{0.5}\text{CoO}_3$ electrode through the SDC electrolyte. This also allows the SDC-Ni electrode to work as the anode in the following reactions



In contrast, the $\text{Sm}_{0.5}\text{Sr}_{0.5}\text{CoO}_3$ electrode acted as the cathode for the following reaction



Here, it should be noted that the cell after experiment was not destroyed at all.

Figure 4 shows the discharge properties of the single-chamber SOFCs using 0-50 wt % SDC-Ni anodes, where the electrolyte and the cathode were the same as those shown in Fig. 2. All these cells could supply current reproducibly, and the voltage drop was the least at an SDC content of 30 wt %. The internal resistances estimated from the impedance spectra of these cells are shown in Table II. The electrode-reaction resistance was the smallest at 30 wt % SDC content. Their scanning electron microscope (SEM) pictures showed that an increase in the SDC content resulted in a formation of SDC network and a destruction of NiO network. It seems that the addition of 30 wt % SDC to NiO leads to the optimum networks of SDC and NiO for the anodic reaction. More important was that their ohmic resistances were close to a value of 3.1 Ω calculated from the ionic conductivity of the SDC electrolyte at 650°C, rather than a value of 27 Ω calculated similarly at 450°C, which corresponds well to the results shown in Fig. 2. Figure 5 shows the corresponding result of the single-chamber SOFCs using $\text{Sm}_{0.4-0.6}\text{Sr}_{0.6-0.4}\text{CoO}_3$ cathodes, where the electrolyte and the anode were the same as those shown in Fig. 2. The discharge properties of these cells were also stable, and the least voltage drop was observed using the $\text{Sm}_{0.5}\text{Sr}_{0.5}\text{CoO}_3$ cathode. This was due to the smallest electrode-reaction resistance of the cell using the $\text{Sm}_{0.5}\text{Sr}_{0.5}\text{CoO}_3$ cathode as shown in Table II. From the SEM observations of these cathodes, it is seen that there was a slight difference in microstructure among them, suggesting that the cathodic-reaction rate is dependent on their electrical conduction, which is determined by the Sr^{2+} content. Therefore, it is concluded that the 30 wt % SDC-Ni and the $\text{Sm}_{0.5}\text{Sr}_{0.5}\text{CoO}_3$ are the best anode and cathode, respectively, among the tested electrode materials. Subsequent experiments were thus carried out using these electrodes.

Figure 6 shows the discharge properties of the single-chamber SOFCs using the two electrodes stated above of different electrode

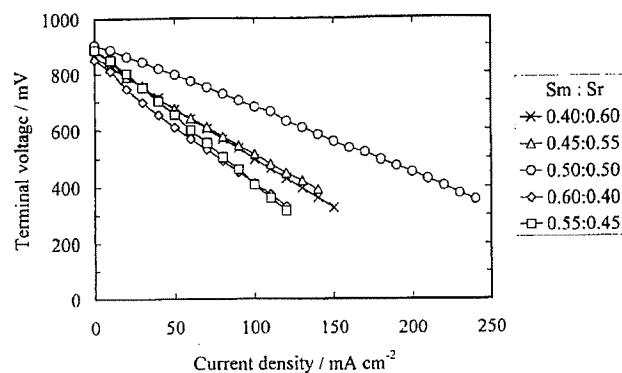


Figure 5. Discharge properties of single-chamber SOFCs using $\text{Sm}_{0.4-0.6}\text{Sr}_{0.6-0.4}\text{CoO}_3$ cathodes in a flowing mixture of butane and air at a heating temperature of 450°C. Anode = 30 wt % SDC-Ni, SDC thickness = 0.5 mm, electrode area = 0.5 cm².

areas. The voltage drop during cell discharge became somewhat smaller as the electrode area increased, thus resulting in a slightly increasing peak power density with increasing electrode area. This can be understood by the fact that the use of a large electrode promotes the partial oxidation of butane over the anode, probably causing a further temperature rise at the anode, the electrolyte and/or the cathode.

Figure 7 shows the discharge properties of the single-chamber SOFCs using the SDC electrolytes of different thicknesses. The voltage drop during cell discharge was strongly dependent on electrolyte thickness, so that the peak power density of the cell increased from 85 to 245 mW cm⁻² with decreasing electrolyte thickness from 0.50 to 0.15 mm. Their impedance spectra further clarified this point. The ohmic resistances of these cells were 4.8 Ω for 0.50 mm, 2.0 Ω for 0.25 mm, and 1.1 Ω for 0.15 mm, where the latter two values were smaller than values of 2.4 Ω for 0.25 mm and 1.4 Ω for 0.15 mm, which were predicted on the basis of the ohmic resistance for 0.50 mm. Furthermore, the electrode-reaction resistance of these cells decreased with decreasing electrolyte thickness: 0.44 Ω for 0.50 mm, 0.42 Ω for 0.25 mm, and 0.27 Ω for 0.15 mm. It can be assumed that the reaction heat which evolved at the anode is better conducted to the cathode through the electrolyte due to the decrease in electrolyte thickness, which results in an additional temperature rise at the electrolyte and/or the cathode. On the other hand, the EMF of the cell remained at almost constant values of ~890 mV for all electrolyte thickness, suggesting that the reduction of Ce^{4+} to Ce^{3+} was not significant in the SDC electrolyte during operation, because when mixed conduction is present, the EMF becomes

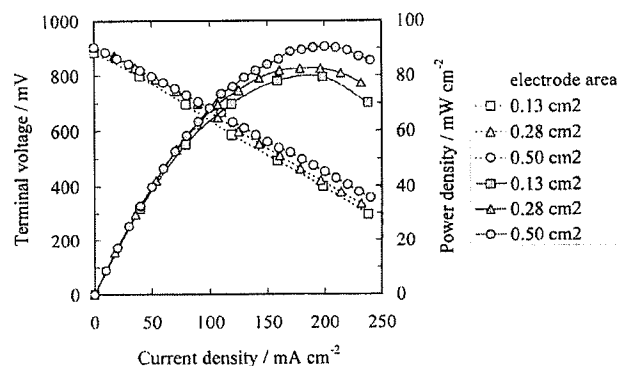


Figure 6. Dependence of performance of a single-chamber SOFC on electrode area at a heating temperature of 450°C. SDC thickness = 0.5 mm.

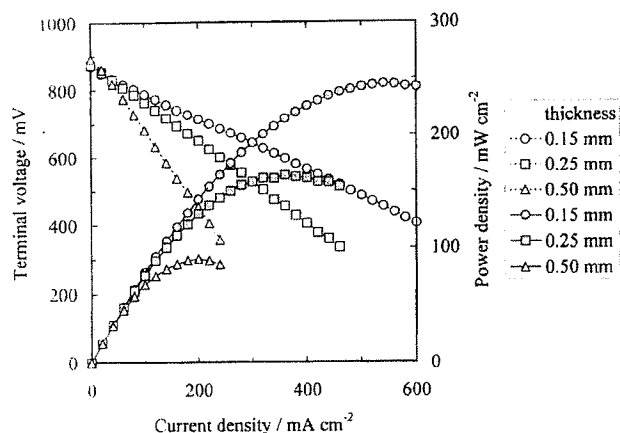


Figure 7. Dependence of performance of a single-chamber SOFC on SDC thickness at a heating temperature of 450°C. Electrode area = 0.5 cm².

smaller as electrolyte thickness decreases.³ This is supported by the fact that the single-chamber SOFC using a YSZ electrolyte gave an EMF of 915 mV under the same conditions as those stated above.

Fuel-cell performance at heating temperatures below 450°C.—The temperatures of the anode and cathode surfaces were measured by supplying a mixture of butane and air at heating temperatures below 450°C. These results are shown in Fig. 8a and b. The exothermic effect of the partial oxidation of butane by oxygen on the two electrode surfaces was confirmed at heating temperatures from 400 to 200°C, below which such an effect disappeared. The increment in the anode temperature was somewhat larger than that

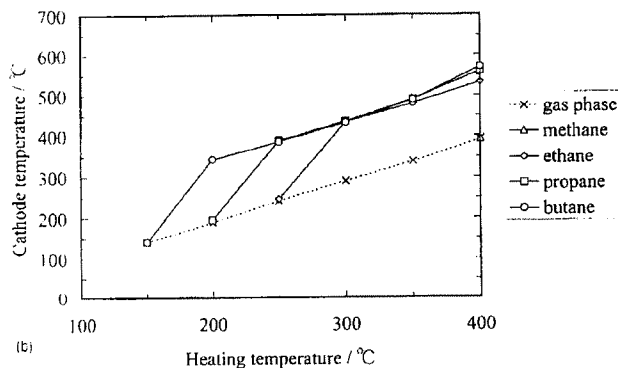
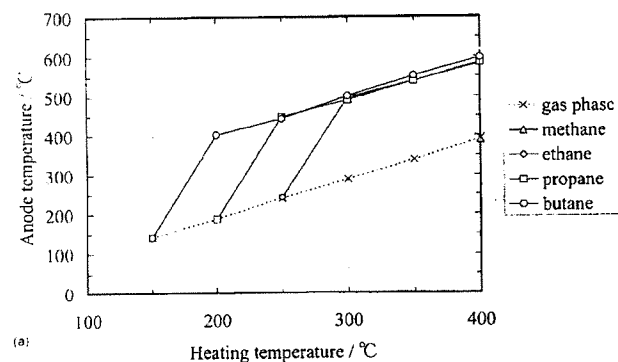


Figure 8. (a) Anode and (b) cathode temperatures in a flowing mixture of different hydrocarbons and air at heating temperatures below 450°C. SDC thickness = 0.5 mm, electrode area = 0.5 cm².

Table III. Catalytic activities of Ni + 30 wt % SDC and Sm_{0.5}Sr_{0.5}CoO₃ electrodes for partial oxidation of hydrocarbons by oxygen.

Temp (°C)	Conversion %				
	CH ₄	C ₂ H ₆	C ₃ H ₈	C ₄ H ₁₀	O ₂
Ni + 30 wt % SDC					
0	0	-	-	-	1
400	-	32	-	-	57
	-	-	34	-	57
	-	-	-	35	54
350	0	-	-	-	1
	-	20	-	-	53
	-	-	30	-	52
	-	-	-	26	46
300	0	-	-	-	0
	-	20	-	-	53
	-	-	23	-	52
	-	-	-	25	46
250	0	-	-	-	0
	-	10	-	-	22
	-	-	24	-	49
	-	-	-	24	46
200	0	-	-	-	0
	-	0	-	-	4
	-	-	6	-	20
	-	-	-	22	45
Sm _{0.5} Sr _{0.5} CoO ₃					
0	0	-	-	-	0
400	-	5	-	-	3
	-	-	5	-	6
	-	-	-	2	1
350	0	-	-	-	0
	-	3	-	-	3
	-	-	1	-	4
	-	-	-	3	0
300	0	-	-	-	0
	-	3	-	-	3
	-	-	3	-	3
	-	-	-	3	0
250	0	-	-	-	0
	-	2	-	-	2
	-	-	2	-	2
	-	-	-	3	1
200	0	-	-	-	0
	-	0	-	-	0
	-	-	0	-	0
	-	-	-	1	1

in the cathode temperature at any heating temperature, and both increments became gradually smaller as the heating temperature decreased. Figure 8a and b also includes the results using methane, ethane, and propane as the fuels for comparison. The lower limit of the exothermic effect was dependent on the hydrocarbon species. This effect did not appear for methane at all the tested heating temperatures, and it disappeared at 250°C for ethane and 200°C for propane.

In order to understand the above dependence, the composition of the outlet gas from the cell having only the SDC-Ni or Sm_{0.5}Sr_{0.5}CoO₃ electrode was measured between 200 and 400°C. The conversions of the hydrocarbons and oxygen, which are based on this measurement, are summarized in Table III. The SDC-Ni anode exhibited relatively high catalytic activities for the partial oxidation of butane at all the tested temperatures, therefore, the exothermic effect appeared between 200 and 400°C as shown in Fig. 8a and b. However, the catalytic activity of the anode for the partial oxidation of the other hydrocarbons became abruptly smaller at heating temperatures of 400 for methane, 250 for ethane, and 200°C for propane, which corresponded roughly to the results shown in Fig. 8a and b.

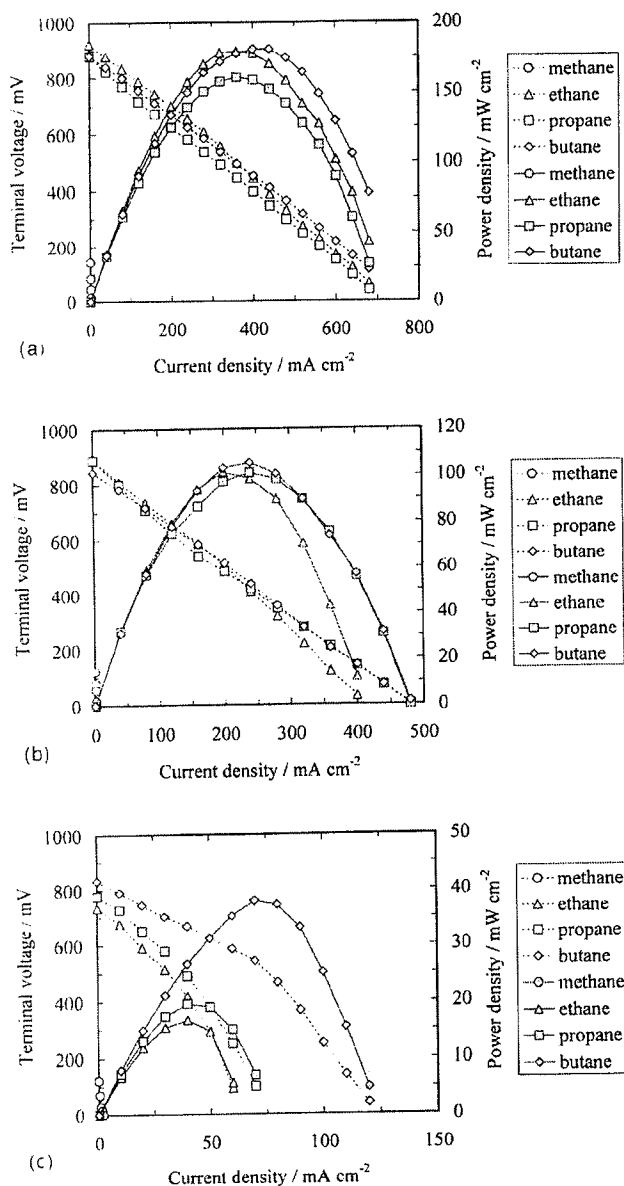


Figure 9. Performance of a single-chamber SOFC in a flowing mixture of different hydrocarbons and air at heating temperatures of (a) 400°C, (b) 350°C, and (c) 300°C. SDC thickness = 0.15 mm, electrode area = 0.5 cm².

The discharge properties of the single-chamber SOFC at heating temperatures between 300 and 400°C were measured using the 0.15 mm thick SDC electrolyte. The results are shown in Fig. 9a, b, and c. At a heating temperature of 400°C (Fig. 9a), the cell exhibited relatively good performance with the hydrocarbons other than methane. The peak power density was still greater than 160 mW cm⁻² using ethane, propane, and butane, although its value was almost 0 mW cm⁻² using methane. Their impedance spectra showed small electrode-reaction resistances below 0.7 Ω, suggesting that the cell performance would be improved further using an even thinner electrolyte film. A similarity in discharge properties among ethane, propane, and butane was also observed at a heating temperature of 350°C, although their peak power densities were reduced to ca. 100 mW cm⁻² (Fig. 9b). At a heating temperature of 300°C (Fig. 9c), however, there was a large difference in discharge properties among

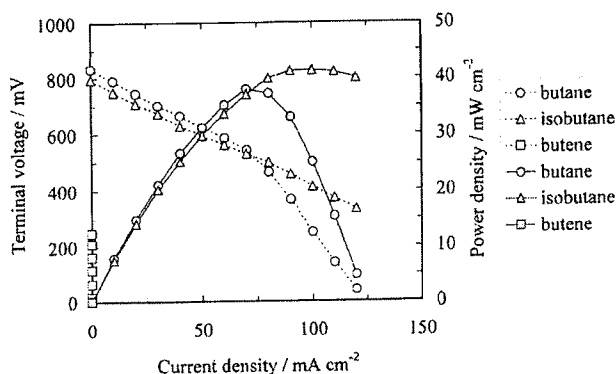
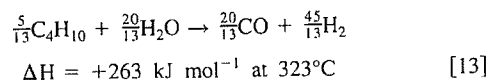
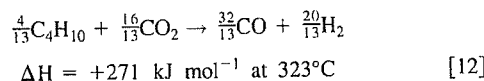
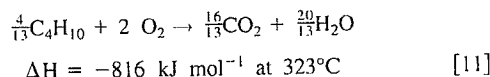


Figure 10. Performances of a single-chamber SOFC in a flowing mixture of C4 hydrocarbons and air at a heating temperature of 300°C. SDC thickness = 0.15 mm, electrode area = 0.5 cm².

the three hydrocarbons: The order of the peak power density was ethane < propane < butane. As shown in Fig. 8a and b, the exothermic effect was still observed using these hydrocarbons under the present conditions; thereby, this would not explain the above difference. An explanation for this difference is provided by the total formation amounts of hydrogen and carbon monoxide and the impedance spectra of the cell: The total formation amounts of hydrogen and carbon monoxide decreased in the order of butane > propane > ethane; The electrode-reaction resistance decreased in the order of ethane (10.6 Ω) > propane (9.3 Ω) > butane (4.7 Ω). It is generally said that the partial oxidation of hydrocarbons by oxygen takes place through the following reactions using butane as an example, although each of these reactions consists of a complex set of elementary steps³³



Reaction 11 is largely exothermic, while Reactions 12 and 13 are endothermic. In addition, Reactions 12 and 13 proceed at very slow rates, especially at reduced temperatures, compared to Reaction 11. Assuming that these also apply to the present case, the rate of Reaction 11 will be only slightly affected by the carbon number of the hydrocarbon, thus causing a temperature rise in the cell, regardless of the hydrocarbon species. However, the rates of Reactions 12 and 13 will be strongly dependent on the carbon number of the hydrocarbon, because their reactivity increases in that order, thereby resulting in an increasing formation amount of hydrogen and carbon monoxide with increasing carbon number of the hydrocarbon. Accordingly, the anodic reaction resistance decreased with increasing carbon number of the hydrocarbon, which provided a difference in discharge properties among the hydrocarbons.

We finally evaluated the discharge properties of the single-chamber SOFC using isobutane and butene as the fuels at a heating temperature of 300°C in order to clarify the above assumption. As shown in Fig. 10, the discharge properties of the cell were improved using the isobutane fuel. As a general view, the reactivity of butane is enhanced when branched to isobutane,³⁴ thus permitting a further decrease in the anodic reaction resistance. The discharge properties of the cell, however, became worse using the butene fuel. After operation, a large amount of carbon was deposited on the anode and

the Pt mesh using butene, although no evidence of the carbon deposition was shown using the other hydrocarbons. This is mainly due to the small H/C ratio of the butene molecule of 2: H/C ratio = 4 for methane, 3 for ethane, 2.7 for propane, and 2.5 for butane. Probably, this carbon deposition would poison the catalytic site on the Ni surface or mechanically destroy the SDC-Ni anode. Because of their similar H/C ratios, one can also expect that the use of pentane or hexane as the fuel would bring about a significant carbon deposition equally on the anode. We thus conclude that butane and isobutane can be successfully used as the fuels in the present single-chamber SOFC, especially at reducing temperatures.

Conclusions

The use of the partial oxidation of butane by oxygen as the internal reforming reaction in a single-chamber SOFC successfully reduced the starting temperature to 450°C or less. This was achieved for two reasons: the evolution of a large quantity of reaction heat and the use of the single-chamber cell design. In addition, the use of an SDC electrolyte together with 30 wt % SDC-Ni and $\text{Sm}_{0.5}\text{Sr}_{0.5}\text{CoO}_3$ electrodes permitted an improved power density with decreasing electrolyte thickness. This offers the possibility that the fabrication of a thin electrolyte film would further enhance the position of the present SOFC as a power source for transportation.

The National Industrial Research Institute of Nagoya assisted in meeting the publication costs of this article.

References

1. J. P. P. Huijsmans, F. P. F. van Berkel, and G. M. Christie, *Solid State Ionics*, **71**, 107 (1998).
2. E. P. Murray, T. Tsai, and S. A. Barnett, *Nature (London)*, **400**, 649 (1999).
3. R. Doshi, Von L. Richards, J. D. Carter, X. Wang, and M. Krumpelt, *J. Electrochem. Soc.*, **146**, 1273 (1999).
4. S. Park, J. M. Vohs, and R. J. Gorte, *Nature (London)*, **404**, 265 (2000).
5. J. Van herle, R. Ihringer, N. M. Sammes, G. Tompsett, K. Kendall, K. Yamada, C. Wen, I. Kawada, M. Ihara, and J. Mizusaki, *Solid State Ionics*, **132**, 333 (2000).
6. T. Hibino, A. Hashimoto, T. Inoue, J. Tokuno, S. Yoshida, and M. Sano, *Science*, **288**, 2031 (2000).
7. B. C. H. Steele, *J. Power Sources*, **49**, 1 (1994).
8. S. Desouza, S. J. Visco, and L. C. Dejonghe, *J. Electrochem. Soc.*, **144**, 35 (1997).
9. M. Gödickemeier, K. Sasaki, L. I. Gauckler, and I. Riess, *J. Electrochem. Soc.*, **144**, 1635 (1997).
10. M. Sahibzada, B. C. H. Steele, K. Zheng, R. A. Rudkin, and I. S. Metcalfe, *Catal. Today*, **38**, 459 (1997).
11. C. Hatchwell, N. M. Sammes, and I. W. M. Brown, *Solid State Ionics*, **126**, 201 (1999).
12. B. C. H. Steele, *Solid State Ionics*, **129**, 95 (2000).
13. W. Huang, P. Shuk, and M. Greenblatt, *J. Electrochem. Soc.*, **147**, 439 (2000).
14. E. J. L. Schouler and M. Kleitz, *J. Electrochem. Soc.*, **134**, 1045 (1987).
15. B. C. H. Steele, I. Kelly, H. Middleton, and R. Rudkin, *Solid State Ionics*, **28-30**, 1547 (1988).
16. M. Mogensen, B. Kindl, and B. Malmgren-Hansen, Abstracts of 1990 Fuel Cell Seminar, p. 195, Phoenix, AZ, Nov 25-28, 1990.
17. B. C. H. Steele, *Solid State Ionics*, **86-88**, 1223 (1996).
18. M. H. R. Lankhorst, H. J. M. Bouwmeester, and H. Verweij, *Solid State Ionics*, **96**, 21 (1997).
19. S. B. Adler, *Solid State Ionics*, **111**, 125 (1998).
20. A. L. Lee, R. F. Zabransky, and W. J. Huber, *Ind. Eng. Chem. Res.*, **29**, 766 (1990).
21. E. Achenbach and E. Riensche, *J. Power Sources*, **52**, 283 (1994).
22. V. D. Belyaev, T. I. Politova, O. A. Marina, and V. A. Sobyenin, *Appl. Catal., B*, **133**, 47 (1995).
23. A. L. Dicks, *Appl. Catal., B*, **61**, 113 (1996).
24. D. Eng and M. Stoukides, *Catal. Rev. Sci. Eng.*, **33**, 375 (1991).
25. S. Bebelis, I. V. Yentekakis, S. Neophytides, P. Tsiakaras, H. Karasali, and C. G. Vayenas, in *Proceedings of the Third International Symposium on Solid Oxide Fuel Cells*, S. C. Singhal and H. Iwahara, Editors, PV 93-4, p. 926, The Electrochemical Society Proceedings Series, Pennington, NJ (1993).
26. T. M. Gür, H. Wise, and R. A. Huggins, *Catal. Lett.*, **23**, 387 (1994).
27. T. Yamada, Y. Hiei, T. Akbay, T. Ishihara, and Y. Takita, *Solid State Ionics*, **113-115**, 253 (1998).
28. G. A. Louis, J. M. Lee, D. L. Maricle, and J. C. Troccoli, U.S. Pat. 4,248,941 (1981).
29. C. K. Dyer, *Nature (London)*, **343**, 547 (1990).
30. P. Moseley and D. Williams, *Nature (London)*, **346**, 23 (1990).
31. T. Hibino and H. Iwahara, *Chem. Lett.*, 1131 (1993).
32. I. Riess, P. J. van der Put, and J. Schoonman, *Solid State Ionics*, **82**, 1 (1995).
33. P. D. F. Vernon, M. L. H. Green, A. K. Cheetham, and A. T. Ashcroft, *Catal. Lett.*, **6**, 181 (1990).
34. J. D. Roberts, R. Stewart, and M. C. Caserio, *Organic Chemistry*, p. 53, W. A. Benjamin, Inc, California (1971).

EXHIBIT 7



High Performance Anodes for SOFCs Operating in Methane-Air Mixture at Reduced Temperatures

Takashi Hibino,^{a,*} Atsuko Hashimoto,^a Masaya Yano,^b Masanori Suzuki,^b Shin-ichiro Yoshida,^b and Mitsuru Sano^b

^aCeramics Research Institute, National Institute of Advanced Industrial Science and Technology (AIST), Nagoya 462-8510, Japan

^bGraduate School of Human Information, Nagoya University, Nagoya 466-0804, Japan

Electrocatalytic oxidation of methane over anodes in single-chamber solid oxide fuel cells, 0-10 wt % Pd-30 wt % $\text{Ce}_{0.8}\text{Sm}_{0.2}\text{O}_{1.9}$ (samaria-doped ceria, SDC)-Ni|SDC| $\text{Sm}_{0.5}\text{Sr}_{0.5}\text{CoO}_3$, was studied in a mixture of methane and air between 450 and 550°C. The addition of a small amount of Pd (0.145 mg cm^{-2}) to the anode significantly promoted the partial oxidation of methane by oxygen to form hydrogen and carbon monoxide, which resulted in electromotive forces of ca. 900 mV from the cell and extremely small electrode-reaction resistances of the anode. The peak power densities, when using a 0.15 mm thick SDC electrolyte, reached 644, 467, and 269 mW cm^{-2} at 550, 500, and 450°C, respectively.

© 2002 The Electrochemical Society. [DOI: 10.1149/1.1430226] All rights reserved.

Manuscript submitted April 12, 2001; revised manuscript received August 13, 2001. Available electronically December 20, 2001.

Fuel-cell cogeneration (heat and electricity) systems will be introduced into homes in the near future, because of their high efficiencies (~80%), low emissions of polluting gases (~5 ppm nitrogen oxides), and little vibration noise (~65 dB). The development of these applications has been directed toward polymer electrolyte fuel cells (PEFCs) operating on hydrogen fuel which is formed by the external reforming of city gas. Direct methane fuel cells have attracted great interest since Murray *et al.* have had success with a solid oxide fuel cell (SOFC) which meets this criterion at operating temperatures around 600°C.¹ Such SOFCs, if applied to residential applications, would have some advantages over PEFCs: they would eliminate the need of an external reformer of city gas, thus permitting an improved energy efficiency and a reduced fabrication cost.² However, the performance of SOFCs below 600°C, so far reported, was far lower than that of PEFCs: For example, the peak power densities at 550°C were 125 mW cm^{-2} using an 8 μm thick yttria-stabilized zirconia (YSZ) film¹ and 195 mW cm^{-2} using a 30 μm thick samaria-doped ceria (SDC) film,³ whereas peak power densities of more than 500 mW cm^{-2} are easily achievable in PEFCs. We also reported that although a single-chamber SOFC using the SDC electrolyte exhibited relatively high peak power densities of 282 and 231 mW cm^{-2} with ethane and propane fuels, respectively, even at 450°C, it showed very small peak power densities of several $\mu\text{W cm}^{-2}$ with methane fuel below 600°C due to its electromotive forces (EMFs) less than 200 mV.⁴

One of the reasons for such low power densities would be insufficient catalytic activity of the used ceria-Ni anodes for the electrochemical or nonelectrochemical oxidation of methane at reduced temperatures. Several studies⁵⁻⁷ on the methane oxidation over supported catalysts showed that methane was activated over supported Ru, Ph, Pd, and Pt catalysts besides supported Ni catalysts. Furthermore, Watanabe and Uchida *et al.* reported that the steam reforming reaction of methane was enhanced by the support of some noble metal catalysts on a SDC anode.^{8,9} In this study, we thus fabricated single-chamber SOFCs with Ni-SDC anodes catalyzed by different metals between 450 and 550°C. As a result, it was found that the addition of a small amount of Pd to the anode significantly improved the performance of the SOFC operating in a mixture of methane and air, which would further enhance the position of SOFCs as a residential cogeneration system.

Experimental

A SDC ($\text{Ce}_{0.8}\text{Sm}_{0.2}\text{O}_{1.9}$) electrolyte and a $\text{Sm}_{0.5}\text{Sr}_{0.5}\text{CoO}_3$ cathode were the same as those used previously.⁴ 0-10 wt % metal oxide

(PdO, PtO_2 , Rh_2O_3 or RuO_2)-30 wt % SDC-containing NiO cermets were used as the anodes in this study. The desired amounts PdO, PtO_2 , Rh_2O_3 , or RuO_2 (each 99.9%, Koch chemicals), SDC (99.8%, Anan Kasei), and NiO (99.9%, Kojundo Chemical Lab) powders was mixed in ethyl carbitol (99.0%, Kishida Chemicals) and then ground using a planetary ball mill with a zirconia mill container and zirconia grinding balls at 180 revolutions per minute (rpm) for 14 h. The paste was smeared on one surface (0.126-0.630 cm^2 area) of the electrolyte disk as thinly as possible with a brush, followed by calcining in air at 1450°C for 1 h. Scanning electron micrographs (SEMs) of the anodes after calcining showed that their thicknesses were typically 8-17 μm . The preparation of the $\text{Sm}_{0.5}\text{Sr}_{0.5}\text{CoO}_3$ powders were described in detail elsewhere.¹⁰ The paste was applied on another face of the electrolyte disk in a manner similar to that stated above and then calcined in air at 900°C for 4 h.

The cell thus fabricated was set up in an alumina tube (15 and 19 mm inner and outer diameters, respectively) as shown in Fig. 1. A Pt wire and a Pt mesh were used as the output terminal and the electrical collector, respectively, for the anode, and an Au wire and an Au mesh were similarly used for the cathode. These metals have been used since we first constructed a series of single-chamber SOFCs.¹¹ Mixtures of methane and air having different volume ratios of methane to oxygen from 1.0 to 2.0 were supplied to the cell at flow rates of 300 mL min^{-1} between 450 and 550°C. The fuel-cell tests were carried out by measuring the terminal voltage between the two electrodes during cell discharge using a galvanostat (Hokuto Denko HA-501) and by measuring the impedance spectrum under open-circuit conditions using an impedance analyzer (Solartron SI-1260). The outlet gas from the cell having only the anode without the Pt mesh or the cathode without the Au mesh was also analyzed

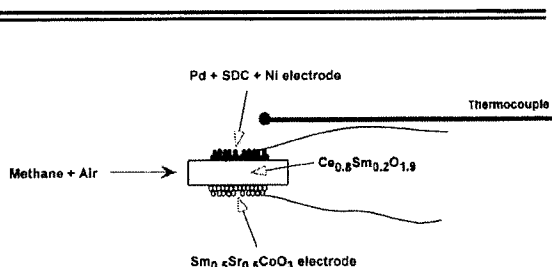


Figure 1. A schematic illustration of a single-chamber SOFC.

* Electrochemical Society Active Member.

* E-mail: thibino@nirin.go.jp

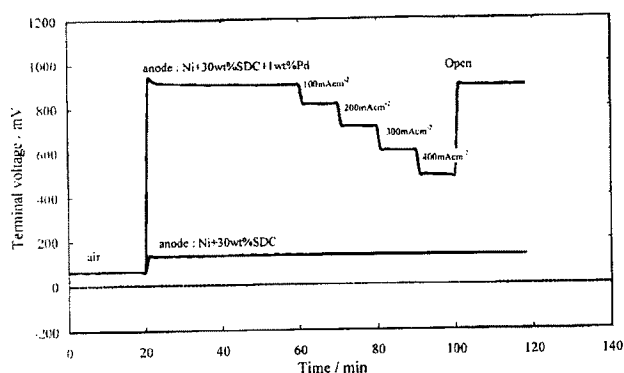


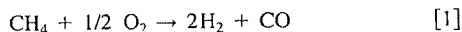
Figure 2. Transient changes in EMF generated from two SOFCs in a mixture of methane and air: PdO content = 1 wt %, electrode area = 0.5 cm², electrolyte thickness = 0.5 mm, CH₄/O₂ = 2/1, operating temperature = 550°C

on a dry basis using on-line gas chromatography (Shimadzu GC-8A). Hydrogen, oxygen, nitrogen, methane, and carbon monoxide were separated using a molecular sieve 5A column at 50°C, and the others were measured using a Porapak Q column between 80 and 140°C.

Results and Discussion

Figure 2 shows the transient changes in the EMF generated from two SOFCs using a 0.5 mm thick SDC electrolyte in a flowing mixture of methane and air at 550°C. The SOFC with a Pd-free anode generated a very small EMF of 110 mV and could not thus supply current practically. These results were in striking contrast to those of the SOFC operating in a mixture of ethane or propane and air as described above: EMFs of ca. 900 mV were generated from the cell.⁴ This can be explained by the fact that methane is the most unreactive among hydrocarbons. However, a significant improvement in the performance of the SOFC was achieved by the addition of 1 wt % PdO to the anode. The EMF generated from the SOFC quickly rose to 941 mV and then reached to a constant value of 910 mV. Current could be reproducibly drawn from the SOFC, where the voltage drop was on the average 105 mV per 100 mA cm⁻². Preliminary experiments showed that the addition of PtO₂, Rh₂O₃, or RuO₂ to the anode had a very slight or small enhancement effect on the performance of the SOFC.

From the analysis of the outlet gas from the cell having only the anode or the cathode (Table I), it was found that the partial oxidation of methane by oxygen proceeded to form a large amount of hydrogen and carbon monoxide over the PdO-containing anode, whereas such an oxidation proceeded at a very slow rate over the PdO-free anode similar to that over the cathode



Therefore, it can be predicted that the PdO-containing anode shows a significantly negative potential based on the following reactions

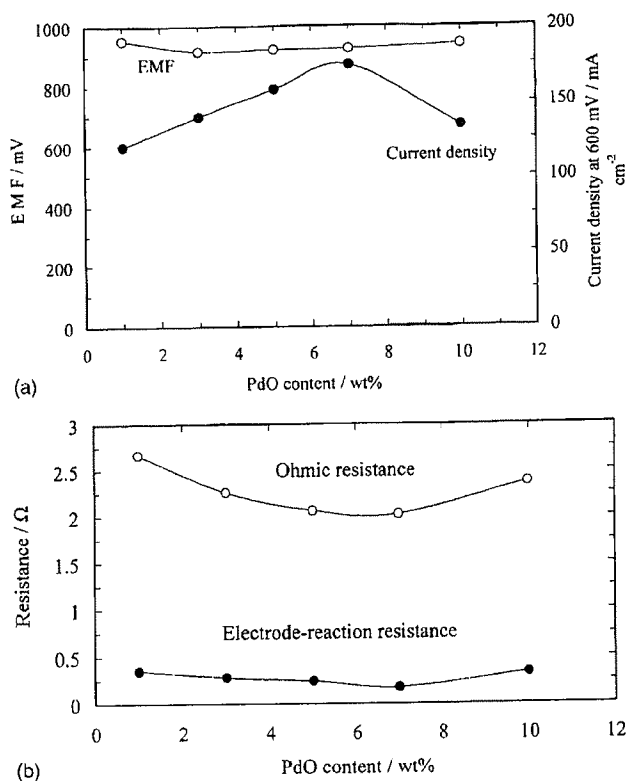
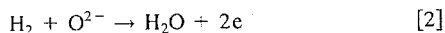
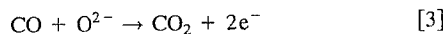
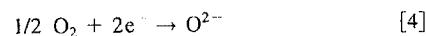


Figure 3. Dependences of SOFC performance on PdO contents: (a) EMF and current density at 600 mV, (b) ohmic and electrode-reaction resistances, electrode area = 0.5 cm², electrolyte thickness = 0.5 mm, CH₄/O₂ = 2/1, operating temperature = 550°C.



On the other hand, the potential of PdO-free anode, as well as the cathode, is determined by the following reaction of a large amount of the unreacted oxygen



As a result, the SOFC with the PdO-containing anode exhibited the large EMF as shown in Fig. 2.

Figure 3a shows the performance of the SOFCs with the PdO-containing anodes having different PdO contents at 550°C. Although the EMF was almost unchanged by the increase in PdO content, the current density at a cell voltage of 600 mV showed a maximum near 7 wt %. The impedance spectra of these SOFCs further clarified this point (Fig. 3b): The order of the ohmic resistance was 2.02 Ω (7 wt %) < 2.06 Ω (5 wt %) < 2.26 Ω (3 wt %) < 2.37 Ω (10 wt %) < 2.67 Ω (1 wt %); the order of the electrode-reaction resistance was 0.17 Ω (7 wt %) < 0.24 Ω (5 wt %) < 0.28 Ω (3 wt %) < 0.33 Ω (10 wt %)

Table I. Catalytic activities of three electrodes for partial oxidation of methane by oxygen at 550°C. The composition of the inlet gas was 30 vol % methane, 15 vol % oxygen, and 55 vol % nitrogen.

Electrode	Conversion percentage		Gas composition percentage			Carbon balance percentage
	CH ₄	O ₂	H ₂	CO	CO ₂	
None	-	-	0	0	0	
1 wt % Pd-30 wt % SDC-Ni	25.9	78.5	5.3	3.3	9.2	102.98
30 wt % SDC-Ni	0.6	1.9	0	0	0.3	100.51
Sm _{0.5} Sr _{0.5} O ₃	0.5	0.8	0	0	0.1	99.82

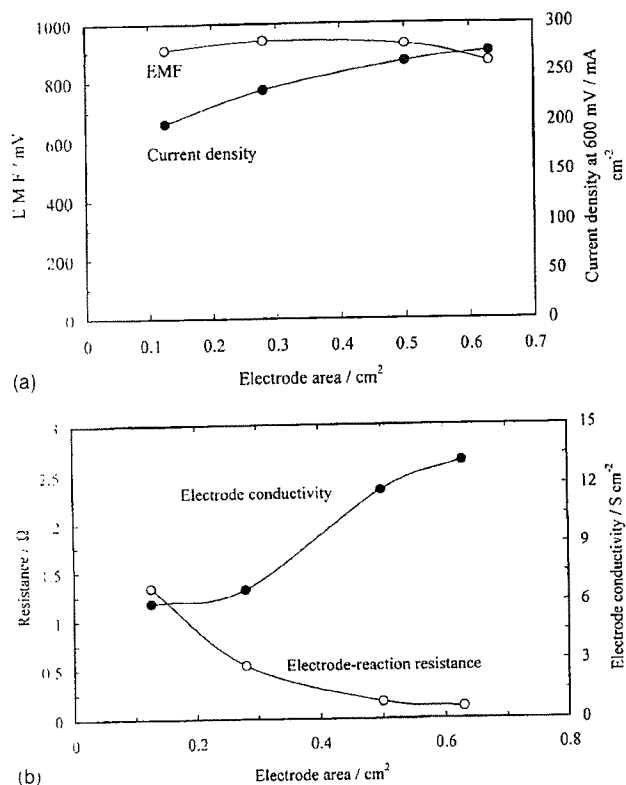


Figure 4. Dependences of SOFC performance on electrode area: (a) EMF and current density at 600 mV, (b) electrode-reaction resistance and electrode conductivity. PdO content = 7 wt %, electrolyte thickness = 0.5 mm, $\text{CH}_4/\text{O}_2 = 2/1$, operating temperature = 550°C.

< 0.35 Ω (1 wt %). An explanation for these orders is provided by the fact that the catalytic activity of the anode for Reaction 1 was the highest near 7 wt % PdO, probably causing a further reduction of Ni(O) to Ni at the anode. Here, it should be noted that the amount of Pd at 7 wt % PdO was just 0.145 mg cm⁻², which is comparable to that of Pt in PEFCs.¹² Although the current price of Pd (\$821 per 1 oz) is somewhat higher than that of Pt (\$598 per 1 oz), the anode in the present SOFC does not require the use of Ru¹³ (\$290 per 1 oz) or Rh¹⁴ (\$2,333 per 1 oz) as the additive to depress poisoning by carbon monoxide, in contrast to the anode in PEFCs. We used the 7 wt % PdO-containing anode in subsequent experiments.

The performance of the SOFCs with different cell sizes was also studied at 550°C. The EMFs were in the range of 909 to 934 mV from 0.126 to 0.500 cm², but it suddenly dropped to 865 mV at 0.630 cm² (Fig. 4a). Although we cannot give a precise solution to the cause, there may be nonuniformity of the gas flow or the temperature in such a cell. The current density at 600 mV became gradually enhanced as the electrode area increased. This enhancement was attributable to a reducing electrode-reaction resistance with increasing electrode area (Fig. 4b): 1.34 Ω (0.126 cm²) > 0.54 Ω (0.280 cm²) > 0.17 Ω (0.500 cm²) > 0.12 Ω (0.630 cm²). The electrode-reaction kinetics are often discussed on the basis of electrode conductivity, σ_e (S cm⁻²) = 1/Re (Ω cm²). σ_e thus estimated was the order of 5.92 S cm⁻² (0.126 cm²) < 6.61 S cm⁻² (0.280 cm²) < 11.7 S cm⁻² (0.500 cm²) < 13.2 S cm⁻² (0.630 cm²). This order can be understood by the fact that the conversion of methane into hydrogen and carbon monoxide was enhanced by the increase in electrode area, thus resulting in an activation of Reactions 2 and 3 at the anode. More important was the extremely small electrode-reaction resistance of 0.12 Ω at 0.630 cm², suggesting that the per-

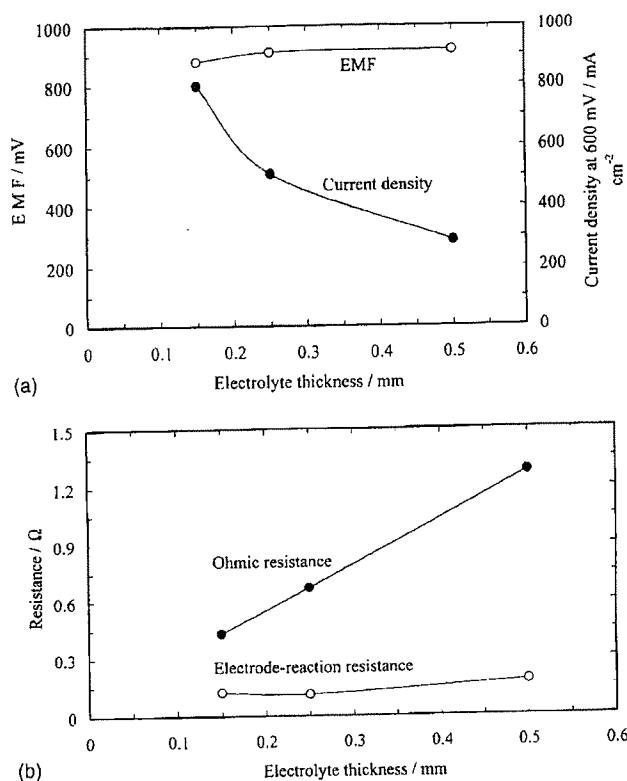


Figure 5. Dependences of SOFC performance on electrolyte thickness: (a) EMF and current density at 600 mV, (b) ohmic and electrode-reaction resistances, PdO content = 7 wt %, electrode area = 0.63 cm², $\text{CH}_4/\text{O}_2 = 2/1$, operating temperature = 550°C.

formance of the SOFC would be further improved using a thinner electrolyte film.

Evidence for the above suggestion is provided by the performance of the SOFCs using the SDC electrolytes with different thicknesses at 550°C (Fig. 5a). The current density at 600 mV using the SDC electrolytes with thicknesses of 0.50, 0.25, and 0.15 mm were 286, 508, and 800 mA cm⁻², respectively. This is simply due to a reduction of the ohmic resistance of the SDC electrolyte (Fig. 5b). The ohmic resistance was reduced from 1.28 to 0.43 Ω with decreasing electrolyte thickness from 0.50 to 0.15 mm, while the electrode-reaction resistance was not significantly dependent on the electrolyte thickness. On the other hand, the EMF remained at almost constant values of ca. 900 mV for all electrolyte thicknesses, suggesting that the reduction of Ce⁴⁺ to Ce³⁺ was not significant in the SDC electrolyte during operation, because when mixed conduction is present, the EMF becomes smaller as electrolyte thickness decreases.¹⁵

The dependence of the performance of the SOFC on operating conditions (e.g., volume ratio of methane to oxygen and operating temperature) was also studied. Reaction 1 shows that the volume ratio of methane to oxygen of 2 corresponds to a stoichiometric value for the partial oxidation of methane by oxygen. However, the peak power density was enhanced when the volume ratio of methane to oxygen was shifted to lean conditions (Fig. 6). Similar dependence was observed in their impedance spectra, where the electrode-reaction resistance was reduced from 0.12 to 0.06 Ω by the decrease in volume ratio of methane to oxygen from 2 to 1. Probably, the increase in oxygen concentration in the gas mixture may raise the rate of Reaction 4 at the cathode. The resulting peak power density reached 644 mW cm⁻² at a volume ratio of methane to oxygen of 1.

Furthermore, Reaction 1 is thermodynamically possible even below 550°C

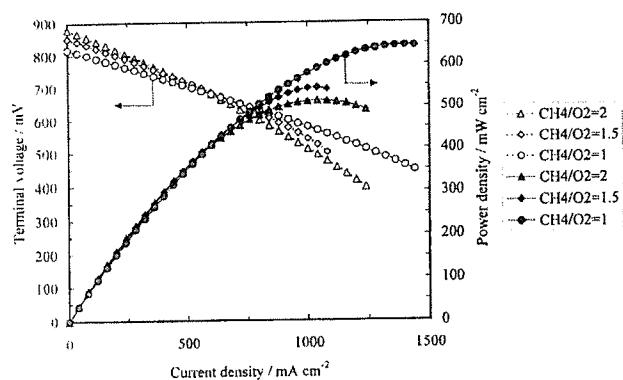


Figure 6. Dependence of discharge properties of a SOFC on volume ratio of methane to oxygen: PdO content = 7 wt %, electrode area = 0.63 cm^2 , electrolyte thickness = 0.15 mm, operating temperature = 550°C .

$$\Delta G^\circ (427^\circ\text{C}) = -220 \text{ kJ mol}^{-1} \quad [5]$$

where ΔG° is Gibbs free energy. The EMFs generated from the SOFC were also higher than 820 mV under such conditions, and the voltage drops per 200 mA were, on the average, 80 mV at 500°C and 150 mV at 450°C (Fig. 7). As a result, the peak power densities were 467 and 269 mW cm^{-2} at 500 and 450°C , respectively. It is noted that these peak power densities were near or higher than those

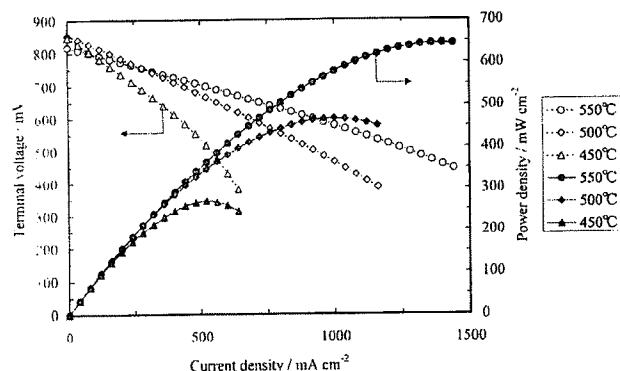


Figure 7. Dependence of discharge properties of a SOFC on operating temperature: PdO content = 7 wt %, electrode area = 0.63 cm^2 , electrolyte thickness = 0.15 mm, $\text{CH}_4/\text{O}_2 = 1/1$.

obtained using ethane or propane fuel,⁴ indicating that the addition of PdO to the anode enhanced the reactivity of methane to those of ethane and propane even at reduced temperatures.

The results described above cannot completely address the feasibility of the present SOFC as a residential cogeneration system. The fuel utilization in the single-chamber SOFCs can never exceed 50%, because methane which passes through the cathode is not used as the fuel. In fact, the fuel utilization in the present SOFC was still a small value of 9.4% even at 644 mW cm^{-2} , which was estimated from the oxide ion flux through the cell and the supplied methane by the assumption that Eq. 1-3 proceeded at the anode. However, a systematic improvement would be possible as: The single-chamber stacked cells can serve as an auxiliary power unit for conventional stacked cells, where their anodes are supplied with the outlet gas from the single-chamber stacked cells. Since the single-chamber cell design provides simple and loosely stacked cells, it could make the power unit less damageable for the thermal shock than the conventional cell design. Therefore, one can initially use the single-chamber SOFCs, and then start the conventional SOFCs.

Conclusions

An improvement in electrocatalytic activity of an SDC-Ni anode for the oxidation of methane was attempted to develop a SOFC for residential applications. Methane was greatly activated over the anode catalyzed by a small amount of Pd, thus providing EMFs of ca. 900 mV and electrode-reaction resistances less than 0.2Ω at 550°C . A significantly high peak power density of 644 mW cm^{-2} was achieved using the SDC electrolyte with a thickness of 0.15 mm.

National Institute of Advanced Industrial Science and Technology assisted in meeting the publication costs of this article.

References

1. E. P. Murray, T. Tsai, and S. A. Barnett, *Nature*, **400**, 649 (1999).
2. C. H. Steele, *Nature*, **400**, 619 (1999).
3. C. Xia, F. Chen, and M. Liu, *Electrochem. Solid-State Lett.*, **4**, A52 (2001).
4. T. Hibino, A. Hashimoto, T. Inoue, J. Tokuno, S. Yoshida, and M. Sano, *Science*, **288**, 2031 (2000).
5. A. T. Ashcroft, A. K. Cheetham, M. L. H. Green, and P. D. F. Vernon, *Nature*, **352**, 225 (1991).
6. D. Dissanayake, M. P. Rosynek, K. C. C. Kharas, and J. H. Lunsford, *J. Catal.*, **132**, 117 (1991).
7. D. A. Hickman and L. D. Schmidt, *Science*, **259**, 343 (1993).
8. M. Watanabe, H. Uchida, M. Shibata, N. Mochizuki, and K. Amikura, *J. Electrochem. Soc.*, **141**, 342 (1994).
9. M. J. Saeki, H. Uchida, and M. Watanabe, *Catal. Lett.*, **26**, 149 (1994).
10. T. Ishihara, M. Honda, T. Shibayama, H. Minami, H. Nishiguchi, and Y. Takata, *J. Electrochem. Soc.*, **145**, 3177 (1998).
11. T. Hibino and H. Iwahara, *Chem. Lett.*, **1993**, 1131.
12. C. Zawodzinski, M. S. Wilson, and S. Gottesfeld, in *Proton Conducting Membrane Fuel Cells I*, S. Gottesfeld, G. Halpert, and A. Landgrebe, Editors, PV 95-23, p. 57, The Electrochemical Society Proceedings Series, Pennington, NJ (1995).
13. P. N. Ross, K. Kinoshita, A. J. Scarpellino, and P. Stonehart, *J. Electroanal. Chem.*, **63**, 97 (1975).
14. P. N. Ross, K. Kinoshita, A. J. Scarpellino, and P. Stonehart, *J. Electroanal. Chem.*, **59**, 177 (1975).
15. R. Doshi, V. L. Richards, J. D. Carter, X. Wang, and M. Krumpelt, *J. Electrochem. Soc.*, **146**, 1273 (1999).

EXHIBIT 8

Compact mixed-reactant fuel cells

Michael A. Priestnall*, Vega P. Kotzeva, Deborah J. Fish, Eva M. Nilsson

Scientific Generics Ltd., Harston Mill, Harston, Cambridge CB2 5GG, UK

Abstract

The compact mixed-reactant (CMR) fuel cell is an important new “platform” approach to the design and operation of all types of fuel cell stacks. Amongst several other advantages, CMR has the potential to reduce polymer electrolyte membrane (PEM) stack component costs by around a third and to raise volumetric power densities by an order of magnitude.

Mixed-reactant fuel cells, in which the fuel and oxidant within a cell are allowed to mix, rely upon the selectivity of anode and cathode electrocatalysts to separate the electrochemical oxidation of fuel and reduction of oxidant. A comprehensive review of the 50-year history of mixed-reactant literature has demonstrated that such systems can perform as well as and, in some circumstances, much better than conventional fuel cells.

The significant innovation that Generics has introduced to this field is to combine the concept of mixed-reactant fuel cells with that of a fully porous membrane electrode assembly (MEA) structure. Passing a fuel–oxidant mixture through a stack of porous cells allows the conventional bipolar flow-field plates required in many fuel cell designs to be eliminated. In a conventional PEM stack, for example, the bipolar carbon flow-field plates may block up to half of the active cell area and account for up to 90% of the volume of the stack and of the order of one-third of the materials costs. In addition to all the advantages of mixed-reactant systems, the “flow-through” mode, embodied in Generics’ CMR approach, significantly enhances mass-transport of reactants to the electrodes and can reduce reactant pressure drops across the stack. Redesigning fuel cells to operate in a CMR mode with selective electrodes offers the attractive prospect of much reduced stack costs and significantly higher stack power densities for all types of fuel cell.

Initial modeling and proof of principle experiments using an alkaline system have confirmed the validity of the CMR approach and the potential for substantial performance improvements. © 2002 Elsevier Science B.V. All rights reserved.

Keywords: Mixed-reactant; Fuel–air mixture; Methanol; Sodium borohydride; Fuel cell

1. Introduction

Conventional fuel cells operate using active but often non-selective electrocatalysts and rely upon a strict segregation of fuel and oxidant to prevent parasitic chemical reactions at the electrodes. Mixed-reactant fuel cells, which have been known for around half a century, rely upon the selectivity of anode and cathode electrocatalysts to separate the electrochemical oxidation of fuel and reduction of oxidant. Without a need for physical separation of fuel and oxidant, there is no longer any need for gas-tight structures within the stack and considerable relaxation of sealing, manifold and reactant delivery structures is possible.

The compact mixed-reactant (CMR) fuel cell is an entirely new concept in which a mixture of fuel and oxidant is flowed through a fully porous anode–electrolyte–cathode

structure. This structure may be a single-cell, series stack or parallel stack and may be in planar, tubular or other geometry. In principle, a CMR cell may be based on polymer, alkaline, phosphoric acid, molten carbonate, solid oxide or any other type of fuel cell chemistry. Whatever the specific geometry or chemistry, for this type of cell to work effectively, the anode and cathode electrocatalysts must be substantially selective—i.e. the anode should be active toward fuel oxidation and tolerant to oxygen, while the cathode should be active toward oxygen reduction and tolerant to fuel.

Selectivity in the electrocatalysts for a mixed-reactant or a CMR fuel cell is needed to minimise mixed potentials at the electrodes which otherwise will reduce the available cell voltage and compromise the efficiency of conversion to electricity. Loss of efficiency reflects the extent of the “parasitic” direct reaction of fuel and oxidant to produce heat rather than electric current. This is directly analogous to the problem of methanol cross-over from the anode compartment to cathode compartment in conventional direct-methanol fuel cells. A range of partially and substantially

* Corresponding author. Tel.: +44-1223-875200;

fax: +44-1223-875201.

E-mail address: mpriestnall@scigen.co.uk (M.A. Priestnall).

URL: <http://www.generics.co.uk>

selective catalysts have become available in recent years, largely as a result of the continuing effort to develop more effective catalysts for direct-methanol fuel cells.

2. Significance of the compact mixed-reactant fuel cell

Two key advantages of operating any fuel cell stack in the flow-through CMR mode are as follows:

- flow-field structures can be eliminated from within the stack;
- mass-transport of reactants to electrodes is much higher than in conventional or mixed-reactant stacks.

These key advantages are supported by those more generally of mixed-reactant systems, which include: reduced manifolding and sealing; single feed supply to one side of fuel cell only; reduced quantities of materials and component count; lower tolerance component manufacturing and easier stack assembly.

The consequence of eliminating the bipolar flow-field plates is a huge reduction in volume and cost of a fuel cell stack. For a polymer electrolyte membrane (PEM) stack this volume reduction could be as high as 80–90%. In several semi-commercial designs of planar solid oxide fuel cell, the ceramic or metal bipolar interconnector is the single most expensive component. Removing it could reduce the stack cost by around 30–60%. Increasing the mass-transport of reactants to the electrodes has the immediate effect of increasing cell current density. The reduction in diffusion boundary layers between reactants and catalyst particles may also reduce the amount of catalyst required per kilowatt of power generated by the cell. The combined effects of increased mass-transport and smaller stack volume should be a large increase in volumetric power density for the stack and a reduction in the power required to pump reactants through the stack.

An example of the potential volumetric power density that a CMR stack may deliver is provided by an experimental programme underway at Generics. In this programme, the performance of a small DMFC stack with a mixed vapour feed of humidified methanol and air will be tested in flow-through mode. The stack is designed to consist of a series of closely spaced fully porous MEAs, with each cell inter-connected electrically by a thin and porous carbon gas diffusion layer (GDL) and no flow-field plate. Assuming that each GDL and MEA sheet is around 100 μm thick then a cell pitch of around 50 cells cm^{-1} should be readily achievable. (This compares with a “conventional” cell pitch of around 2–5 cells cm^{-1} .) Using existing selective cathode materials, we anticipate that it should be possible to achieve at least 50 mA cm^{-2} at a cell voltage of 0.4 V in CMR mode. If this moderate cell performance can be achieved at this cell pitch, the stack should achieve a volumetric power density of 1000 W l^{-1} , approximately equivalent to that of a conventional hydrogen-fuelled PEM stack.

With the lower fuel efficiencies resulting from today’s generally poorly selective electrocatalysts in CMR mode, one challenge associated with very high stack densities will be cooling. Although cooling is readily achieved in all-liquid fuel cells, this issue may limit the maximum power density of gas-phase CMR systems until improved electrocatalysts are developed specifically for them.

3. History of mixed-reactant fuel cells

As has been observed many times elsewhere, the history of the fuel cell goes back more than one and a half centuries. In that period many individuals and organisations have devoted considerable efforts and resources to the invention, development and demonstration of various fuel cell technologies. One such technology that has been investigated for alkaline, solid oxide, polymer and direct-methanol fuel cells is the “mixed-reactant” or “single-chamber” fuel cell [1–33].

Starting in the 1950s, when nuclear fission plants were under intense development, fuel cell engineers examined the possibility of radiolytic splitting of water into hydrogen and oxygen followed by electrochemical recombination of the gas mixture to generate electricity. Fuel cell stack geometries with alkaline electrolytes (anion membrane or KOH) were tested by Grüneberg and others of Varta and Siemens in which the oxygen in a stoichiometric $\text{H}_2 + 0.5 \text{O}_2$ gas mixture was first depleted to below the flammability limit at a selective cathode (e.g. C, Ag, Au)—i.e. a cathode capable of reducing oxygen molecules to oxygen ions but incapable of oxidising hydrogen gas to ions [1]. To complete the cell reaction, the depleted gas mixture was subsequently exposed to an anode electrocatalyst (e.g. Pt, Pd) that promoted hydrogen oxidation. In a later variant, in which the same gas mixture was delivered to each electrode, using a silvered nickel cathode and Pd–Pt anode, Goebel et al. [2], operated a liquid alkaline fuel cell at room temperature on a 9% $\text{O}_2 + 91\% \text{H}_2$ oxyhydrogen gas mixture. This cell delivered an open circuit voltage (OCV) of 1.0 V and a current density of 4 mA cm^{-2} at 0.4 V.

Around the same time as Grüneberg and Goebel, in 1961, Grimes et al. [3] of Allis Chalmers built and operated a 600 W direct-methanol mixed-reactant alkaline fuel cell. A series-connected 40-cell stack of 25 cm \times 25 cm solid bipolar Pt–Ni–Ag electrodes was supplied with a liquid reactant mixture consisting of hydrogen peroxide (0.1–1 wt.%) and methanol (2–10 wt.%) in a 0.5–7 M potassium hydroxide solution and delivered up to 40 A at 15 V. In single-cell tests using a solid anion membrane as electrolyte, an OCV of 0.41 V was measured in the reactant mixture compared to 0.81 V when methanol and hydrogen peroxide were supplied separately in KOH solution to the Pt anode and Ag cathode. Analysis of reaction products determined that the net reaction in the cell was the oxidation of methanol to potassium methanate (formate), possibly either by direct

electrochemical reaction for which the theoretical cell voltage is 1.88 V, or via disproportionation of a chemically generated methanal (formaldehyde) intermediate for which the EMF would be 0.94 V. Quantitative comparison of the reaction products with the charge passed by the cell indicated that significant direct chemical reaction occurred between the reactants (as opposed to electrochemical oxidation). Further tests indicated that this chemical short circuiting was primarily catalysed at the platinum electrode. Although not a particularly fuel efficient cell, the Grimes' device was clearly a powerful and early demonstration of the feasibility of liquid-phase mixed-reactant fuel cells.

Also in 1961, Eyraud described another gas-phase mixed oxygen–hydrogen device in which a micro-porous alumina support flooded with condensed moisture from the humid gas mixture acted as a film electrolyte [4]. In this case the Ni–Al₂O₃–Pd cell was operated as a sensor with OCV varying from –0.35 to +0.6 V, depending upon gas composition (no power was drawn from this cell). Then, in 1965, extending Eyraud's work on film electrolytes, van Gool, described for the first time, a further variant of the mixed-reactant fuel cell, the “surface-migration” cell [5]. In this geometry, two closely spaced selective electrodes (anode and cathode) are positioned on the same side of an insulating substrate with a film electrolyte between them. While such a geometry could be operated with separate feeds of hydrogen and oxygen, van Gool suggested that the close electrode spacing (~1 µm) required for a film electrolyte would make gas separation impracticable. For the selective anode electrocatalyst he suggested that a metal with a stable or partly stable hydride and unstable oxide (e.g. Pt, Pd, Ir) would be an appropriate starting point for experimentation; for the selective cathode, a metal, such as silver with unstable hydride and stable oxide. van Gool also suggested that the metals W, Ni and Fe which catalyse the dissociation of methane and ethane below ~200 °C, might work as effective anodes in a mixed-reactant system based on hydrocarbon fuels, in which oxygen or oxygen ions are available to mitigate carbonisation of the anode. No experimental work was reported by van Gool.

There was a gap of 14 years before Louis et al. [6] of United Technologies tested a single-cell variant of van Gool's [5] mixed-reactant “surface-migration” cell. In the UTC approach, a supported thin-film (3 µm) alumina electrolyte was employed, along with closely spaced (300–400 µm gap) supported Pt anode and SrRuO₃ cathode. Each electrode was 5 µm thick and 2.0 cm × 0.5 cm in area. With a single humidified mixed gas feed of 4% O₂, 4% H₂ in nitrogen, an OCV of 0.67 V was obtained at room temperature and, at peak power, a current density of 0.82 µA cm^{–2} at 0.39 V. UTC went on to describe a surface strip-cell geometry in which multiple pairs of surface electrodes are interconnected electrically in series and in which several of such layers are connected in parallel. Alternative electrolyte and selective anode and cathode electrocatalysts (e.g. zirconia, LaCo_{0.5}Ru_{0.5}O₃, LaMnO₃) were also suggested.

In 1990, Moseley and Williams [7] of AEA Technology described a similar room temperature Pt-oxide–Au surface-migration cell, which they had tested as a sensor in various gas mixtures. Using a porous metal (W, Sn) oxide as substrate for the sputtered metal electrodes and for condensation of an aqueous film electrolyte, they discovered that this cell generated an OCV of up to 0.5 V in humid air alone. Adding small amounts (up to approximately 1%) reducing (fuel) gases, such as H₂, CO, NH₃ or EtOH to the gas mixture, they found that the OCV of the cell increased approximately as the log of the concentration of the reducing gas. The authors reasoned that the OCV response in ambient air was a result of the different mixed potentials established by oxygen reduction and metal oxidation at the respective gold and platinum electrodes. Introduction of an additional fuel gas, they believed, mainly affected the mixed potential at the Pt electrode.

Also in 1990 (although with a Patent priority in 1988), Dyer, who was actually working on hydride batteries at Bell Communications Research, described a quartz-supported thin-film mixed-reactant fuel cell that operated with active but apparently non-selective electrodes [8–11]. As with the systems described by Eyraud et al. [4], van Gool [5] and Louis et al. [6], Dyer used a hydrated alumina film as an electrolyte (0.5 µm). In his system, however, the electrodes, which are positioned on either side of the alumina film, can be identical and are either Pt or Pd. Only one electrode of the thin-film cell is exposed to the fuel (H₂, CH₄, MeOH)-oxidant (air, O₂) mixture, while the other side is supported by an impermeable substrate. Dyer found, in his initial experiments with hydrogen–air gas mixtures, that the outer or first Pt electrode was negative (i.e. was the anode), while the inner Pt electrode was positive (cathode). OCV varied over a range of ~0.2–1.1 V, depending upon gas composition, with OCV > 0.95 V when the gas mixture consisted of at least 50% H₂. Perhaps the most important factor contributing to the magnitude and polarity of the observed OCV is that the inner Pt electrode was treated in boiling water to convert an initial < 50 nm coating of Al metal to boehmite phase alumina. It is likely that in this preparation process the Pt surface itself was oxidised. Compared to Pt metal, Pt-oxide has been reported to be a reasonably selective cathode, i.e. promoting O₂ reduction at the expense of H₂ oxidation [12]. A secondary contribution to OCV may be from the differential oxygen reduction/electrode oxidation reactions occurring in the presence of a hydrous electrolyte film (Moseley and Williams [7] observed potentials up to 0.5 V). A third but possibly weaker contributor to the observed behaviour of Dyer's cell may be that a concentration gradient in the local gas mixture is established either by gettering of hydrogen at the exposed electrode or by differential diffusion rates between oxygen and hydrogen in the pinhole-free alumina layer [9,13]. An alternative explanation, based on the relative ability of the two electrodes to catalyse the formation of hydrogen peroxide (the inner electrode being more active), was given by Ellgen, of

Kerr-McGee, which provided the untested basis for a 1991 Patent which claimed a Pt–Pd alloy as a preferred cathode, simultaneously active toward chemical formation and electrochemical reduction of H_2O_2 , and an anode that is inhibited toward peroxide formation but active toward hydrogen oxidation [14].

Dyer was able to reverse the polarity of his cell by changing the outer electrode to Ni. This reflects Grüneberg's original mixed-reactant cell of the 1950s which featured selective depletion of oxygen as the gas-phase mixture was exposed first to a hydrogen-inert cathode and then to a hydrogen-active anode [1]. Dyer was also able to draw $\sim 1\text{--}5\text{ mW cm}^{-2}$ from his $\text{H}_2\text{--O}_2$ Pt–Pt cell with cell voltage falling by $\sim 0.2\text{--}0.3\text{ V}$ per decade of current in the range $0.1\text{--}3.0\text{ mA cm}^{-2}$. He proposed that his thin-film fuel cell would be particularly suitable as an integrated power source in planar electronic circuits and, if deposited on a flexible substrate, could also be packaged in a compact stack form (e.g. spirally wound) to replace conventional batteries, potentially with the fuel-oxidiser mixture being supplied in liquid form [10,15]. An efficiency improvement to Dyer's cell was suggested by Taylor (also of Bell Communications), involving patterning the outer electrode and coating it with a fuel-permeable, oxygen-impermeable barrier to increase anode selectivity to fuel and the permeability of the cell to oxygen [16]. A later (Motorola, 1996) improvement to the general mixed-reactant cell for battery-type applications included an absorbent material to eliminate water discharge [17].

In 1990, approximately concurrent with Dyer's report [9], Wang et al. [18] of GTE Laboratories, filed Patents on a two-interconnected-chamber mixed-reactant Pt–YSZ–Pt SOFC. Although a mixed-reactant yttria-stabilised zirconia (YSZ) electrolyte cell was described previously in Louis et al. [6] Patent, this was the first time such an elevated-temperature cell had been demonstrated in practice. The mechanism of operation of Wang's cell is not entirely clear, but seems to be via either differential flow rates of the methane–air mixture to each electrode or via an initial electrical pulse (in the range of several millivolts to volts) that may establish one Pt electrode as anode and the other as cathode. It is stated that the device will operate as a fuel cell only up to 450°C and can be operated on any reducing gas and with alternative electrolytes and with different electrodes (e.g. Pt–Au). At 350°C , Wang's Pt–YSZ–Pt cell provided an OCV of 0.95 V and a current of $70\text{ }\mu\text{A}$ at 0.65 V in a methane (10%)–air mixture. A second embodiment of the device, which was reported to give much improved performance at up to 600°C , appears to supply the fuel (ethane or methane)–air mixture to only one side of the cell, with the other side possibly being exposed to air.

Continuing the development of mixed-reactant SOFCs, in 1993, Hibino and Iwahara reported a high-temperature "single-chamber" solid oxide fuel cell operating on a methane–air mixture [19,20]. At 950°C , Hibino's Ni–YSZ–YSZ–Au single-cell delivered an OCV of 0.35 V

and, at peak power, 15 mA cm^{-2} at 0.16 V in a 2:1 $\text{CH}_4\text{:O}_2$ mixture. GC analysis of the off-gas from each electrode showed that the Ni–YSZ anode was an effective catalyst for the partial oxidation of methane to hydrogen and carbon monoxide, while the gold cathode was a much less effective catalyst for partial oxidation. The measured gas compositions at each electrode corresponded reasonably well with the Nernstian partial pressure of oxygen at each electrode, calculated from the respective half-cell potentials (-0.9 and -0.2 V , Pt–YSZ reference). This, combined with OCV = 0 V measured when the cell was supplied with air, N_2 or H_2 alone or when both electrodes were identical, led Hibino to conclude that cell EMF is largely due to the local oxygen concentration gradient generated by the difference in catalytic activity (toward partial oxidation of methane) between the two electrodes. Hibino also reasoned that the high cathodic overpotential (0.5 V at 10 mA cm^{-2}), due to gold's poor activity toward oxygen adsorption, diffusion and reduction, could be improved by replacing the oxygen electrolyte with a proton conductor. In subsequent experiments, Hibino was able to increase the peak specific power of his mixed-reactant SOFC from $\sim 2\text{ mW cm}^{-2}$ (0.5 mm YSZ electrolyte) to 166 mW cm^{-2} (0.5 mm $\text{BaCe}_{0.8}\text{Y}_{0.2}\text{O}_3$) [21,22]. In this latter system, at 950°C , a Pt anode and Au cathode were used, reducing both electrode overpotentials to $<50\text{ mV}$ at $\sim 200\text{ mA cm}^{-2}$ and giving an OCV of 0.8 V and current density of 400 mA cm^{-2} at 0.42 V . It was also found that performance of an Au–YSZ–Pt mixed-reactant cell could be significantly improved by surface doping of the YSZ with Pr to render it electronically conducting [23].

Separate measurements by Gödicke in 1997 at ETH-Zurich [24] on a Au–TZP–Pt (TZP = 0.3 mol% YSZ) single-cell, over a range of methane–air compositions, indicated an equilibrium oxygen partial pressure, $p(\text{O}_2)^{\text{eq}}$, at the Pt anode of 10^{-17} atm and a non-equilibrium $p(\text{O}_2)^{\text{neq}}$ at the Au cathode of 0.18 atm at 700°C in a 3:2 methane:air ratio. OCV for this cell was 0.8 V (corresponding with the Nernstian voltage expected from the measured $p(\text{O}_2)$ values), with a current density of $\sim 10\text{ mA cm}^{-2}$ at 0.6 V and $\sim 30\text{ mA cm}^{-2}$ at 0.2 V . These results support Hibino's results and analysis of mixed-reactant SOFCs.

A theoretical analysis of Hibino's and Iwahara [19] and Dyer's [9] results of single fuel cells operating in fuel–air gas mixtures was given by Riess et al. [25]. With a uniform oxygen partial pressure supplied to each electrode, Riess started with the proposition that the asymmetry required to drive an ionic current through the electrolyte must originate from a difference in the catalytic properties of the two electrodes. He showed that an ideal mixed-reactant cell will provide identical OCV and $I\text{--}V$ behaviour to that of a conventional fuel cell when one electrode is reversible towards oxygen adsorption and completely inert to fuel, and the other exhibits reversible fuel adsorption and is completely inert to oxygen. He argued that the actual OCV measured in Hibino's cell was lower than the theoretical value because imperfect catalyst selectivity promoted

direct fuel-oxygen reaction which reduced the chemical potential across the electrolyte. One additional conclusion of Riess' analysis is that the electrolyte does not need to be impervious to fuel oxidant or reaction products.

Logically, Hibino recently tested the practicality of a conventional Ni-YSZ-La_{0.8}SrMn_{0.2}O₄ SOFC single-cell in mixed-reactant mode, obtaining an OCV of 0.8 V at 950 °C and at peak power, $\sim 300 \text{ mA cm}^{-2}$ at 0.4 V with an inlet gas mixture consisting of 19% CH₄, 16% O₂ and 65% N₂ [26,27]. He has also demonstrated that an intermediate-temperature (500 °C) SOFC with 0.15 mm Ce_{0.8}Sm_{0.2}O₂ (SDC) electrolyte (or with other electrolytes), Ni-SDC anode and Sm_{0.5}Sr_{0.5}CoO₃ cathode can operate effectively in "single-chamber" mode when supplied with gas mixtures of methane, ethane, propane or LPG in air [28,29]. In the SDC cell, supplied with an ethane (18%)-air mixture at 500 °C, OCV was $\sim 0.9 \text{ V}$ and at peak power, a current density of $\sim 800 \text{ mA cm}^{-2}$ at $\sim 0.5 \text{ V}$ was measured. In all the cases, measurements of electrode off-gas compositions support Hibino's original conclusion (and Riess' later analysis) that cell OCV is determined largely by the oxygen concentration at each electrode which itself is determined by the extent of partial oxidation of the hydrocarbon at each electrode. Hibino uses this as the basis of a Patent [30] on a series-connected surface strip-cell SOFC geometry (exposed to a gas mixture on one side only), similar in many respects to the "surface-migration" cell proposed by van Gool in 1965 [5] and later patented in series-connected form by Louis et al. [6].

In related work at ETH-Zurich, Joerger [31] described a further variant on the strip-cell SOFC geometry. In the ETH design, each side of a zirconia (TZP) electrolyte sheet is coated with a series of alternating and physically separated anode and cathode electrode strips, with each alternated pair interconnected electrically with gold wire. Additionally, the electrodes on the two sides are arranged so that anodes are opposite cathodes and electrically connected anode-cathode pairs are opposite electrically separate cathode-anode pairs. Electrical connection to an eight cell arrangement of this type was made to the outer anode (Pt) and cathode (Au) on one side of the electrolyte (TZP) sheet, giving an OCV of $\sim 4.5 \text{ V}$ at 700 °C in a methane-air mixture. The connection geometry suggests that the intention in this design is for oxygen ions to be conducted across the thickness of the TZP electrolyte (i.e. between opposite electrodes), rather than along the surface of the TZP, as would be the case in a "surface-migration" strip-cell (i.e. between adjacent electrically separate electrodes). Clearly both ion conduction paths are possible in such a design—risking ionic short-circuiting—with the preferred path being determined largely by electrode separation distances. Recently, Zhu et al. [32] at RIT-Stockholm proposed an essentially identical geometry that solved the issue of ionic short circuiting by replacing the single zirconia electrolyte layer with a double electrolyte sandwich of YSZ (50 μm)-Al₂O₃ (0.5–1 mm)-YSZ (50 μm). The alumina support acts as a barrier to oxygen

ion transport, so that each side of the series-connected strip-cell design acts purely in a surface-migration mode. Zhu's design also included stacking of many such layers in a manner similar to that proposed previously by Louis et al. [6].

Very recently, researchers from IFC and U. Texas [33] demonstrated the feasibility of a mixed-reactant direct-methanol PEM cell, showing that performance in mixed-reactant mode with selective electrodes could exceed that in conventional mode when identical rates of fuel and oxidant are supplied to anode and cathode, respectively. They also conducted a design study in which the dimensions of a series of mixed-reactant surface strip-cells were optimised. In the single-cell tests, a two-phase reactant mixture of 1 M methanol solution ($3 \text{ cm}^3 \text{ min}^{-1}$) and air ($3 \text{ dm}^3 \text{ min}^{-1}$) was supplied to both sides of a conventional geometry membrane electrode assembly (MEA) at 80 °C. The 32 cm^2 MEA was a Nafion-117 electrolyte coated on one side with a hydrophobic Pt-Ru C-black (5 mg cm^{-2}) anode, and on the other with iron tetramethoxyphenyl porphyrin (FeTMPP), a methanol-tolerant cathode material. Half-cell experiments were also carried out on these electrodes (with Pt counter electrode) and also on another selective cathode electrocatalyst, Ru-Se-Mo (5 mg cm^{-2}). The half-cell measurements demonstrated that, in this system, there was no significant reaction between oxygen and methanol at the anode and that the main effect of the entrained air (or entrained nitrogen) in the mixed-feed was to impede mass-transport of the fuel to the anode at current densities above 100 mA cm^{-2} . At the cathode, half-cell measurements again showed little significant difference between operation in mixed-reactant mode and conventional mode, a 40 mV drop in OCV being measured for FeTMPP in mixed-reactant mode while a $\sim 20 \text{ mV}$ increase in OCV was measured for Ru-Se-Mo.

Cell performance was compared in mixed-reactant mode and in conventional mode (air supplied to cathode; MeOH to anode). For both cathode systems, the OCV (0.5–0.6 V) in mixed-reactant mode was virtually identical to that in conventional mode, while slightly higher current densities were measured for the mixed-reactant systems: at 0.3 V current densities were approximately 12 and 16 mA cm^{-2} for the Ru-Se-Mo cathode, and 23 and 33 mA cm^{-2} for the FeTMPP cathode, in mixed-reactant and selective modes, respectively. One possible explanation for the slightly higher current densities in mixed-reactant mode could be that methanol crossed-over from the cathode side to the anode side by permeation through the electrolyte membrane (driven by depletion of methanol at the anode). If this is the explanation, it is important to note that it is only possible because in their experiments the IFC and U. Texas team supplied the mixed-reactant cell with twice the amount of methanol ($3 \text{ cm}^3 \text{ min}^{-1}$ to both anode and cathode) supplied to the conventional DMFC ($3 \text{ cm}^3 \text{ min}^{-1}$ to anode only).

In the mixed-reactant DMFC, one could argue that methanol cross-over offers a performance advantage—quite the opposite to the situation in a conventionally operated PEM

DMFC. In the latter case, methanol leaks constantly from anode compartment to cathode compartment where it reacts at the unselective cathode electrocatalyst (typically Pt), thereby lowering its potential as well as wasting fuel through direct chemical reaction. This has its most significant effect on fuel efficiency (the ratio of electrical energy output of the cell to heat of combustion of fuel entering the cell) when the conventional DMFC cell is being operated at low current densities. The IFC and U. Texas team were able to show that the fuel efficiency of their mixed-reactant DMFC using a selective FeTMPP cathode remained higher than that of a conventional geometry DMFC with non-selective Pt cathode up to a current density of $\sim 100 \text{ mA cm}^{-2}$. Of course, this efficiency improvement would be evident in a conventional DMFC also, if Pt were replaced by FeTMPP. This is one of the primary reasons why selective cathode materials, such as FeTMPP and Ru–Se–Mo were investigated in the first place.

The 50-year history of mixed-reactant fuel cell systems has demonstrated convincingly that they can deliver performance comparable to that of conventional fuel cells, that multiple cells can be stacked in series and that the mechanisms by which they work are well understood in terms of catalyst selectivity and local chemical gradients generated at the electrodes. Moreover, the range of work carried out in this area demonstrates that the mixed-reactant approach is applicable to gaseous and liquid systems, to systems operating over a wide range of temperatures, to alkaline, solid oxide and PEM fuel cell types and, by implication, to all fuel cell types.

The key advantages of mixed-reactant systems identified by the various workers in this field can be summarised as follows:

- more compact designs possible because manifolding simplified;
- surface strip-cell geometry enables series cell connections and exposure to reactant on just one side of structure;
- supported thin-film cell with porous electrolyte and surface electrode enables exposures from just one side;
- higher power densities possible by closer stacking of thin-film and strip-cell geometries;
- lower fabrication costs possible from continuous coating of supported thin-film and strip-cell structures;
- lower cost and more reliable systems because sealing requirements reduced or eliminated.

Key disadvantages of mixed-reactant systems are as follows:

- selective (as well as active) catalysts required to prevent polarisation losses and fuel inefficiencies due to parasitic side reactions;
- fuel cell exhaust may contain a larger proportion of more dilute unreacted fuel than in conventional anode exhaust;
- fuel (non-reacting) dilutes oxidant concentration (or partial pressure) at cathode (Nernst potential very slightly reduced);

- oxidant (non-reacting) dilutes fuel concentration (or partial pressure) at cathode (Nernst potential very slightly reduced).

At their best, with ideally selective and active anode and cathode electrocatalysts, with identical geometries and fuel and oxidant activities, mixed-reactant single-cells should have identical performance to conventional fuel cells. In certain types of cell, for example, where fuel cross-over depresses performance, or where reaction products may depress electrocatalyst activity, it appears possible for mixed-reactant cells to out-perform conventional separate-reactant cells. At present, ideally selective catalysts are not available for fuel cells and those substantially selective electrocatalysts that do exist are not as active as conventional fuel cell electrocatalysts toward either fuel oxidation or oxygen reduction. Although there are presently no significant efforts to develop selective anode or cathode electrocatalysts for mixed-reactant fuel cell systems, there are significant efforts in the fuel cell community to develop methanol-tolerant cathode materials for DMFCs as one means of helping to alleviate the problem of methanol cross-over. These electrocatalysts are also ideal candidates for the cathodes of mixed-reactant DMFCs and are a starting point for a more substantial development effort for catalysts designed to enable the full benefits of mixed-reactant systems.

4. Development of CMR systems

Generics has begun initial experimental and theoretical investigations of CMR technology. The approach we are following is first to demonstrate proof of principle in single-cells and small stacks, secondly to develop a valid theoretical understanding of how CMR fuel cells work and thirdly to demonstrate significant performance in pre-prototype devices. This approach, we believe, will enable us to work toward demonstrating the applicability and value of the CMR approach to all the main types of fuel cell (PEM, AFC, PAFC, MCFC and SOFC).

The proof of principle of mixed-reactant fuel cells is already well established by the 50-year history of such systems. Our focus has been to demonstrate that the CMR approach—in which a hydrodynamic flow of mixed reactants moves through a porous cell or stack—also works in principle. At Generics we have used a dissolved-reactant alkaline system as the basis of our initial proof of principle experiments. A series of half-cell, single-cell and stacked-cell (series and parallel) experiments were carried out using a commercial anode of Pt–carbon–PTFE catalyst on Ni-mesh (EL05&06, Electro-Chem-Technic) and cathode of MnO_2 –PTFE on Ni-Mesh (EL01&02, Electro-Chem-Technic—note: backing layer of PTFE was removed). For flow-through experiments, porosity of the electrodes was increased by perforating them with a square array of pinholes.

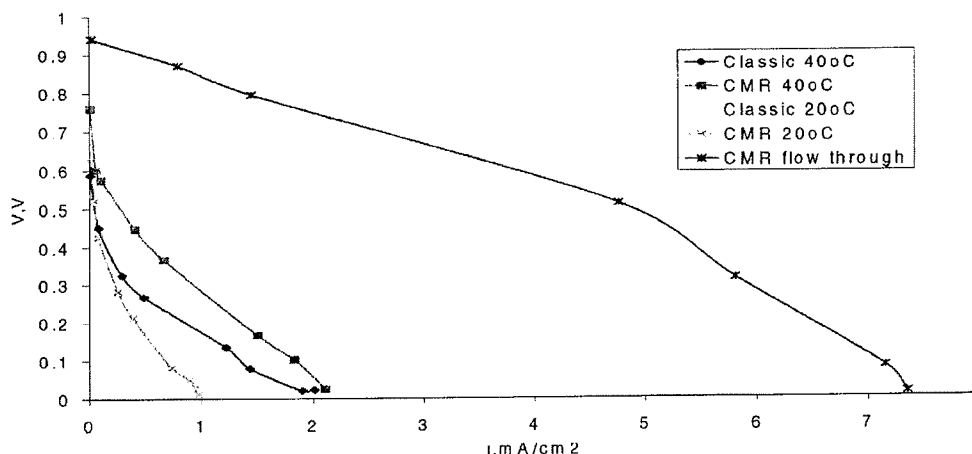


Fig. 1. Performance of flow-through CMR mode (20 °C) compared with mixed-reactant (static CMR) and conventional (classic) modes.

Electrolyte was a 6 M or 10 M solution of potassium hydroxide. Oxidant was air, either dissolved in the electrolyte, dissolved in water, or entrained as bubbles in the electrolyte. Fuel was either methanol dissolved in electrolyte or 0.008 M sodium borohydride (NaBH_4) dissolved in electrolyte.

A three-chamber tubular rig was constructed enabling separate reactant supply to each chamber and also sequential reactant flow through the three chambers. Each chamber was 4 cm in length and were separated by a single anode and single cathode sealed across the diameter of the rig by ϕ -rings. External electrical connections were made to the electrodes. In one series of experiments, the performance of an alkaline single-cell in the rig was compared in conventional separated-reactant mode, mixed-reactant mode and in CMR flow-through mode (Fig. 1). In the conventional and mixed-reactant (non-flow-through) modes the electrodes were separated by a 4 cm depth of free 10 M KOH electrolyte, filling the central chamber of the rig.

In the conventional mode, a 0.008 M (3 g l^{-1}) solution of NaBH_4 in 10 M potassium hydroxide (KOH), de-aerated with bubbled nitrogen, was fed to the anode chamber while 10 M KOH saturated with dissolved air was fed to the cathode. In non-flow-through mixed-reactant mode the NaBH_4 -KOH solution was first saturated with bubbled air and then supplied separately to both anode, and cathode chambers. In the CMR flow-through mode the same reaction mixture was supplied to the anode chamber, where it flowed through a perforated anode, through the central chamber and then through a perforated cathode before exiting the cathode chamber. In each mode, fluids entirely flooded the three chambers and were pumped through the electrode chambers at a constant rate of 2.5 ml min^{-1} .

Current-voltage data from the three experiments are shown in Fig. 1. At 20 °C, the conventional ("classic" in Fig. 1) mode of fuel cell operation gave identical results to that of the non-flow-through mixed-reactant mode ("CMR"

in Fig. 1). At 40 °C, OCVs and current densities were higher in both cases, with the performance in mixed-reactant mode exceeding that in conventional mode. CMR flow-through mode (which was measured only at 20 °C) gave significantly higher performance than either the conventional or mixed-reactant modes. These results suggest, firstly, that the electrodes in this alkaline system are highly selective toward the respective desired half-cell reactions. Secondly, they suggest that the presence of both reactants at one or other of the electrodes operate in some way to reduce electrode overpotential. Speculative mechanisms could include local decomposition of NaBH_4 to H_2 gas at the cathode surface disrupting the local boundary layer and improving oxygen transport to the cathode, or perhaps through local dissolved oxygen reacting at the anode to increase the rate at which adsorbed reaction products are cleared from the platinum catalyst surfaces. Thirdly, and probably the most significant effect, the results demonstrate that mass-transport of reactants to the electrode catalysts in a CMR flow-through regime considerably exceeds that in a conventional or in a mixed-reactant "flow-by" regime. In the latter, diffusion boundary layers may be substantial and a smaller volume or surface area of catalyst may be exposed to reactant. Overall, this comparison between the three modes of operation supports the various earlier studies reported in the literature on mixed-reactant fuel cells and clearly shows a potential advantage in operating a single fuel cell in CMR flow-through mode.

As part of the second stage of our approach to CMR systems development, we have developed two simple computer models of direct-methanol CMR behaviour based on initial assumptions of the main electrochemical mechanisms and flow modes that determine CMR cell polarisation performance. We anticipate that these models will become increasingly robust and more sophisticated as they are developed and refined through a process of experimental testing and verification. The purpose of the models is to

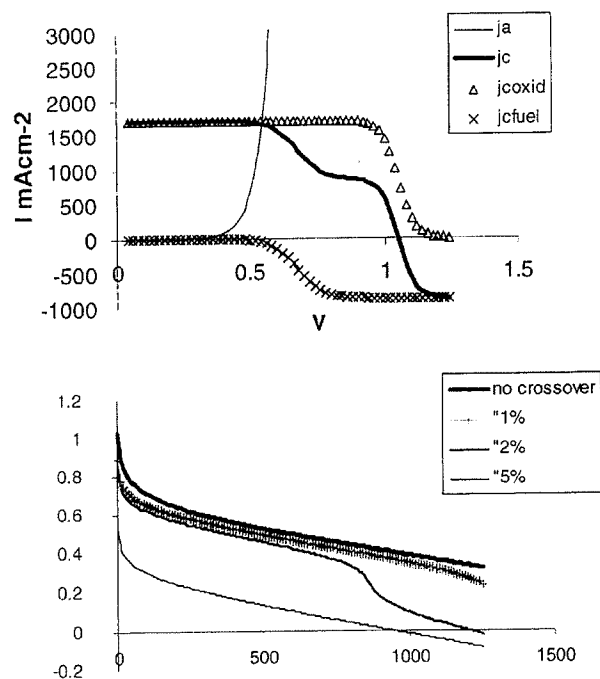


Fig. 2. Simulation of effects on performance of methanol cross-over in a conventional DMFC behaviour using a CMR model. (Upper graph) Simulated half-cell polarisation data for a conventional DMFC with 2% methanol cross-over using a CMR model; (Lower graph) simulated single-cell polarisation data for a conventional DMFC with 0–5% methanol cross-over using a CMR model.

enable the likely performance of future designs of CMR systems to be predicted with reasonable confidence, for example, to help define measurable characteristics required for suitable active materials and to optimise specific microstructures.

The first of our mathematical models of CMR is based on the Butler–Volmer equation that describes electrode potentials and current density in terms of exchange current density and charge transfer coefficients for the various reactions occurring at each electrode. We initially tested the model by using it to predict the expected performance of a “conventional” DMFC with differing extents of fuel cross-over, populating the model with data extracted from Tafel measurements in the literature [34]. The upper graph in Fig. 2 shows predicted anode (j_a) and cathode (j_c) polarisation curves for a DMFC with 2% methanol cross-over, where j_c is the summed result of the competing oxygen reduction ($j_{c_{oxid}}$) and methanol oxidation ($j_{c_{fuel}}$) reactions occurring at the cathode. The lower graph in Fig. 2 shows predicted cell polarisation curves for a range of methanol cross-over, where each cell curve is calculated from the potential difference of curves $j_c - j_a$ at fixed current. This first electrochemical model assumes that the same reactant mixture is supplied to both electrodes and treats the limits to mass-transport of the reactants simply as a pre-defined maximum flux of each reactant to both electrodes. It does not distinguish, therefore, between the flow-through or flow-across

regimes and does not take into account diffusional boundary layers at the electrodes. Despite this gross simplification, with an assumed fully methanol-selective anode and a completely non-selective cathode, the simulated polarisation curves are comparable to those reported experimentally for the “conventional” DMFC.

In the second of our modeling approaches, we have used a commercial finite element package, Femlab (Comsol AB, Stockholm), to begin to compare the effects of mixed-reactants in different flow regimes on cell polarisation. The single-cell is a direct-methanol PEM MEA consisting of a GDL–Pt–Nafion–Pt/Ru–GDL sandwich (120 μ m GDL, 10 μ m catalyst, 20 μ m electrolyte), where the GDL surfaces are 50% blocked on each side by an interdigitated flow-field current collector. The reactant mixture is a hypothetical single phase 50:50 (v/v) mixture of 1 M methanol and air. The model assumes that in all cases only fuel reacts at the anode and oxygen at the cathode. The model also assumes that in a mixed-reactant environment the cell voltage is 150 mV below standard EMF for the DMFC to allow for less than ideal selectivity of the electrocatalysts. The main basis of the flow model is D’Arcy’s law, which describes the rate of flow of a fluid through a porous network in terms of a specific permeability constant for the network and the viscosity of the fluid. Interdigitated reactant supply to each electrode (as opposed to serpentine flow) is used in the conventional separated-reactant (case 1) and mixed-reactant cases (case 2). In the CMR flow-through case (case 3) the cathode catalyst layer is treated as either flooded with liquid (case 3a) or with gaseous air (case 3b)—oxygen in the cathode backing is in gaseous form in both cases. In all cases the reactant flows were driven at a constant pressure differential of 0.5 atm (Fig. 3).

The results show that at a constant supply pressure the different operating modes are likely to result in very different cell performances. The major difference between case 1 and case 2 is accounted for by the much lower flux of dissolved oxygen to the cathode (compared to gaseous oxygen in case 1) and by the 50% dilution of methanol at the anode by inclusion of air in the mixed-reactant feed. The remaining difference is mainly accounted by the polarisation loss assumed for non-ideal selectivity. The major difference between case 2 and case 3a is the larger and more uniform oxygen supply to the active layer (also more fuel reaches the anode). This results in a more uniform current density distribution and thus a lower polarisation of the electrode. In case 3b, where the liquid mixture does not flood the cathode layer (as would be the case in a gas–reactant system), the resistance to diffusion of oxygen across the cathode is much lower (than in case 3a), increasing the flux of reactants and therefore the current density. The decreased mass-transport resistance makes it possible for the current to be distributed more uniformly and also lowers the kinetic polarisation. Differences between case 3 and case 1 are primarily due to the differences in resistance to reactant flow and to the assumed polarisation loss. In the model, the

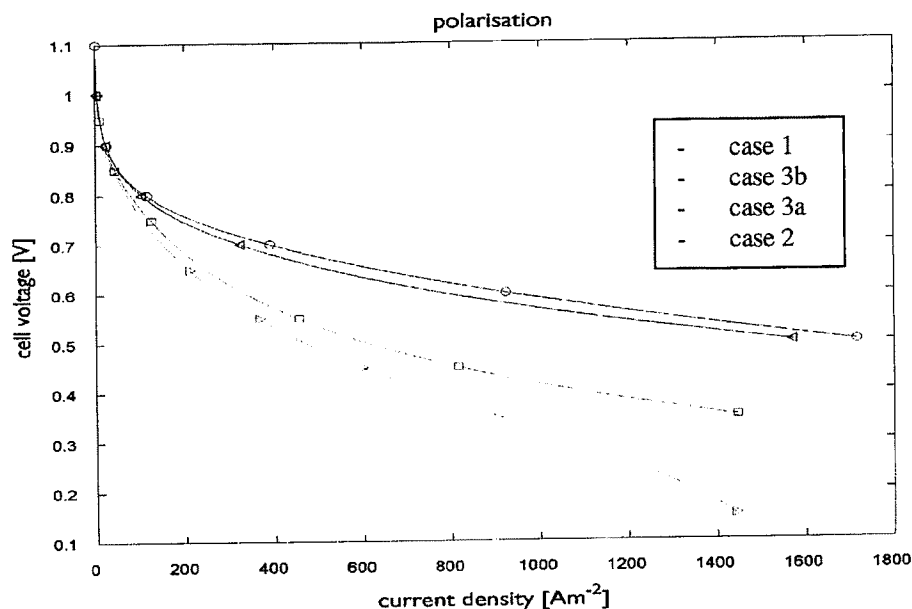


Fig. 3. Predicted polarisation curves for PEM-DMFC operating in conventional mode (case 1), mixed-reactant (non-flow-through CMR) mode (case 2) and CMR flow-through mode (case 3).

permeability of the electrolyte membrane is assumed to be 10% of that of the GDL material. It should therefore be possible to significantly improve the flux of reactants through the cell in CMR mode (case 3) by thinning the electrolyte layer and also by increasing its permeability. Additionally, for purposes of direct comparison in the model, it is assumed that the MEA in case 3 has two GDLs and current collectors that partially block the GDLs. In what might be an ideal flow-through CMR stack, only one GDL should be required to separate each cell and no other current collector or gas distribution structure is required between each cell. With design improvements, such as these, it should be possible to significantly increase the flux of reactants in a CMR system and thereby increase cell current density well above that modeled in case 3b. Furthermore, in this model an interdigitated forced-flow is applied in case 1 rather than the more conventional diffusional serpentine reactant flow adopted in most current fuel cell designs. This suggests that if the mass transfer resistance of a diffusion boundary layer were included in case 1, an even larger advantage could be identified for the CMR mode.

5. Safety of mixed-reactant and CMR systems

Mixing a fuel and oxidant within a fuel cell raises immediate concerns of potential explosion. In reality, a fuel cell stack is largely filled with electrolyte, electrode and separator materials, which will act as a heat sink, eliminating the possibility of explosion. Analogous systems, such as metal-foams or gauzes are well known as means to prevent explosion in storage or usage of explosive mixtures. The

remote possibility of sustained combustion within a mixed-reactant fuel cell will be limited to any open gas supply channels with the structure.

Evidence of the mixed-reactant fuel cells—even high-temperature SOFCs—built and tested in the last 50 years supports the view of safety in these systems. It is, of course, possible to operate with gaseous fuel:oxidant ratios below the explosive limit of the reactants, as several researchers have done. It is also possible to operate with reactant mixtures diluted in an inert carrier, such as nitrogen or water. In liquid mixed-reactant systems, the heat capacity of the liquid medium provides additional protection against any possibility of explosion.

In a CMR fuel cell, where flow of reactants occurs through a porous stacked structure, the elimination of open gas flow channels eliminates any possibility of either sustained combustion or explosion, whatever the mixed-reactant composition. Safety will need to be proved ultimately, of course, by impact, explosion and combustion tests of actual CMR devices.

6. Conclusion

For developers of all of today's fuel cell systems, CMR technology offers immediate benefits in cost, size, power density and reliability at the likely expense of some loss in efficiency. For direct-methanol fuel cells, CMR offers the prospect of an increase in fuel efficiency, as well as these advantages. In the future, with the development of more selective electrocatalysts, the overwhelming advantages of operation in the CMR mode suggest it could displace today's

conventional separate-reactant fuel cell in many application areas.

Acknowledgements

Thanks are due to Prof. Keith Scott of Newcastle University and Dr. Ed Fontes of Comsol AB, for their assistance in the development of fuel cell models.

References

- [1] G. Grüneberg, W. Wicke, E. Justi, British Patent GB994448 (1961) also equivalent French Patent FR1321373 (1961).
- [2] G. Goebel, B.D. Struck, W. Vielstich, in: W. Vielstich (Ed.), English translation by D.J.G. Ives, *Fuel Cells—Modern Processes for the Electrochemical Production of Energy*, Wiley/Interscience, New York, 1965, pp. 374–376, ISBN: 0471906956.
- [3] P.G. Grimes, B. Fielder, J. Adam, *Proc. Annu. Power Sources Conf.* 15 (1961) 29–32.
- [4] C. Eyraud, J. Lenoir, M. Géry, *Acad. des Sci.* 252 (1961) 1599–1600.
- [5] W. van Gool, *Philips Res. Rep.* 20 (1965) 81–93.
- [6] G.A. Louis, J.M. Lee, D.L. Maricle, J.C. Trocciola, US Patent 4248941 (1979/1981).
- [7] P.T. Moseley, D.E. Williams, *Nature* 346 (1990) 23.
- [8] C.K. Dyer, US Patent US 4863813 (1988/1989) and reissued US Patent Re.34248 (1990/1993).
- [9] C.K. Dyer, *Nature* 343 (1990) 547–548.
- [10] C.K. Dyer, US Patent 5094928 (1990/1992).
- [11] R. Pool, *Science* 247 (1990) 1034–1035.
- [12] S. Gottesfeld, *Nature* 345 (1990) 673.
- [13] T.E. Mallouk, *Nature* 343 (1990) 515–516.
- [14] P.C. Ellgen, US Patent 5162166 (1991/1992).
- [15] C.K. Dyer, US Patent 4988582 (1990/1991).
- [16] T.M. Taylor, US Patent 5102750 (1990/1992).
- [17] S.M. Scheifers, D.H. Closterman, M.K. Chason, K.W. Wyatt, US Patent 5723229 (1996/1998).
- [18] D.Y. Wang, D.T. Kennedy, B.W. MacAllister, US Patent 5100742 (1990/1992); also EU Patent Appl. 91102546,8.
- [19] T. Hibino, H. Iwahara, *Chem. Lett.* 7 (1993) 1131–1134.
- [20] T. Hibino, K. Asano, H. Iwahara, *Nippon Kagaku Kaishi* 7 (1994) 600–604.
- [21] K. Asano, T. Hibino, H. Iwahara, Solid oxide fuel cells IV, in: M. Dokiya, et al. (Eds.), *The Electrochem. Soc., Proc. Ser.*, PV 95-1, Pennington, NJ, 1995, pp. 58–66.
- [22] K. Asano, T. Hibino, H. Iwahara, *J. Electrochem. Soc.* 142 (10) (1995) 3241–3245.
- [23] K. Asano, H. Iwahara, *J. Electrochem. Soc.* 144 (9) (1997) 3125–3130.
- [24] M. Gödickemeier, D. Nussbaum, C. Kleinogel, L.J. Gaukler, in: *Proceedings of the Joint International 192nd Meeting of Electrochemical Society; Proceedings of the Joint International 48th Meeting of the International Society of Electrochemical*, Paris, France, 31 Aug.–5 Sep., 1997, Abstract no. 2191.
- [25] I. Riess, P.J. van der Put, J. Schoonman, *Solid State Ionics* 82 (1995) 1–4.
- [26] T. Hibino, S. Wang, S. Kakimoto, M. Sano, *Electrochem. Solid-State Lett.* 2 (7) (1999) 317–319.
- [27] T. Hibino, Japanese Patent JP 2000-243412 A2 (1999/2000).
- [28] T. Hibino, A. Hashimoto, T. Inoue, J.-I. Tokuno, S.-I. Yoshida, M. Sano, *Science* 288 (2000) 2031–2033.
- [29] T. Hibino, A. Hashimoto, T. Inoue, J.-I. Tokuno, S.-I. Yoshida, M. Sano, *J. Electrochem. Soc.* 147 (8) (1997) 2888–2892.
- [30] T. Hibino, K. Ushiki, Y. Kuwabara, Japanese Patent JP 02910977 B2 (1995/1998).
- [31] M. Joerger, in: *Proceedings of the Joint International 192nd Meeting of the Electrochemical Society Inc.; Proceedings of the Joint International 48th Annual Meeting of International Society of Electrochemical*, Paris, France, 31 August–5 September 1997, Abstract.
- [32] B. Zhu, G. Meng, B-E. Mellander, *J. Power Sources* 79 (1999) 30–36.
- [33] S. Calabrese Barton, T. Patterson, E. Wang, T.F. Fuller, A.C. West, *J. Power Sources* 96 (2001) 329–336.
- [34] K. Scott, W. Taama, J. Cruickshank, *J. Appl. Electrochem.* 28 (1998) 289–297.

EXHIBIT 9

CNN.com

CNN.com nature

Editions | myCNN | Video | Audio | Headline News Brief | Feedback

[MAINPAGE](#)[WORLD](#)[U.S.](#)[WEATHER](#)[BUSINESS](#)[SPORTS](#)[TECHNOLOGY](#)[SPACE](#)[HEALTH](#)[ENTERTAINMENT](#)[POLITICS](#)[LAW](#)[CAREER](#)[TRAVEL](#)[FOOD](#)[ARTS & STYLE](#)[BOOKS](#)[NATURE](#)[IN-DEPTH](#)[ANALYSIS](#)[LOCAL](#)[EDITIONS:](#)[CNN.com Europe](#)[change default edition](#)[MULTIMEDIA:](#)[video](#)[video archive](#)[audio](#)[multimedia showcase](#)[more services](#)[E-MAIL:](#)

Subscribe to one of our news e-mail lists.

Enter your address:

go

[Or:](#)[Get a free e-mail account](#)[DISCUSSION:](#)[message boards](#)[chat](#)[feedback](#)[CNN WEB SITES:](#)[myCNN.com](#) [CNSI](#)
[allpolitics](#) [CNNfr](#)[AsiaNow](#)[En Español](#)[Em Português](#)[Svenska](#)

'Hot' fuel cells get cooler and cooler

ENN®

June 16, 2000

Web posted at: 12:41 p.m. EDT (1641 GMT)

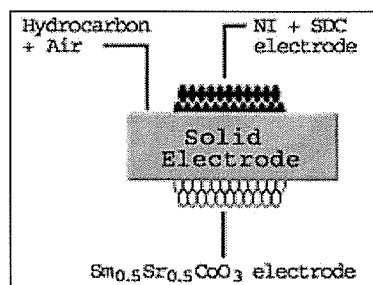
By Environmental News Network staff

Fuel-cell technology is cool. It offers the promise of low-emission power generation for everything from cars to entire metropolitan areas. And Japanese researchers say they have built a fuel cell that runs efficiently at temperatures as low as 932 degrees Fahrenheit.

This temperature is very cool for fuel cells and means the cell can run on regular hydrocarbon fuels such as methane without an accumulation of carbon to clog the apparatus. A paper on the technology appears in today's issue of *Science*.

"What they got was very impressive performance at lower temperatures," said Raymond Gorte, a professor of chemical engineering at the University of Pennsylvania. Gorte and colleagues also built a fuel cell that avoids carbon buildup. They reported the results March 16 in *Nature*.

Conventional solid oxide fuel cells extract electricity from hydrocarbon fuels by converting the hydrocarbons to hydrogen inside the cells. Hydrogen reacts with oxygen from the air in such a way that electrical power is generated.



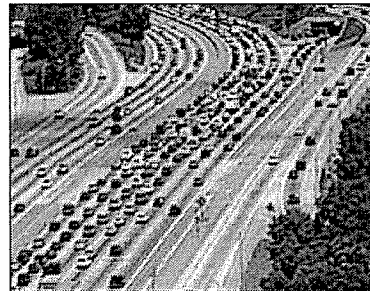
Instead of relying on hydrogen for fuel, a single-chamber, solid-oxide fuel cell uses a flowing mixture of hydrocarbon and air

In conventional solid-oxide fuel cells, carbon atoms join together and clog the fuel cell instead of joining with oxygen to form carbon dioxide.

Gorte's team overcame this problem by developing a material that does not promote the formation of carbon-carbon bonds. Thus, the apparatus does not get fouled by carbon buildup.

The Japanese researchers, led by Takashi Hibino of the National Industrial Research Institute of Nagoya, developed a single-chamber fuel cell with unique materials that operates at temperatures cool enough to deter carbon buildup.

"In principle (the technology) could be applied to a regular type of fuel cell,"



Fuel-cell research using lower operating temperatures makes the future of lower-emission power more feasible for everything from cars to entire metropolitan areas

CNN.com NewsNet

CNN Sites

Search

CNN.com

Find

NATURE

TOP STORIES

[New hurdles hamper](#)[Galapagos oil spill cleanup](#)[Insight, Prius lead the hybrid-powered fleet](#)[Picture: Indonesia's Merapi volcano erupts](#)[\(MORE\)](#)

CNN.com

TOP STORIES

[Up to 2,000 killed in India quake; fear of aftershocks spreads](#)[Clinton aide denies reports of White House vandalism](#)[New hurdles hamper Galapagos oil-spill cleanup](#)[Two more Texas fugitives will contest extradition](#)[\(MORE\)](#)**BUSINESS**[Playing for Iraq's jackpot](#)[Coke & smoke bite Dow](#)[Sun Microsystems posts tiny profit](#)[\(MORE\)](#)

MARKETS 4:30pm ET, 4/16

DJIA ↓ 144.70 8257.60

NAS ↑ 3.71 1394.72

S&P ↓ 10.90 879.91

Get Quote

SI.com **SPORTS**[Jordan says farewell for the third time](#)[Shaq could miss playoff game for child's birth](#)[Ex-USOC official says athletes bent drug rules](#)

[Norge](#)
[Danmark](#)
[Italian](#)

FASTER ACCESS:
[europe](#)
[japan](#)

TIME INC. SITES:

Go To ...

CNN NETWORKS:

CNN
CNN INTERNATIONAL
CNN Headline NEWS

[more networks](#)
[transcripts](#)

SITE INFO:

[help](#)
[contents](#)
[search](#)
[ad info](#)
[jobs](#)

WEB SERVICES:

[CNN e-store](#)

said Gorte. "What they are doing is working at low enough temperatures that carbon buildup doesn't occur."

It may take several years of development to work out glitches and get the technology ready for industrial use, according to Subash Singhal, who heads the fuel cell research program at Pacific Northwest National Laboratory in Richland, Washington.

However, the Department of Energy recently launched a \$35-million-a-year program known as the Solid State Energy Conversion Alliance to bring the technology to the marketplace. If successful, cool fuel cells that run on ordinary hydrocarbon fuels may be in operation within the decade.

Copyright 2000, Environmental News Network, All Rights Reserved

RELATED STORIES:

[Ordinary energy powers new fuel cell](#)
 March 23, 2000
[Fuel-efficient cars primed to outrun gas prices](#)
 March 31, 2000
[Alternatives to gas-powered vehicles are in the works](#)
 March 15, 2000
[Better cars just down the road](#)
 January 2, 2000
[y: Automakers pumped about fuel cell potential](#)
 December 1999

RELATED ENN STORIES:

[Ordinary energy powers new fuel cell](#)
[Fuel cells, the next generation: lean, mean and clean](#)
[Synthetic enzyme produces hydrogen cheaply](#)
[Being off the grid appeals to rich folks](#)
[Fuel cells power brave new energy world](#)

RELATED SITES:

[The National Industrial Research Institute of Nagoya](#)
[Science](#)
[Raymond Gorte](#)
[Fuel Cells 2000](#)
[National Fuel Cell Research Center](#)

Note: Pages will open in a new browser window
External sites are not endorsed by CNN Interactive.

Search CNN.com

Find

(MORE)

→ [All Scoreboards](#)

WEATHER

US Zip go [All cities](#)

WORLD

[Quake help not fast enough, says Indian PM](#)

U.S.

[Bush: No help from Washington for California power crunch](#)

POLITICS

[Bush signs order opening 'faith-based' charity office for business](#)

LAW

[Prosecutor says witnesses saw rap star shoot gun in club](#)

TECHNOLOGY

[Napster to launch fee-based service](#)

ENTERTAINMENT

[Can the second 'Survivor' live up to the first?](#)

HEALTH

[Heart doctors debate ethics of testing super-aspirin](#)

TRAVEL


[Nurses to aid ailing airline passengers](#)

FOOD

[Texas cattle quarantined after violation of mad-cow feed ban](#)

ARTS & STYLE

[Ceramist Adler adds furniture to his creations](#)

 (MORE HEADLINES)

[Back to the top](#)

© 2001 Cable News Network. All Rights Reserved.
[Terms](#) under which this service is provided to you.
 Read our [privacy guidelines](#).